Performance Evaluation of Pavements with Cement Stabilized Layer using MEPDG Program and LTPP Data

by

Shahbaz Khan, Ph.D.

A Thesis Submitted to the

School of Graduate Studies

In partial fulfillment of the requirements for the degree of

Master of Engineering

Faculty of Engineering and Applied Science

Memorial University of Newfoundland

October 2021

St. John’s Newfoundland and Labrador Canada

Executive Summary

The spring season causes melting of wintry ice in pavement structures. Therefore, transportation agencies use axle load limits to protect the pavement from deterioration during springtime. The use of cement treated base (CTB) in the pavement structure can provide a prospect to overcome this problem. Studies conducted in U.S., South Africa, and India suggests that the use of CTB improves overall performance of pavement structure. In the present work, long term pavement performance (LTPP) data from U.S. and Canada for pavement sections with cement treated base were studied. To better understand the design performance of cement-treated pavement, a mechanistic empirical pavement design guide was used and road sections with different climatic conditions were investigated. A parametric study consisting of seven variables, each at two levels (high and low) were considered. These included asphalt thickness, cement treated base thickness, elastic modulus of cement treated base layer, modulus of rupture, crack spacing, traffic, and speed along with the following three categorical variables: subgrade (coarse and fine), moisture (wet and dry), and temperature (freeze and no freeze). Factorial analysis consisting of a 2^k design of resolution V was considered in the design of the experiment, and a total of 128 factors were considered for the analysis. All the combinations were run in the Mechanistic-Empirical Pavement Design Guide (MEPDG) by AASHTOWare and response variables such as international roughness index, total permanent deformation, asphalt layer rutting, asphalt total fatigue cracking (bottom-up cracking+ reflective cracking), asphalt total transverse cracking (thermal cracking + reflective), asphalt thermal cracking, and top-down asphalt cracking were considered. The response was analyzed using DoE and the factors that affect the performance of CTB pavement were determined. The results are presented for each response and all the assumptions of the response are met. Furthermore, apart from the best suited factors for pavement design, the MEPDG

results suggest that the CTB layers' reflective cracking is a major distress in the design of these pavements. In general, surface cracks follow the same pattern as cracks in the base, and are therefore called "reflection" cracks. As stated before, the use of CTB design can provide a chance to improve the loading condition during the spring season. However, the stress concentrations and cracking in the base layer can develop on top of the asphalt surface as well. The failure of semi-rigid pavements due to reflective cracking is somewhat discouraging. The literature suggests using geotextile, aggregate interlayer and chip seal between the CTB layer and asphalt layer as a potential solution to the problem. In the present research, the use of aggregate interlayer was attempted to solve this problem. This type of pavement system is named Inverted Pavement and is used in only a few states in the United States such as Louisiana. However, the AASHTOWare software, which is the most popular pavement design software in the U.S., has some issues in terms of versatility of the pavement structure.

To be specific, the MEPDG program can not analyze the performance of an inverted pavement system. Therefore, to better understand the use of this pavement structure, a different software was used. A pavement software named CROSSPAVE which can run the aforesaid structure was employed. The results of MEPDG are superior to CROSSPAVE as it gives performance in terms of distress that occur in the pavement system while the CROSSPAVE output only gives stress and strain. These strains/stresses were correlated to the distresses in terms of the number of repetitions using empirical equations.

Therefore, another parametric study was carried out to understand the factors affecting the inverted pavement stress/strains at critical locations. Similar to the previous analysis, the DoE analysis was carried and critical factors affecting the design of inverted pavement are listed.

Acknowledgments

First and foremost, I would like to thank Allah for providing me good health, a good state of mind, and a way to finish this thesis. All praise and thanks to Allah; without his help, it wouldn't be easy to complete this degree.

Furthermore, I would like to thank my Supervisors Dr. Kamal Hossain and Dr. Carlos Bazan. I want to thank them for mentoring, sincere advice and supervising me. Dr. Hossain's dedication to his work is excellent and his desire to work on innovative projects is impressive. I have learned a lot from him; and the calmness of Dr. Bazan was always reassuring and it is a kind of support you always look for as a student and fellow human and I admire his knowledge and compassion.

I have to acknowledge the support from the team members of the Advanced Road & Transportation Engineering Lab (ARTEL) at the Memorial University of Newfoundland. All the group chats and tea chats were helpful. I love the way the team members were supportive and collaborative during their tenure. I want to sincerely thank all of them especially to Surya for providing access to MEDPG and DoE software through his contact. It meant a lot in this journey. I acknowledge the effort of Towhidul and Alyssa for sincere advice and for proofreading the thesis.

Finally, I would like to acknowledge the support, prayers and advice of family members and friends. I am grateful to my parents, brothers, sister, and wife for their love, affection, and care.

TABLE OF CONTENTS

LIST OF FIGURES

LIST OF TABLES

Acronyms

CTB	Cement Treated Base
MEDPG	Mechanistic Empirical Pavement Design Guide
LTPP	Long Term Pavement Performance
LCA	Life Cycle Assessment
LCCA	Life Cycle Cost Analysis
DoE	Design of Experiment
AC	Asphalt Concrete
ANOVA	Analysis of Variance
IRI	International Roughness Index
BT	Bituminous Top
CBR	California Bearing Ratio
AASHTO	American Association of State Highway and Transportation Officials
HRB	Highway Research Board
HMA	Hot Mix Asphalt
MSA	Million Standard Axles
SHRP	State Highway Research Program
FHWA	Federal Highway Administration
GPS	General Pavement Section
SPS	Specific Pavement Section
ABP	Area Bound by Performance curve
USACE	U.S. Army Corps of Engineers
PCC	Plain Cement Concrete
CPR	Cold in Place Recycling
JCP	Jointed Concrete Pavement
CRCP	Continuously Reinforced Concrete Pavement
ATB	Asphalt Treated Base
MERRA	Modern-Era Retrospective analysis for Research and Applications
WIM	Weight In Motion
UCS	Unconfined Compressive Strength
AC	Asphalt Concrete
LTE	Load Transfer Efficiency
PG	Performance Grade

CHAPTER 1: INTRODUCTION AND REVIEW OF LTPP

1. Introduction

Pavement is designed with the main purpose of protecting the subgrade and providing a safe riding quality. The design life of a flexible pavement is generally 20 years. Normally, the pavement is sufficiently thick to cater to these basic needs. The design traffic and strength of the subgrade plays a vital role in the crust composition of any type of pavements. The load distribution in flexible pavement occurs through grain-to-grain contact, whereas the slab action of the concrete layer is responsible for the load distribution of the rigid pavements. Flexible pavement distresses such as rutting, cracking (longitudinal, transverse), and potholes are common during the service period of the pavement. Therefore, to achieve the objective of safe riding quality above the minimum serviceability of the pavements, different maintenance strategies such as routine maintenance (crack sealing, pothole repair, spray patching, shallow patching and drainage improvement), periodic maintenance (slurry seal, chip seal, micro surfacing, and full depth patching), and rehabilitation (reconstruction, resurfacing, milling and resurfacing, hot in place recycling and cold in place recycling) are done (Haas and Kazmierowski, 1996).

The U.S. Army Corps of Engineers (USACE) developed a pavement design procedure based on the CBR value of the subgrade (Huang, 2004). Different flexible pavement design methods such as AASHTO 93, Hveem and Mechanistic-Empirical have been used to better understanding the performance of pavements.

1.1 AASHTO Road Test

The AASHTO road test is a landmark test for the performance evaluation of pavements. The 27-million-dollar project was conceived formerly by AASHO to test the performance of Portland cement concrete and asphalt concrete pavement as well as a few short-span bridges.

The purpose of the project was to study the performance of a pavement, historically known as the AASHO Road Test, 1961 (HRB, 1962). Figure 1.1 shows the test layout of the now called AASHTO road test.

Figure 1.1: Test setup layout for the AASHTO road test (HRB, 1962)

Success of the AASHO road test

Road test results from AASHO were historically significant. It led to the following improvements in flexible pavement design practice.

- The design equation for flexible pavement was developed;
- The data from this road test was used to develop the design guide of 1961, 1972, 1981, 1986, and 1993;
- The structural number concept was developed to accommodate for different environmental and subgrade conditions;
- The procedure for determining effective soil resilient modulus was developed and pavement serviceability index concept was implemented in pavement design.

Limitation of the AASHO road test

- The design equations are based on the results of traffic tests over a two-year period. The long-term effects of traffic, temperature and moisture on the reduction of serviceability were not included;

- The equations were developed for a set of conditions applicable to a given climatic setting with a specific set of pavement materials and subgrade soils. The average climate at the test site for summer and winter temperatures are 76 F and 27 F respectively with an average annual precipitation of about 34 inches. The average depth of frost penetration is about 28 inches. The subgrade soils consist of A-6 and A-7-6 that are poorly drained, with CBR ranging from 2 to 4;
- One type of HMA, granular base and subbase was used in this road test;
- The design procedure is based on the cumulative expected 18 kips (80 kN) equivalent single axle load. The load used in the equations was based on the outcome of operating vehicles with identical axle loads and configuration (as opposed to mixed traffic).
- The original design equations were purely based on the results of the AASHTO road test but were modified later by theory and experience to take care of other subgrade and climatic conditions;
- The resilient modulus of a layer (asphalt layer) is replaced with the dynamic modulus.

The further improvements led to the development of the rutting and fatigue equation for the pavement distress criteria used by Shell and Asphalt Institute (Huang, 2004). In addition, new pavement design software were developed for the design of flexible pavement such as BISAR, ELSYSM, CIRCLY, ILLIPAVE, and 3-D Move. However, the actual design of the pavement system still did not consider the pavement maintenance and actual field performance in the design. Therefore, a long-term pavement performance study was taken up to better understand the actual field performance of the pavement in different conditions.

1.2 Long Term Pavement Performance (LTPP)

1.2.1 Objectives of LTPP

The goal of LTPP is to extend the life of pavements by investigating the long-term performance of different pavement designs, as originally constructed or rehabilitated, under various conditions. The LTPP program established six objectives:

- Evaluate pavement design methods;
- Improve the design methods and strategies for rehabilitating pavements; improve the design equations for new and reconstructed pavements;
- Determine the effects of loading, environment, material properties and variability, construction quality, and maintenance levels on pavement distress and performance;
- Determine the effects of specific design features on pavement performance; and
- Establish a national long-term pavement performance database (Walker and Cebon, 2011).

To better understand the performance of pavement after the AASHTO test, the LTPP studies were taken up by State Highway Research Program (SHRP) in 1987. Later, Federal Highway Administration (FHWA) took up the project. The mission of LTPP was to collect and store performance data from across North America (many U.S. states and Canadian provinces took part in the study) to better understand pavement design, construction, rehabilitation, maintenance, preservation, and management.

1.2.2 LTTP test sections

The total number of pavement sections in LTPP consisting of both asphalt pavement and concrete pavement is around 2581. However, only 394 of these sections are now active, for which data are still collected. All the data are available online through LTPP infopave website (LTPP, 2018). These are a rich source of pavement performance data across North America. The road sections are distributed between the United States and Canada. The number of sections found within Canadian provinces are 141, the distribution of which is shown in Table 1.1. The distribution of sections in the United States is presented in Table 1.2.

Table 1.1: Canadian LTPP road sections

Section ID	Name	Number of Section
81	Alberta	17
82	British Columbia	4
83	Manitoba	26
84	New Brunswick	4
85	Newfoundland	3
86	Nova Scotia	1
87	Ontario	36
88	Prince Edward Island	3
89	Quebec	20
90	Saskatchewan	27

Table 1.2: U.S. LTPP Road sections

Section ID	Name	Number of Section	Section ID	Name	Number of Section
1	Alabama	68	31	Nebraska	44
2	Alaska	6	32	Nevada	71
4	Arizona	158	33	New Hampshire	1
5	Arkansas	59	34	New Jersey	30
6	California	126	35	New Mexico	44
8	Colorado	68	36	New York	26
9	Connecticut	10	37	North Carolina	50
10	Delaware	33	38	North Dakota	22
11	District of Columbia	1	39	Ohio	58
12	Florida	38	40	Oklahoma	73
15	Hawaii	4	41	Oregon	17
16	Idaho	25	42	Pennsylvania	49
17	Illinois	42	43	Puerto Rico	4
18	Indiana	56	44	Rhodes Island	1
19	Lowa	66	45	South Carolina	9
20	Kansas	67	46	South Dakota	36
21	Kentucky	19	47	Tennessee	38
22	Louisiana	22	48	Texas	217
23	Maine	18	49	Utah	105
24	Maryland	32	50	Vermont	5
25	Massachusetts	3	51	Virginia	31
26	Michigan	75	53	Washington	54
27	Minnesota	82	54	West Virginia	5
28	Mississippi	46	55	Wisconsin	72
29	Missouri	109	56	Wyoming	24
30	Montana	38			

1.2.3 LTPP General and Specific test sections

The LTPP test sections consist of general pavement studies (GPS) sections and specific pavement studies (SPS) sections. The GPS sections include existing pavements and overlays and the SPS sections include newly constructed pavements and overlays. Most sections were designed to be 152 m long. The material and design were typical of North American standard practice. Table 1.3 shows the LTPP GPS planned sections. There are a total of 976 GPS sections. Later, more pavement sections were added to study the effect of more variables in pavements. The noted difference in SPS and GPS sections was that SPS sections were more controlled than GPS sections. There are a total of 1793 SPS sections. Table 1.4 shows the specific pavement sections.

Table 1.3: LTPP General Pavement Section

GPS sections	Specifications	Number of Sections
GPS-1	Asphalt Concrete Pavement in Granular Base	233
GPS-2	Asphalt Concrete Pavements on Bound Base	144
GPS-3	Jointed Concrete Pavements	133
GPS-4	Jointed Reinforced Concrete Pavements	69
GPS-5	Continuously Reinforced Concrete Pavement	85
GPS-6	Asphalt Concrete Overlay of Asphalt Concrete Pavements	421
GPS-6 A	Existing AC Overlay on AC Pavement	64
GPS-6 B	AC Overlay with Conventional Asphalt Cement on AC Pavement, No Milling	123
GPS-6 C	AC Overlay with Modified Asphalt Cement on AC Pavement, No Milling	53
GPS-6 D	Multiple AC Overlays with Conventional Asphalt Cement on AC Pavement, No Milling	29
GPS-6 S	AC Overlay on AC Pavement with Milling and/or Fabric Pre-treatments	236
GPS-7	Asphalt Concrete Overlay of Portland Cement Concrete Pavements	143
GPS-7A	Existing AC Overlay on PCC Pavement	35
GPS-7B	AC Overlay with Conventional Asphalt Cement on PCC Pavement, with CPR or No Pre-treatment	58
GPS-7C	AC Overlay with Modified Asphalt Cement on PCC Pavement, with CPR or No Pre-treatment	23
GPS-7D	Multiple AC Overlays with Conventional Asphalt Cement on PCC Pavement, with No Pre-treatment	10
GPS-7F	AC Overlay on PCC Pavement, with Slab Fracture Pre-treatment	4
GPS-7 R	Intensive Concrete Pavement Restoration of PCC without Overlay	1
GPS-7 S	AC Overlay on PCC Pavement with Pre-treatment	54
GPS-8	Bonded Portland Cement Concrete Overlay	
GPS-9	Unbounded Portland Cement Concrete Overlay of Portland Concrete Pavements	26

Table 1.4: LTPP Specific Pavement Section

SPS	Specifications	Number of Sections
SPS-1	Strategic Study of Structural Factors for Flexible Pavements	246
SPS-2	Strategic Study of Structural Factors for Rigid Pavements	207
SPS-3	Preventive Maintenance Effectiveness of Flexible Pavements	445
SPS-4	Preventive Maintenance Effectiveness of Rigid Pavements	220
SPS-5	Rehabilitation of Asphalt Concrete Pavements	204
SPS-6	Rehabilitation of Jointed Portland Cement Concrete Pavements	170
SPS-7	Bonded Portland Cement Concrete Overlay of Portland Cement Concrete Pavements	39
SPS-8	Study of The Environmental Effects in the Absence of Heavy Load	53
SPS-9	Validation of Strategic Highway Research Program Asphalt Specification and Mix Design	137
SPS-9C	Superpave Asphalt Binder Study, AC Overlay on CRCP	7
SPS-9J	Superpave Asphalt Binder Study, AC Overlay on JCP	38
SPS-9N	Superpave Asphalt Binder Study, New AC Pavement Construction	50
SPS-9O	Superpave Asphalt Binder Study, AC Overlay on AC Pavement	42
SPS-10	Warm Mix Asphalt Overlay of Asphalt Pavement	72

1.2.4 Climate

The climate plays a major role in the performance of a pavement. Table 1.5 shows the different types of climates covered in the LTPP study. To define the wet and freeze climate, the limits of minimum precipitation of 508 mm per year and freeze index of 83°C days are used. Table 1.5 shows the different climatic regions (Daleiden et al., 1994).

Table 1.5: Different climate region in the LTPP dataset

Climatic Region	Annual Rainfall, mm	Freezing Index, 83°C	Sections
Dry, Freeze	<508	>83	422
Dry, No Freeze	<508	<83	321
Wet, Freeze	>508	>83	908
Wet, No Freeze	>508	<83	930

The temperatures and precipitation levels affect the performance of pavements. The geographic regions with a cold climate can be affected by the frost and freezing of the roadbed materials. The silty soil is affected by frost heave. Frost heave occurs when moisture present in the soil expands through freezing action. The temperature in the pavement also affects the oxidation process that can increase the viscosity properties. In the presence of moisture, one of the mechanisms for the deterioration of asphalt is the debonding effect (Daleiden et al., 1994).

Researchers such as Perera and Kohn (2001) studied the effect of all environmental zones and individual environmental zones on the rate of change of IRI values. IRI stands for international roughness index. This pavement index used to rate the riding quality of the pavements. Among the four climatic regions, the wet freeze zone has more effect on the change in the IRI values on asphalt pavements. The authors concluded that the most significant factors affecting the IRI were lower pavement thickness, lower annual precipitation, low number of wet days, higher freezing indices, and high fine content in the base layer. Silt content between 5-15% in the subgrade caused frost related heave and it was found to be a significant factor affecting IRI. Similarly, for wet no freeze zones, the IRI was affected by high plasticity and moisture index of subgrade, high fine content in the base layer (more than 50% passing sieve #200), and high fine content in the subgrade. Moreover, in dry freeze zones, the higher rate of roughness was caused by higher annual precipitation, freezing indices, and higher fne content in the base layer. Furthermore, in dry no freeze zones, the high roughness rate was affected by higher mean annual temperature and subgrade type, especially higher plastic limit, i.e., clay soil.

The variation of climatic regions in North America (Jackson et.al, 2006; Chen et. al., 2019) due to geopraphic location is shown in Figure 1.2.

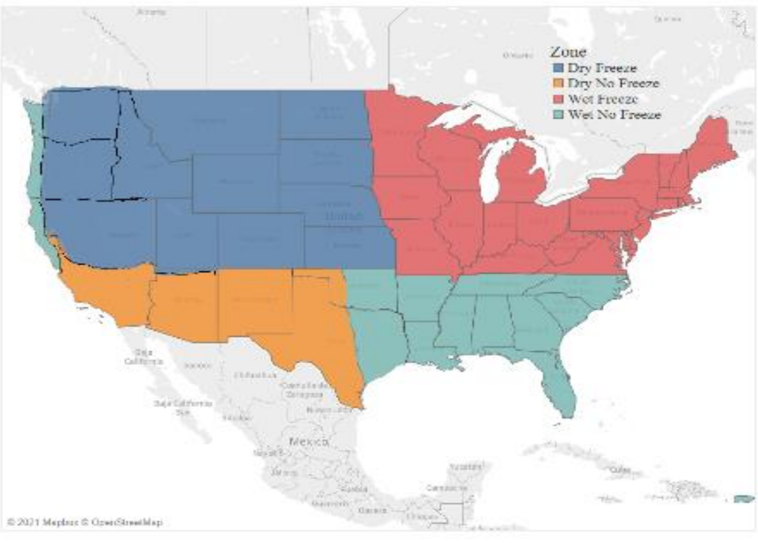

Figure 1.2: Different climatic region in LTPP (Chen et al, 2019)

Some states such as Texas, Oklahoma, Oregon, California, and Nevada have mixed climate and vary within the states itself. For example, Texas and Oklahoma have both dry no freeze and wet no freeze climatic zones.

Furthermore, researchers have studied the effect of frost action on pavement performance and life cycle cost analysis. Also, they have explored the use of local calibration factor in Mechanistic-Empirical Design of New and Rehabilitated Pavement for the pavement management system (Jackson et al., 2006). The variation of frost penetration in different geographic locations is illustrated in Figure 1.3.

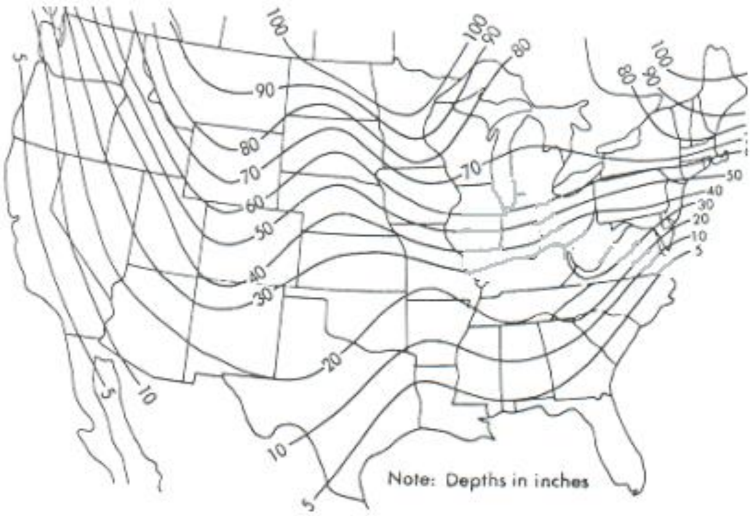

Figure 1.3:Frost penetration depth variation in North America

1.2.5 Material

The LTPP test sections consists of a different material type including asphaltic material, Portland cement concrete, and aggregate. Table 1.6, Table 1.7 and Table 1.8 show the distributions of LTPP sections for subgrade type, base type and surface type respectively. The handling of laboratory material testing has been detailed in the long-term pavement project laboratory material testing and handling guide (Simpson et al., 2007).

Table 1.6:Subgrade type considered in the LTPP dataset

Subgrade Type	Section
Coarse	1437
Fine	1144

Table 1.7:Base type considered in the LTPP dataset

Base Type	Section
Bound	1169
Unbound	1468

Table 1.8:Surface type considered in the LTPP dataset

Surface Type	Section
Asphalt Concrete Pavement	1823
Continuously reinforced concrete pavement	124
Joint plain concrete pavement	668
Joint reinforced concrete pavement	216

The application of different moisture damage resistance additive such as liquid anti-stripping agent used in wet freeze climate, as shown in Figure 1.4.

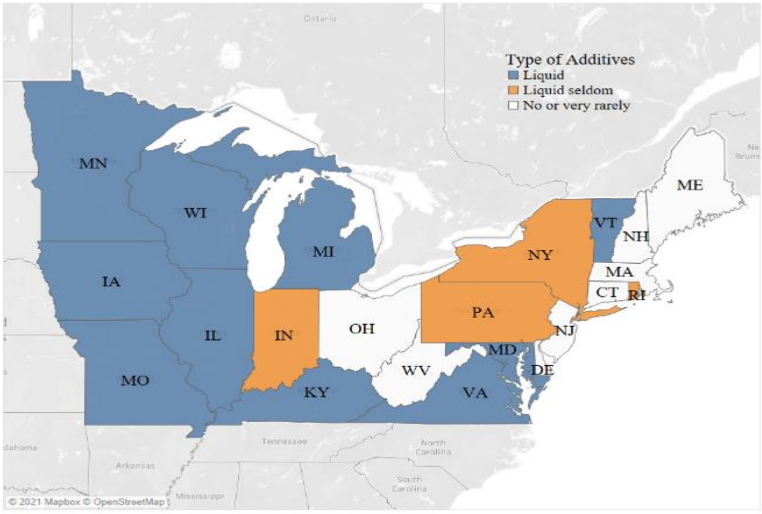

Figure 1.4:State using moisture damage treatment for wet freeze

1.2.6 Traffic

The LTPP consists of different road categories depending on the traffic, as shown in Table 1.9.

Table 1.9:Different traffic set considered in the LTPP dataset

Roadway Functional class	Sections
Rural Local Collector	33
Rural Major Collector	42
Rural Minor Arterial	167
Rural Minor Collector	9
Rural Principal Arterial-Interstate	862
Rural Principal Arterial- Other	1137
Urban Collector	5

Urban Monir Arterial	17
Urban Other Principal Arterial	173
Urban Principal Arterial- Interstate	73
Urban Principal Arterial- Freeways or Expressways	63

It was found that a 1 % increase in overloading due to traffic causes a 1.8 % reduction in pavement life. The relationship between the overloading and reduction in pavement life was found to be linear and independent of pavement structure and traffic loading variation (Wang et al., 2015).

The axle load in the flexible pavement can be measured using weighing motion. However, the system depends on pavement temperature and vehicle speed. It has been reported that the error in the measurement of vehicle weight is caused by the distribution of vertical and horizontal stress (Burnos and Rys, 2017).

1.2.7 Maintenance in LTPP sections

The LTPP sections are divided based on the four categories from a maintenance perspective, as shown in Table 1.10. The possible distress in flexible pavements includes alligator cracking, edge joint cracking, reflection cracking, shrinkage cracking, slippage cracking, rutting, corrugation, depression, upheaval, potholes, raveling, polished aggregate, loss of aggregate, and flushing asphalt. These may be caused by structural failures, component mix issues, and moisture problems, in addition to temperature issues or moisture penetration. To increase the pavement life and prolong the pavement performance, maintenance and rehabilitation of the pavement are carried out. The maintenance includes patching & routine maintenance, fog seal, surface treatment, and slurry seal. The rehabilitation includes surface recycling, thin overlay, open-graded surface, structural overlay, structural recycling, and reconstruction. These maintenance and rehabilitation are applied to specific pavement distress and are shown in Table 1.10.

Table 1.10:Different maintenance considered in the LTPP study sites

Maintenance and Rehabilitation	Section
Maintenance only	1723
Maintenance and Rehabilitation	776
No Maintenance and Rehabilitation	431
Rehabilitation only	1211

To study the effectiveness of pavement rehabilitation through LTPP, the researcher (Ahmed et al. 2013) has taken eight flexible pavement rehabilitation treatments. The aggregate and disaggregate post-performance models were used for determining the effectiveness of treatment. The roughness reduction and estimated treatment service and area bound by the performance curve (ABP) curve were used to evaluate criteria. Results suggested that compared to the recycled mix, the virgin mix was found to be more effective. Treatment performed on good pavement condition resulted in a better outcome than treatment performed on poor pavement condition. The prediction model consists of treatment type, added layer thickness, level of surface preparation and mix type. When comparing 2-inch treatment with 5-inch treatment, the 5-inch treatment was more effective in estimated service life and ABP.

Furthermore, in LTPP, the distresses are collected based on the uniform distress definition. This is done to maintain uniformity in the pavement data and replication of the dataset throughout the program. The most notable document for pavement distress identification is the distress identification manual for long-term pavement performance (Miller and Bellinger, 2003). The definition of each level of severity is discussed to avoid any discrepancy in data collection throughout the program.

For example, to measure the alligator cracking, the severity measured in sq. meter is divided in three levels; low, medium and high. The definitions are given below:

- “Low: An area of cracks with no or only a few connecting cracks; cracks are not spalled or sealed; pumping is not evident;

- Moderate: An area of interconnected cracks forming a complete pattern; cracks may be slightly spalled; cracks may be sealed; pumping is not evident;
- High: An area of moderately or severely spalled interconnected cracks forming a complete pattern; pieces may move when subjected to traffic; cracks may be sealed; pumping may be evident."

Through LTPP, the researcher (Ker et al., 2008) has improved the accuracy of fatigue prediction by using a generalized linear model and generalized additive model assuming Poisson distribution and the quasi-likelihood estimation method. The model's significant term as given in equation 1.1 includes yearly KESALs, pavement age (age), annual precipitation (precip), annual temperature (temp), critical tensile strain (ε_t) under the asphalt-concrete surface layer, and freeze-thaw (ft) cycle for the prediction of fatigue cracking.

$$\text{Fatigue Cracking} = e^{(-18.08+0.943(\text{age})^{0.5} + 0.832\log(\text{kesal}) + 0.121\,(\text{precip})^{0.5} + 0.869(\text{temp})^{0.5} + 31.489\,(1000\varepsilon_t)^2 + 3.242\log(\text{ft}))}$$

……………………………………………………………………………………...Equation 1.1

A study was conducted to measure the performance of fatigue cracking in flexible pavement. Based on the thickness of the surface layer, the type of the base and the base thickness in different site conditions (subgrade and climate), the type of the base was found to be a critical factor, and the asphalt treated base (ATB) demonstrated the best performance. This may be due to fatigue life extension given due to the ATB base type. The drainage and base type jointly affected the performance of the pavement. The wet freeze climate has shown more fatigue cracking. The base thickness was an insignificant effect on the fatigue performance of pavement, whereas the fine-grained soil has shown the worst effect on the performance. The analysis was done using ANOVA, logistic regression and discriminant analysis (Haider and Chatti, 2009).

Some researchers have studied the performance of rehabilitation by comparing IRI before and after treatment using ANOVA and reported that there is not a significant difference between pre-treatment IRI, milling versus no milling, virgin versus recycled and overlay thickness. However, the researchers used a limited amount of data (Daleiden et al. (1998), Perera and Kohn (1999)).

1.2.7.1 Preventive Maintenance

In order to reduce the rate of deterioration in the pavement, the concept of preventive maintenance was brought forward. Preventive maintenance means applying a treatment to the pavement to increase its serviceability and delay the pavement deterioration, prior to the observation of any severe distresses. The application of a treatment and its specific timing has serious performance implications to pavements. The importance of preventive treatment can be judged by a public survey in Arizona, California, and Washington where the general public indicated that they are willing to pay more taxes to get better-maintained roads (Jackson, 2001). The preventive treatments are applied at the early stages of pavement life. Treatments applied too late are ineffective, failing to prolong the life of the pavement. The preventive treatments applied for concrete pavements includes full-depth concrete pavement repair, joint sealing, crack sealing, joint and surface spall repair, diamond grinding, undersealing and load transfer restoration. The preventive treatments for flexible pavements include crack filling/ crack sealing, fog seals, slurry seals, scrub seals, micro-surfacing, chip seals, thin overlay, and ultrathin friction courses. In LTPP, many sections are preserved with a thin overlay, slurry seal, crack seal, and chip seal (Peshkin et al., 2004).

Thin overlay

The thin overlay is a small non-structural layer to the pavement. The purpose is to improve pavement surface condition, protect pavement structure, reduce the pavement deterioration rate, correct surface deficiencies, reduce permeability, and improve the ride quality of the pavement (Wang and Wang 2013). A thin overlay can range from 19-38mm in thickness (0.75 -1.5 inch) (Peshkin et al., 2004).

Slurry seal

The slurry seal is a mixture of emulsified asphalt, well-graded fine aggregate, water, and mineral filler that has a creamy, fluid-like appearance when applied. As a hard-wearing surfacing for pavement preservation, the slurry seal can be used for sealing aged pavements, filling minor cracks, restoring skid resistance, and enhancing aesthetic appearance (Wang and Wang 2013). A mixture of well-graded aggregate (fine sand and mineral filler) and asphalt emulsion is spread over the entire pavement surface with either a squeegee or spreader box attached to the back of a truck. It is effective in sealing low-severity surface cracks, waterproofing the pavement surface, and improving skid resistance at speeds below 64 km/h (30 mph). The thickness of a slurry seal layer is generally less than 10 mm (0.4 in.) (Peshkin et al., 2004).

Chip seal

Chip seal is the application of a bituminous binder immediately followed by the application of aggregate. The aggregate is then rolled and embed into the binder. Multiple layers may be placed, and different types of binder and aggregate can be used to address specific distress or traffic situations (Wang and Wang 2013). Asphalt (commonly an emulsion) is applied directly to the pavement surface (1.59 to 2.27 L/m^2 [0.35 to 0.50 gal/yd^2]) followed by the application of aggregate chips (8 to 27 kg/m^2 [15 to 50 lb/yd^2]), which are then immediately rolled to imbed chips in the asphalt. The treatment seals pavement surface and improves friction.

Crack seal

Crack filling is employed for cracks that undergo little movement. Sealants used are typically thermo-plastic (bituminous) materials that soften upon heating and harden upon cooling. Crack seal requires thorough crack preparation and often requires the use of specialized, high-quality materials placed either into or above working cracks to prevent the intrusion of water and incompressible materials. The main purpose of crack sealing is to prevent the percolation of water through pavement cracks (Wang and Wang 2013). Crack sealing refers to a sealant operation that addresses “working” cracks, i.e., those that open and close with changes in temperature. It typically implies high-quality materials and good preparation (Peshkin et al., 2004).

The benefit of preventive maintenance includes but is not limited to reduced user costs, improved pavement performance and increased safety. It has been reported that the need for major rehabilitation is delayed with preservative maintenance, which in turn results in life cycle cost savings (Peshkin et al., 2004). Therefore, for a given pavement, there is an optimal age or condition (or a range of age or condition) where the benefit/cost (B/C) ratio associated with a chosen treatment is maximized; this is defined as the optimal timing for the treatment. Table 1.11 summarizes the different preventive maintenance treatments and their climatic, traffic, life expectancy, and cost.

Table 1.11:Characteristics of different preventive treatment in flexible pavement

Type of Treatment	Preferable Climatic Condition	Traffic	Life Expecta -ncy	Cost
Thin Overlay	Can be applied in all-weather condition	Not affected by traffic	7-10 Year	\$2.09 -\$2.39 /m^2 for dense-graded mix and \$1.5 – 1.7/m^2 for open-graded mix
Slurry Seal	Can be applied in all-weather condition but best performances reported in a dry and warm climate with low daily temperature variation	Affected by truck traffic	3-5 Year	\$ 0.84- 1.14 /m^2 for a single application and 1.32 /m^{2}for double application
Chip Seal	All-weather condition	Normally applied to low volume road but capable of performing in high traffic road	4-7 Year	\$ 0.9 – 1.08 /m^2
Crack Seal	Can be applied in all-weather condition but best performances reported in warm climate with low daily temperature variation	Not affected by traffic	2-6 Year	\$1-5 per linear m

To study the different preventive maintenance treatments based on roughness, alligator cracking, longitudinal cracking, transverse cracking, rutting, and friction from LTPP, the failure probability based on survival analysis of different performance indicators was used. The result shows that from 354 sections chip seal was the best treatment followed by thin asphalt overlay, slurry seal, and fog seal. However, the chip seal has suffered aggregate loss causing friction loss. The factors considered are traffic, climate, pavement structural capacity and pre-treatment pavement performance. The poor pre-treatment performance has significantly affected the failure. High structural capacity provided better performance of the treatment surface. Results show that the warm climate causes rutting and friction loss. In addition to treatment type, materials, and construction quality, the author recommended other factors such as pavement surface preparation and treatment method can also affect pavement performance (Dong and Huang, 2015).

For SPS sites regarding cracking and rutting, the various types of surface treatments tested at the SPS 3 experiment were not effective at improving pavement conditions. Results showed that to improve pavement roughness, a thin overlay is the best treatment option, followed by the placement of a slurry seal coat. Placing chip and crack seal treatments did not show a significant impact on pavement roughness (Bayomy et. al., 2006).

The research to determine the effectiveness of different treatments after 6 years of service for sections in poor condition shows that the pavement in good condition has twice the chances of survival than in poor condition. The good and bad conditions are defined based on the distress on the surface layer. The overall median survival time for thin overlay, slurry seal and crack seal were 7, 5.5, and 5.1 years respectively. Chip seals outperformed thin overlay, slurry seal, and crack seal treatments with respect to controlling the reappearance of distress. However, when distress such as IRI, rutting and fatigue are considered, thin overlay treatment is the most effective treatment, followed by chip seal and slurry seal. Thin AC overlays also had the most significant effect on long-term rutting control among thin AC overlays, chip seals, slurry seals, and crack seals. In wet freeze environments, the crack seal treatment performed very well whereas crack seal performance in the other two regions was not as successful (Carvalho et. al., 2011).

From the data obtained from the field, it has been reported that 40% of the sites have construction problems in the application of maintenance treatments, especially chip seal. Also, for SPS sites experiments were not effective at improving pavement conditions (IRI) with different surface treatments. A thin overlay is the best treatment option to improve the IRI, followed by the placement of a slurry seal coat. Placing chip and crack seal treatments did not show a significant impact on pavement roughness (Hall et. al., 2002).

1.2.8 Life cycle cost analysis (LCCA)

LCCA has been used for pavement preservation in many studies. For example, the LCCA concept was used in a pavement study in Texas for over 1400 projects. When compared to chip seals, microsurfacing, and thin overlays, thin chip seals have a significantly lower LCCA. In terms of cost effectiveness, chip seal is the most effective and thin overlays is the least effective among the different treatments. Microsurfacing is, in general, more expensive than chip seals but less costly than thin overlays (Zuniga-Garcia et. al., 2018).

The effectiveness of preventive maintenance is studied in terms of life extension, relative benefit, and benefit-cost ratio for chip seal in four climatic zones of the U.S.A. The initial condition of pavement has been classified as smooth, medium and rough based on IRI. The smooth pavement shows the highest life extension, relative benefit, and benefit-cost ratio. Chip seal treatment effectiveness showed no correlation to climatic conditions or to traffic levels (Mamlouk and Dosa, 2014). The majority of U.S. states consider LCCA (Gu and Tran, 2019) in its analysis for the pavement selection and it is shown in Figure 1.5.

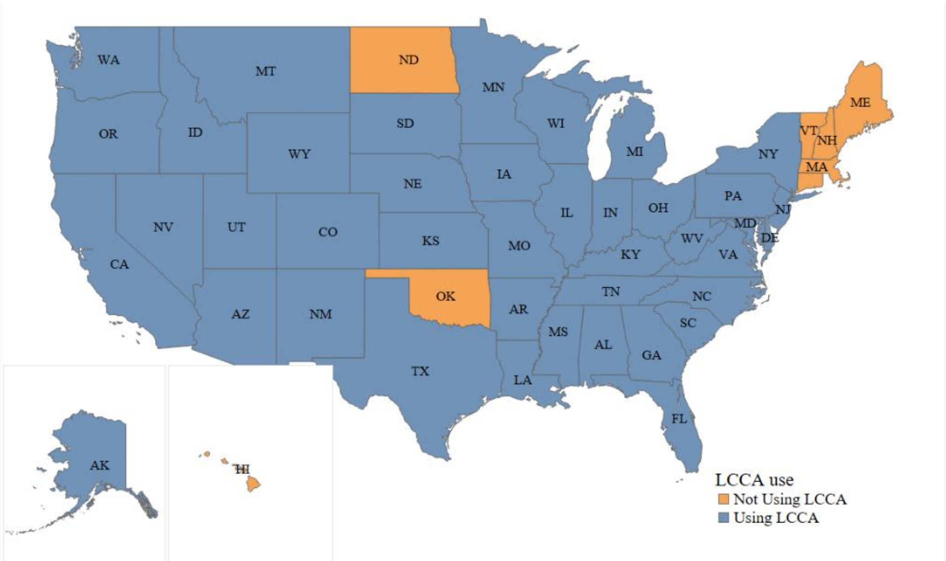

Figure 1.5: Use of LCCA for pavement type selection in the U.S. by state

The LCCA experience in Canada (primarily used in Alberta, Saskatchewan, Manitoba, Ontario, Quebec, and New Brunswick) is found to be variable from pavement type selection, asset management, pavement design, and preservations for pavement type selection (Babashamsi et. al., 2016). Currently, there are two computation approaches to conducting an LCCA: deterministic and probabilistic methods. The deterministic approach assigns a fixed and discrete value to each LCCA input variable. In the probabilistic method, the value of each LCCA input can be variable and defined by a probability distribution function. The probabilistic LCCA accounts for uncertainty and variation in input variables, but the deterministic LCCA is much easier to perform and compare its results (Gu and Tran, 2019).

1.2.9 Mechanistic-Empirical Pavement Design Guidelines (MEPDG)

The LTPP developed various online applications for pavement engineers and researchers from their large database, such as the LTPP climate tool, LTPPBind online, MERRA climate data for MEPDG, LTPP jointed concrete pavement data for MEPDG local calibration, axle load distribution factors, LTPP dynamic modulus prediction, pavement performance forecast, WIM cost analysis, forward calculated stiffness, AASHTO 1998 rigid pavement design, distress identification manual, pavement loading user guide, and LTPP infopave.

The mechanistic pavement design procedure has overcome most of the drawbacks AASHTO of the empirical pavement design. The inclusion of different vehicle loading patterns and combinations instead of ESALs, better characterization of material properties, historical temperatures for the pavement, and improved reliability of the pavement design leads to better performance prediction for different types of pavements. The AASHTOWare Pavement Mechanistic-Empirical (ME) software, also named as Mechanistic-Empirical Pavement Design Guide (MEPDG) software, is a robust pavement design software that is based on field pavement performance. Fundamentally, this software is based on four categories: material properties (both asphalt and base layers), traffic volume and distribution, climate, and structural design. In this study, all the structural and historical climate data were obtained from the Long-Term Pavement Performance (LTPP) program database. The performance prediction models for the MEPDG are calibrated nationally from the field data obtained from the Long-Term Pavement Performance (LTPP) data, Minnesota pavement test track (MnROAD) and the FHWA accelerated loading facility. It should be noted that the nationally calibrated performance models may or may not fit the local conditions. As a result, the performance prediction models may require local calibrations. The LTPP database serves as a major source of information for local calibration of the performance equations in the absence of local management system data. The LTPP sections are used in many calibration studies, as shown in Table 1.12.

Table 1.12:Previous local calibration of MEPDG attempts

Location	**Parameter**	**Author**	**Data**
Alabama	Rutting and Fatigue	Guo, 2013	NCAT
Arizona	Rutting, Fatigue and Roughness	Souliman et al., 2010	LTTP
Idaho	Dynamic Modulus	El-Badawy et al.,2014	Lab
Louisiana	Rutting	Wu et.al., 2013	Department data
New Mexico	Rutting, Fatigue and Roughness	Tarefder and Rodriguez-Ruiz, 2013	LTTP and Department data
North Carolina	Rutting and Bottom-up Cracking	Muthadi and Kim, 2008	LTTP and Department data

Location	Parameter	Author	Data
Ohio	Transverse Cracking and Rutting	Mahella et al., 2009	LTTP
Oregon	Rutting and Fatigue	Williams and Shaidur, 2013	Department data
Virginia	Rutting and Bottom-up Cracking	Smith and Nair, 2015	Department data
Wisconsin, Ohio and Michigan	Longitudinal and Alligator Cracking	Kang and Adams	Department data
Wyoming	Rutting, Fatigue and Thermal Cracking	Bhattacharya et al., 2015	LTTP/Non-LTTP
Texas	Rutting	Banerjee et al., 2009	LTTP
Ontario	Rutting and Bottom-up Cracking	Yuan et al., 2017	Department data

1.2.10 Summary

LTPP is a huge source of pavement performance data. These data include the design, construction, performance, climate and subgrade conditions. Many studies were conducted to better understand the performance of pavement in terms of different characteristics such as designs, pavement materials, and maintenance systems. Additionally, researchers have recommended the use of LCCA for different preservation techniques to determine the best options. LTPP dataset is very rich after North America's AASHTO road test, which are considered a pioneer for the development of new design guidelines. One such design method developed is the Mechanistic-Empirical Pavement Design Guidelines.

1.2.11 Potential GAP in LTPP

There are many different pavement research gaps available in the pavement system that can be addressed with the LTPP dataset. The following presents a summary of gaps that were identified during this research:

- Effect of traffic data input levels (level 1, 2 and 3) on Mechanistic-Empirical Pavement Design Guide outputs;
- Modeling and predicting truck loading patterns for pavement design;
- Evaluation of in-place air voids on the performance of asphalt pavements using LTPP data;

- Field versus laboratory volumetric and mechanical properties;
- Using multi-objective optimization to enhance calibration of performance models in the Mechanistic-Empirical pavement design guide;
- Applying long-term pavement performance data to pavement preservation roadmap;
- Traffic data sensitivity of hourly versus daily data in performance;
- Effect of multiple axles loading group on pavement performance.

In this thesis, the scope of the work is limited to the cement-treated pavement from the LTPP dataset and study its design factors from MEPDG and design of experiment analysis.

CHAPTER 2: METHODOLOGY

2.1 Introduction

As discussed in the previous chapter, the LTPP has performance data with cement stabilized layers. The dataset is divided into four different climatic zones, namely dry freeze, dry no freeze, wet freeze, and wet no freeze. This research aims to understand the performance of cement stabilized bases in pavements. The cement-treated bases are basically used in cement treated semi-rigid pavements and inverted pavement and cement treated semi-rigid pavements.

2.2 Cement Treated Pavement and Inverted Pavement

Flexible pavements follow a stress distribution pattern in which wheel load is distributed from the top layer to the bottom layer through grain-to-grain contact. The strong layer is used at the top, whereas the weak layer (i.e., subgrade) is used at the bottom. The critical locations of strains are at the bottom of the asphalt layer and on top of the subgrade. Some alternatives to the flexible pavement are the semi-rigid pavements, concrete pavements, and inverted pavement systems.

Semi-rigid cement-treated pavements are basically a transition pavement system between flexible and rigid pavements. The semi-rigid pavement system consists of subgrade, unbound/bound subbase, bound base treated with cement and an asphalt layer. The inverted pavement is defined as a pavement system in which the cement-bound layer supports a low strength unbound layer above it. In both inverted pavement and semi-rigid pavement, the cement stabilized layer is the main load-carrying layer. The layer gains strength as cement binds the aggregate particles together. The amount of cement used is generally conservative to limit the high heat of hydration and thus shrinkage cracking in the layers. The unconfined compressive strength (UCS) is the main strength criteria of this layer along with the durability. The UCS value is dependent on the cement content and Figure 2.1 suggests the UCS value used by a different agency for the design of cement-treated layers. In general, the UCS value is kept low to limit shrinkage cracking in the layer. In addition, gravel materials have been shown to be less prone to shrinkage cracking than fine materials.

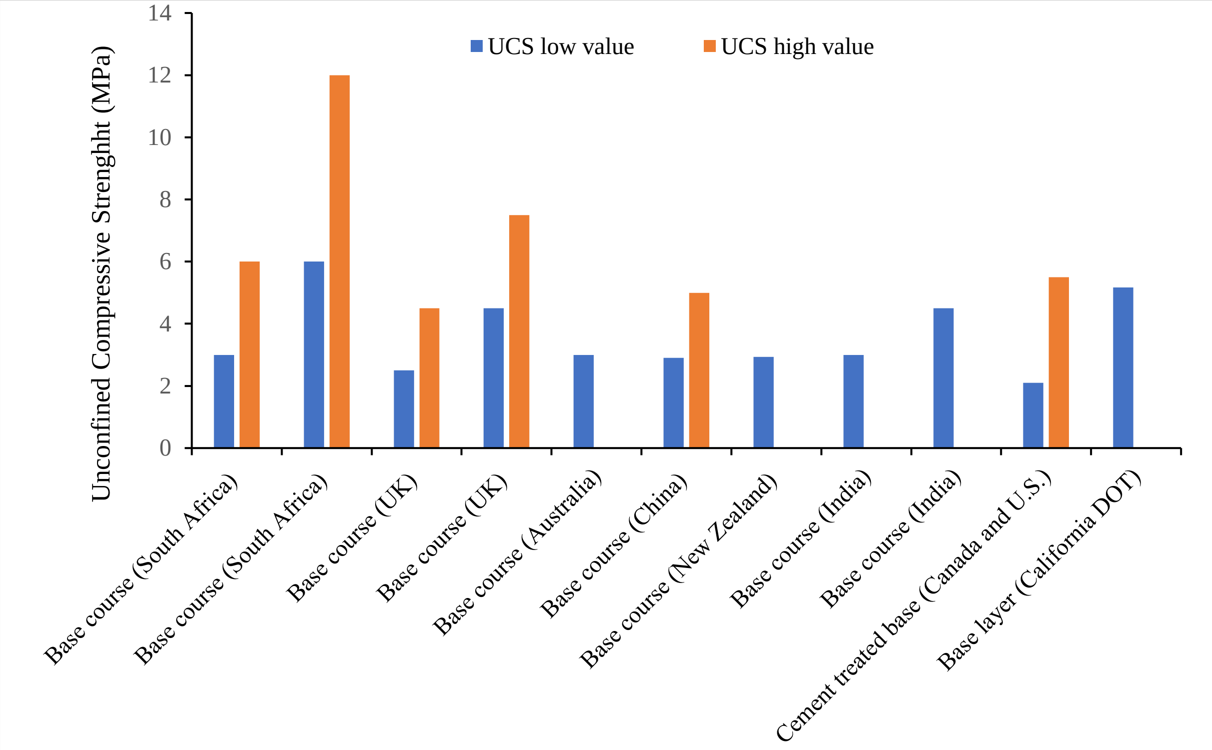

Figure 2.1: Unconfined compressive strength in cemented base layer

The main distress factors considered in the design of a semi-rigid pavement in North America are terminal IRI (in/mile), total rutting (all layers and subgrade), AC rutting, AC total fatigue cracking (bottom up+ Reflective) (%), AC bottom-up cracking (% lane area), AC thermal cracking (ft/mile), AC top-down fatigue cracking (ft/mile), and fatigue fracture of chemically stabilized layer (%) (MEPDG, 2010). However, in these pavements, the bottom-up cracking is generally within the safe limit, whereas reflective cracking and fatigue fracture of the chemically stabilized layer are among the main distress methods. In the past, aggregate interlayers, geotextiles, and chip seals were used to solve this problem. By placing an aggregate interlayer over a cement-treated base and asphalt concrete layer, inverted pavements are created. Figure 2.2 presents the schematic diagram of the inverted pavement system, in which cement stabilized layer cracking is arrested by the granular layer, geotextile, and chip-seal. However, in the present case, the main focus is only on the use of the granular layer. The unbound layer acts as a crack relief layer. It has a high bearing capacity and was sealed by an asphalt layer of 12 to 50 mm (Tutumluer, 2013). For inverted pavement, the critical location of stress/strain is at the bottom of the cemented layer (tensile strain) and at the top of the subgrade (compressive strain). Typically, in a flexible system, the aggregate layer is placed over the subbase layer and thicker HMA layers are placed on top of an aggregate layer, whereas an inverted pavement basically consists of a rigid cement-treated base layer, thin asphalt layer, and a sandwiched compacted aggregate layer between the two (Papadopoulos et al., 2016).

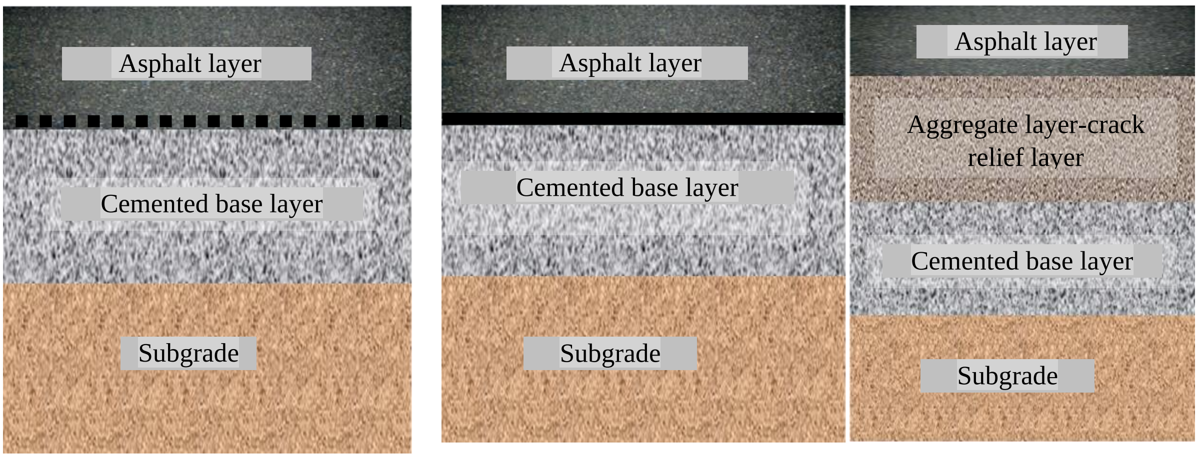

a) Chip seal between CTB and asphalt layer

b) Geotextile between CTB and asphalt layer

c) Inverted pavement system

Figure 2.2:Different cement stabilized pavement system to prevent reflective cracking (Wayne and David, 2004)

The stress distribution in an inverted pavement is different from the conventional pavement. For the conventional pavement system, the modulus value decreases from top to bottom according to the structural capacity of the layer. The modulus value distribution in the inverted pavement is different from that of a conventional pavement. The distribution of modulus in inverted pavement systems is like semi-rigid pavements. The strongest layer with the highest modulus in the inverted pavement is the cemented base layer. Papadopoulos and Santamarina recently reported that the use of a thin asphalt layer in inverted pavement acts as a membrane (seal coat for bottom layers) rather than a beam (Papadopoulos and Santamarina, 2017). The inverted pavement system has been more effective in protecting the subgrade layer as compared to the conventional pavement systems because of the stronger base layer (Santamarina and Papadopoulos, 2014). These types of pavement are also known as upside-down pavement, sandwich pavement, stone interlayer pavement and G1 base pavement (Lewis et al., 2012).

The Louisiana Department of Transportation studied the performance of a stone interlayer section with a cement stabilized base for a period of 20 years. After 20 years of service, a rut depth of 6.6 and 4.3 mm was reported for the stone interlayer and control section respectively. The average cracking density of 34.7% was found in the stone interlayer, whereas the control section has had a cracking density of 56.3%. In terms of the deflection test, the control section exhibited relatively stiffer behavior than the stone interlayer test section (Chen et al., 2014). A researcher in South African also studied the long-term performance of this type of pavement and the study showed the inverted pavement system performed at least equal to the conventional pavement system. The details of the findings can be found in this report (Litwinowicz and De Beer, 2013). From a construction viewpoint, the inverted pavement does not require special machinery and can be constructed using conventional techniques (Papadopoulos and Santamarina, 2017). Also, the cement stabilized materials can have 36% less thickness when compared with conventional pavement (Kumar and Sharma, 2013). In some design procedures, for example, in the South African system, it was recommended that the modulus value for inverted pavement's crack layer need be 450 MPa. To attain this modulus value, they used high-quality crushed rock also known as the G-1 base layer (Theyse et al., 1996). The aggregate layer in this pavement acts as a cushion between the asphalt and cemented layer and it reduces the risk of propagation of reflective cracking from the cemented layer to the asphalt layer (Barksdale and Todres, 1983; Papadopoulos et al., 2016). The aggregate layer which is near the load is in horizontal compression (Tutumluer and Barksdale, 1995). Also, the stiffness of the aggregate layer increases with an increase in load (Terrell et al., 2003). Many studies (Lewis et al., 2012; Halsted C, 2006) reported that the inverted pavement is a cost-effective system because it uses a reduced thickness of the HMA layer.

2.3 Methodology

The methodology utilized in this study is divided into two phases.

Phase 1

- Initially, the dataset from the LTPP was extracted and cement treated base layer sections were studied including the lower and higher values of pavement thickness, subgrade type, moisture, and temperature of the sections.
- Thereafter, different factors representing the pavement design were considered and MEPDG software was used to study the response of the input parameters.
- Finally, the response generated from MEPDG was used in the Design of Experiment software and main factors affecting the design of pavement were studied.

Phase 2

- This phase identifies the inverted pavement system as a means of mitigating failures found in the MEPDG study, such as reflective cracking.
- Similar to phase 1, a parametric study was taken up to study the factors affecting the design of inverted pavement using CROSSPAVE software application.
- Finally, the response generated from software application was used in the Design of Experiment and main factors affecting the design of pavement were studied.

CHAPTER 3: LTPP DATA AND MEPDG ANALYSIS

3.1 Scope and Objective of this Chapter

The scope of this chapter is to better understand the LTPP sections for the different pavement design parameters. Variations of factors such as layer thickness of asphalt and cement-treated base (CTB), subgrade type, traffic, temperature, and moisture were considered from LTPP sections. A few other notable parameters are unavailable in the LTPP sections, such as variation of speed and some properties of CTB such as elastic modulus, modulus of rupture, and crack spacing. These parameters came from input values of MEPDG program. The goal of this chapter is to conduct a comprehensive study for different distresses occurring in the cement-treated pavement for different climate zones.

3.2 Description of LTPP Cement Treated Sections and MEPDG Input

There is a total of 144 sections in the LTPP with bound bases in 37 different regions of the United States and Canada. The dataset contains different types of bound bases, namely cement base and asphalt base. However, the scope of this work is limited to the cement-treated pavement only. The different cement-treated sections available in the pavement design are given below in Appendix I.

Furthermore, the LTPP sections contain bound bases together. The above table shows the cement treated bound layer sections. Similarly, the asphalt bases bound sections are available and can be classified based on different subgrade conditions as given below:

- Experiment type- *asphalt on cement-treated bases;*
- Surface type- *asphalt layer;*
- Base type- *Cement-treated base;*
- Subgrade type- *fine grained; coarse grained*;
- Climatic region- *all climate considered.*

The LTPP sections on coarse grained and fine-grained soil are shown in Table 3.1 and Table 3.2.

Table 3.1: LTPP Section on coarse grained soils

State	**Cement bound layer section number**
California	8
Georgia	4
Louisiana	1
Mississippi	4
New Jersey	1
North California	2
North Dakota	1
Virginia	2
Wyoming	8
Total	**31**

Table 3.2: LTPP Section on fine grained soils

LTPP State	**Cement bound layer section number**
Arkansas	2
California	3
Maryland	2
Mississippi	3
North Carolina	2
Oklahoma	3
Oregon	1
Tennessee	2
Texas	5
Virginia	2
Alberta	1
Total	**26**

A major benefit of the LTPP dataset is that all the sections have been classified systematically and any set of factors/parameters in the pavement design can be retrieved either separately or with other parameters. Similarly, the criteria of the wet and dry regions are based on the precipitation received annually. The threshold limit for distinction in wet and dry regions in the LTPP dataset is 508 mm/year. Any value below this limit is considered dry and above this limit is considered a wet region in the LTPP. The schematic diagram for precipitation at one LTPP sections in Wyoming is given in Figure 3.1 and similarly, the freezing index is shown as an example in Figure 3.2.

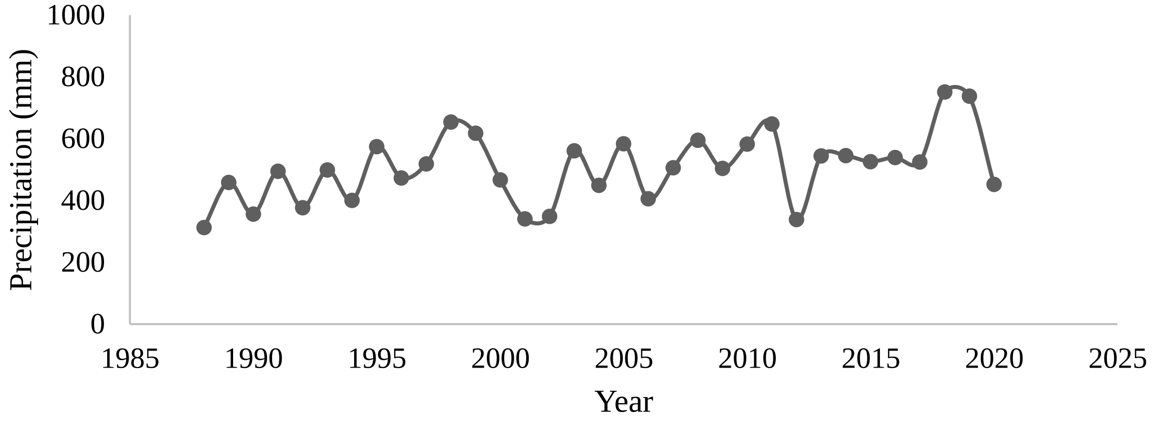

Figure 3.1: Precipitation variation with time in Wyoming

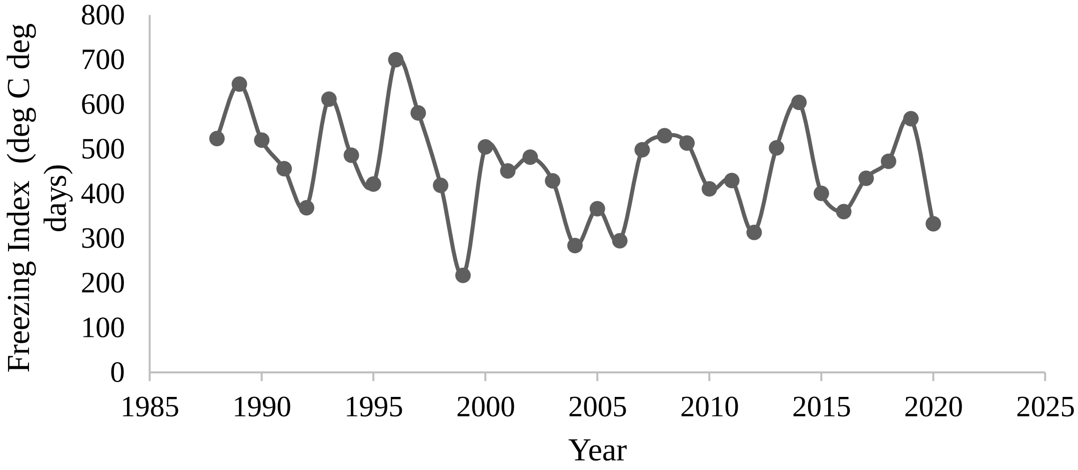

Figure 3.2: Freezing Index variation with time in Wyoming

The scope of the present research is limited to the analysis of cement treated base layers in the LTPP dataset and other sources. The schematic diagram for the cement treated base layer from the LTPP dataset is presented in Figure 3.3.

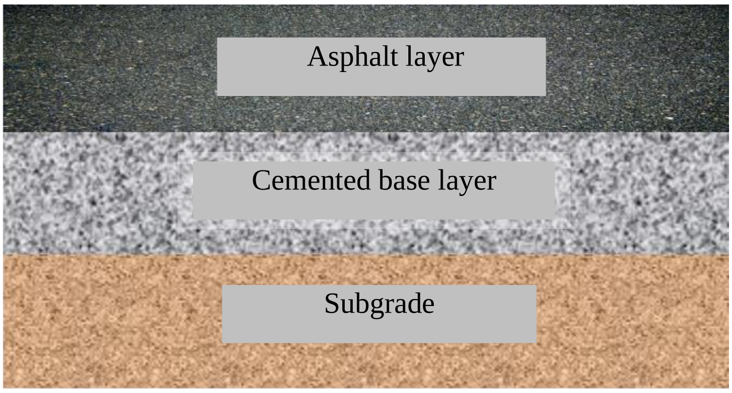

Figure 3.3: Cemented treated base semi rigid pavement

The cement treated base layer is treated with cement depending on the strength requirement. Normally, unconfined compressive strength (UCS) is the criteria for the design of the cement in the cement treated layers. However, to reduce the shrinkage issue in the cement treated layers, the cement content is kept low, so the high rate of the heat of hydration can be mitigated. The schematic representation of UCS values for cement treated sections in the LTPP dataset is given in Figure 3.4. Unfortunately, the cement content data could not be located in the dataset to better represent the UCS and cement content relation. However, a researcher has quoted the cement content values back in the year 2006 (Hanson, 2006), but that could not be verified as the cement content reported in some of the sections in the literature is very high and the data extracted from the LTPP dataset does not include cement content percentages. Therefore, it is not reported here.

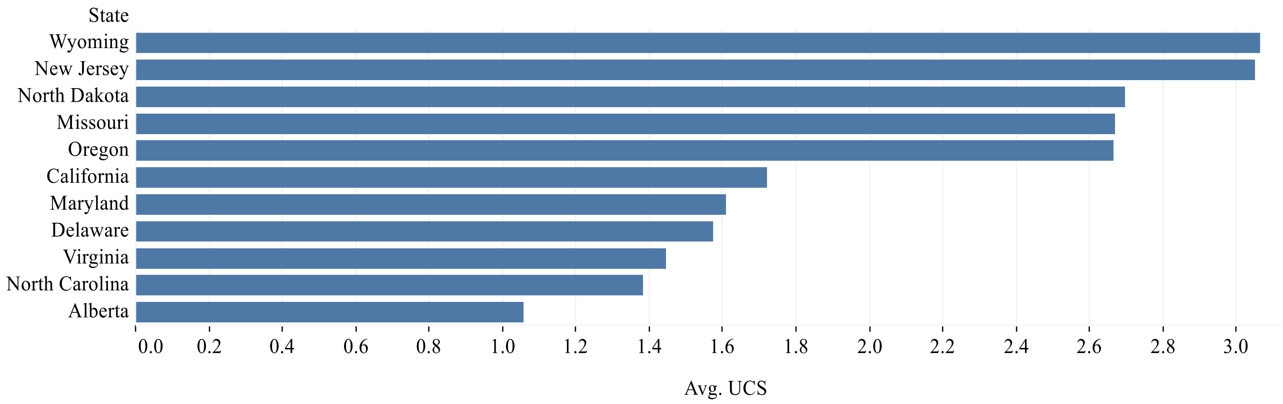

Figure 3.4: Unconfined compressive strength of the different sections in LTTP dataset

The traffic data in terms of annual daily truck traffic is available for the sections in LTPP. Traffic is one of the important parameters for the design of any type of pavement. The schematic chart for traffic is shown in Figure 3.5.

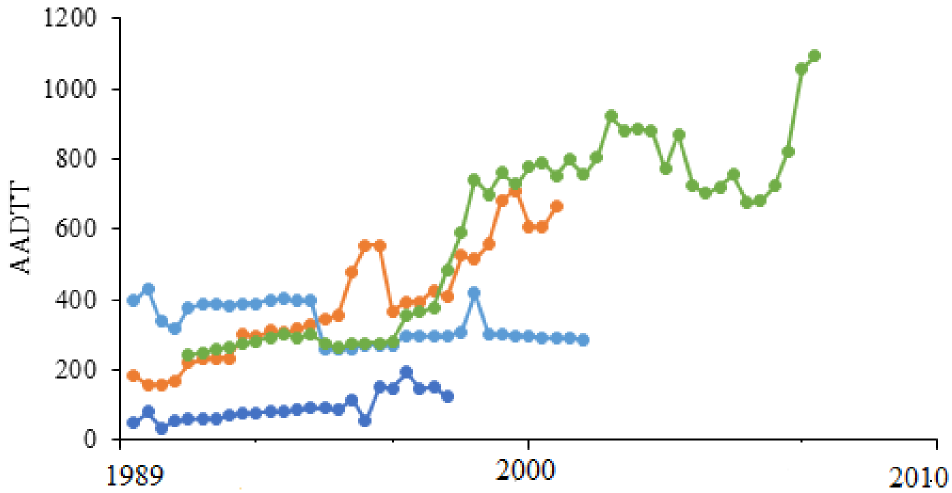

Figure 3.5:Traffic variation with time in some CTB sections

The LTPP sections are classified as Rural Minor Arterial (10 sections), Rural Principal Arterial others (28 sections), or Rural Principal Arterial - interstate (7 sections) (Hanson, 2006). The traffic levels in these sections is not very high.

Similar datasets are available for the all-other sections for the bound bases from General Pavement Section-2. The datasets for cement treated base layer thickness and asphalt layer thickness is given in Figure 3.6.

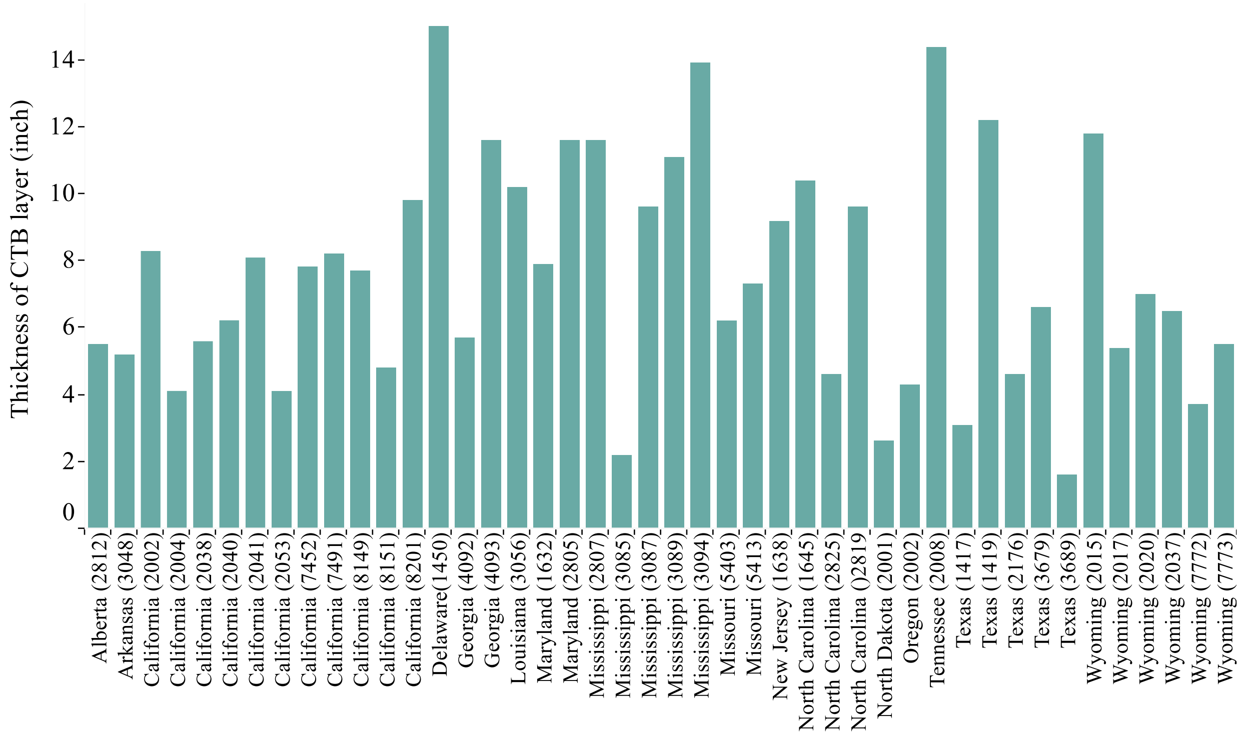

Figure 3.6:Thickness of cement treated layer (inch) of the different sections in LTTP

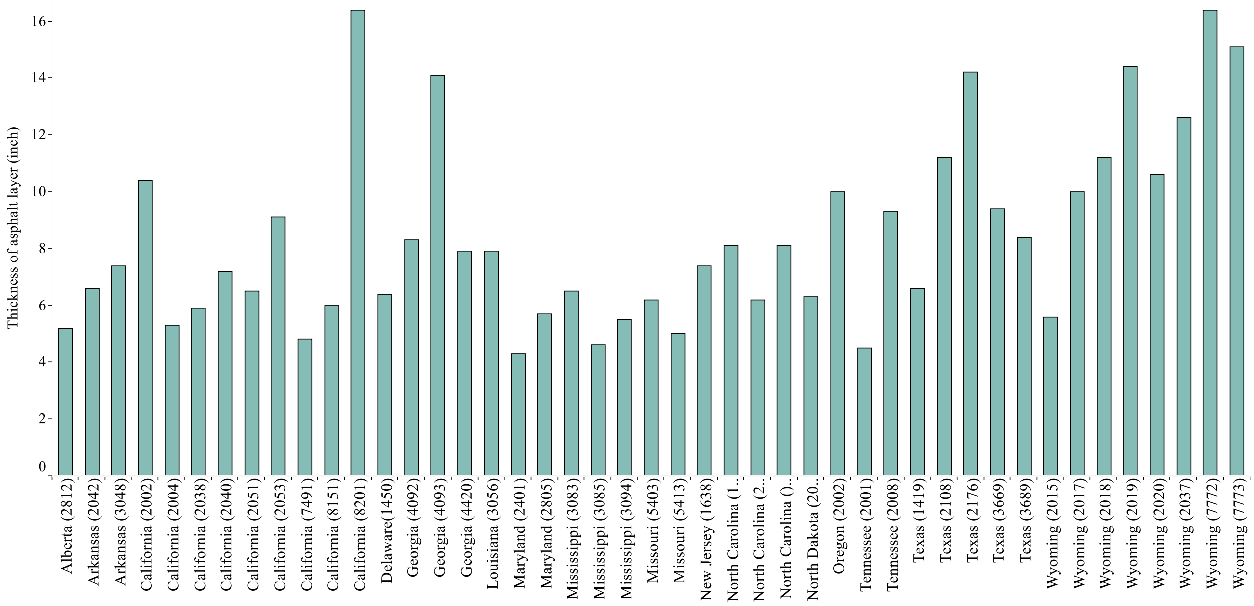

Figure 3.7:Thickness of asphalt layer (inch) of the different sections in LTTP

Also, the data for distress such as cracking, rutting and International Roughness Index (IRI) is available for all the sections. A schematic picture of the distresses in the Wyoming section is given in Figure 3.8.

Figure 3.8: CTB section on Wyoming observed to be in distress (LTPP, 2018)

It is important to recall that the LTPP sections are divided according to the type of different parameters. Two such important parameters in the design of pavement are moisture and temperature. The moisture is either wet or dry and the temperature is either freeze or no freeze. The sections with combination of these states are given below. Some states have two types of weather conditions in the LTPP dataset.

- **Dry No Freeze** - Arizona, Colorado, Nevada, New Mexico, Oregon, Texas and California.
- **Dry Freeze** - Wyoming, Utah, Idaho and Nevada.
- **Wet Freeze** - Colorado, Connecticut, Delaware, Illinois, Indiana, Iowa, Kansas, Maryland, Michigan, Minnesota, Missouri, Montana, Nebraska, Nevada, New Jersey, New York, North Dakota, Ohio, Oregon, Pennsylvania South Dakota, Utah, Vermont, Virginia, Washington, West Virginia, Wisconsin, Wyoming, Alberta, British Columbia, Manitoba, New Brunswick, Ontario, Prince Edward Island, Saskatchewan, and Quebec.
- **Wet No Freeze** - Alabama, Arizona, Arkansas, California, Delaware, Florida, Georgia, Kansas, Louisiana, Maryland, Mississippi, Missouri, New Jersey, North Carolina, Oklahoma, Oregon, Puerto Rico, South Carolina, Tennessee, Texas and Virginia.

There are different factors that affect the performance of cement-treated pavements, such as climatic conditions (temperature and moisture), traffic (AADTT), speed of vehicle, asphalt thickness, cement-treated base thickness, elastic modulus, crack spacing, presence of subbase layer, and modulus of rupture. These factors are studied here using the factorial design in the design of experiment. Only subbase layer thickness is not considered in the present case because the available majority of the LTPP sections do not have a subbase layer. Also, the subbase thickness is not very sensitive to the design of the pavement performance in comparison to the modulus, temperature and load levels. Also, the temperature cycles per day were the main reason for the reflective cracking in the cement stabilized base pavement (Su et al., 2017).

Table 3.3 shows the factors and their level values based on the LTPP and MEPDG recommended values. These factors were found to affect the design of cement-treated pavements as suggested in the published literature.

Table 3.3:Factors for MEPDG Analysis and Inputs

S.No	Factors	Low	High	Comment
1	Subgrade	Fine- A-6	Coarse- A-1-a	Soil type- Coarse and Fine type classification Soil selection based on LTPP dataset
2	Temperature,	Freeze	No Freeze	Representative sections from LTPP dataset are chosen from the available sections.
3	Moisture	Dry	Wet	
4	Traffic, AADTT	200	1500	Low and intermediate value of traffic was selected to represent the effect of traffic
5	Crack Spacing	10 ft	25 ft	Parameter in MEPDG
6	Speed	20 kmph	60 kmph	Slow- and fast-moving vehicle
7	Asphalt thickness	40 mm (1.57 inch)	300 mm (11.8 inch)	Representative thickness is chosen from LTPP asphalt layer variation among different sections.
8	Cemented base layer thickness	110 mm (4.33 inch)	320 mm (12.59 inch)	Representative thickness is chosen from LTPP asphalt layer variation among different sections.
9	Elastic Modulus	1.5 million psi	2 million psi	Minimum and intermediate elastic modulus value in MEPDG
10	Modulus of rupture	150 psi	300 psi	Minimum and intermediate value in MEPDG

The values of each of the parameters were carefully selected to represent the wide range of datasets in the LTPP. The minimum elastic modulus of cement--treated layer is selected in the MEPDG design. But from a research perspective, it would have been ideal if there was a mean to change the elastic modulus since it is directly dependent on the compressive strength of the layer. There were other parameters in the pavement design such as load transfer efficiency, unit weight, and poisson's ratio that can affect the design; however, they were not considered in the present work due to literature recommendations (Hossain et al., 2017), and reason for which is discussed below.

- The default value of load transfer efficiency (LTE), thermal conductivity and heat capacity is recommended in MEDPG. The LTE parameter variation of 50% to 90% did not produce any difference in predicted distresses.
- Default values for unit weight and Poisson ratio could be assumed as 150 pcf and 0.2, respectively.
- Modulus of elasticity value of 1.5 million psi is generally recommended.

- There is no effect of default transverse crack spacing on any other predicted distresses except for transverse reflective cracks irrespective of CTA modulus.
- The 7-day unconfined compressive strength of 600 to 800 psi would increase over time; therefore, a value of 200 psi for the modulus of rupture would be reasonable for design purposes with consideration of the high variability in the field-measured strength and stiffness. In our case, a low value of 150 psi and a high value of 300 psi is chosen.

Figure 3.9 shows the schematic diagram of the MEPDG input screen for the design of semi-rigid pavement and Figure 3.10 shows the different options for the input of the data in the software.

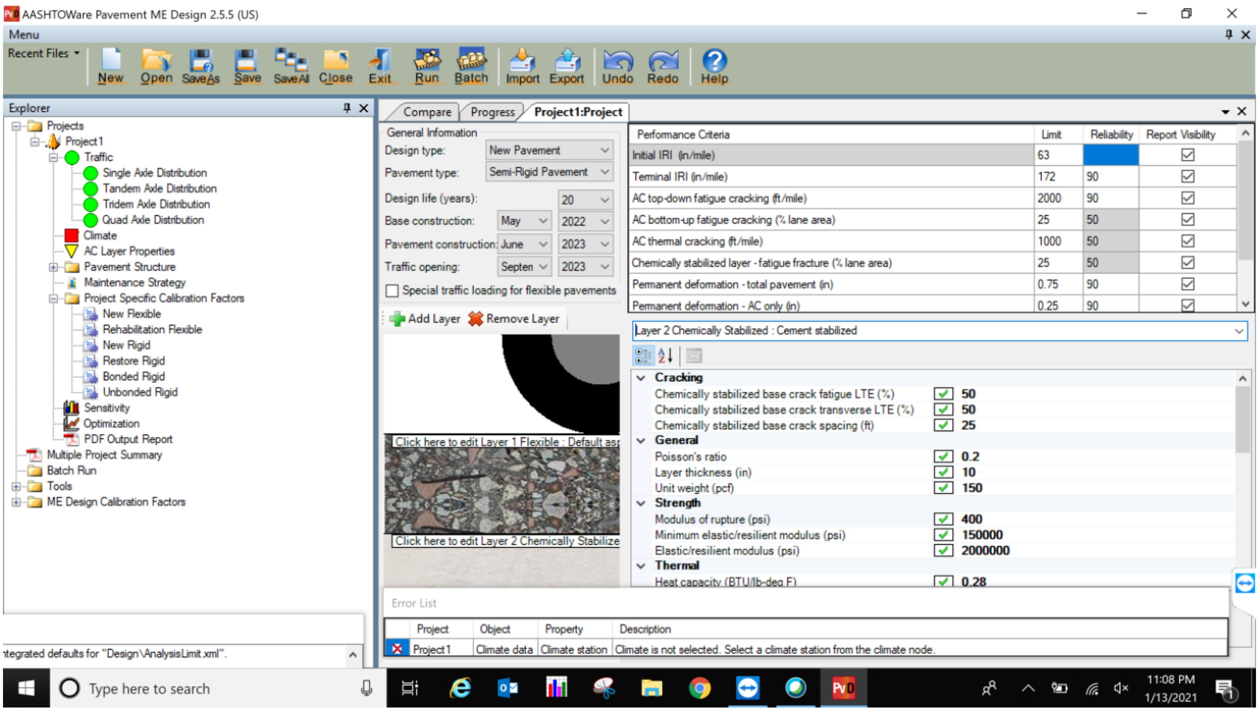

Figure 3.9:Design page of MEPDG software for the pavement system

3.3 Performance Criteria selected for the design of pavement

Performance verification forms the basis of the acceptance or rejection of a trial design evaluated using ME Design. The design procedure is based on pavement performance and therefore, the critical levels of pavement distresses tolerated by agencies (different departments of transportation) at the selected level of reliability needs to be specified by the user. The distress types considered in the design of a semi-rigid pavement are terminal IRI (in/mile), total rutting (all layers and subgrade), AC rutting, AC total fatigue cracking (bottom up+ Reflective) (%), AC bottom-up cracking (% lane area), AC thermal cracking (ft/mile), AC top-down fatigue cracking (ft/mile), and fatigue fracture of chemically stabilized layer (%). Table 3.4 shows the threshold value of the distresses considered in the design.

Table 3.4: Distress criteria used in the current pavement design using MEPDG

Output distress	Distress limit	Reliability Criterion Used
Terminal IRI (in/mile)	172	90
Total Pavement Deformation (inch)	0.75	90
AC Total Fatigue Cracking (bottom up+ Reflective) (%)	25	90
AC Total Transverse Cracking (Thermal + Reflective)(%)	2500	90
AC Bottom-up Cracking (% lane area)	25	50
AC Thermal Cracking (ft/mile)	1000	50
AC Top-Down Fatigue Cracking (ft/mile)	2000	90
AC Permanent Deformation (inch)	0.25	90
Fatigue fracture of chemically stabilized layer (%)	25	-

- Performance Criteria: Table 3.5 presents the list of performance indicators used for the design of semi-rigid pavement. This individual distress is set to the desired level of reliability.
- Limit: Table 3.5 shows the desired limit for each performance indicator. For example, IRI desired limit is 172 in/mile. This is the threshold values of the performance indicators used in the design. Similar values are indicated for other distresses in Table 3.5.
- Reliability: The pavement reliability limits are shown in Table 3.5. The reliability concept deals with the probability at which the predicted distresses and smoothness will be less than the limits over the design period.

- Terminal IRI (in./mile): The terminal IRI is the maximum limit for IRI distress upto which the defined IRI distress is safe. Above this limit, the input parameter should be relooked into to obtain the value within the limit.
- AC top-down fatigue cracking (% lane area); AC bottom-up fatigue cracking (% lane area), AC thermal cracking (ft./mile); Chemically stabilized layer fatigue fracture (percent); Permanent deformation - total pavement (in.); Permanent deformation - AC only (in.); AC total transverse cracking: thermal + reflective (ft./mile):

  The distresses listed above are some of the performance parameters used in the design of semi-rigid pavement. The limit and reliability controls for this criterion allows for the not-to-exceed limit for surface-initiated fatigue cracking at the end of the design life at a specified reliability level to be defined.

Input parameter used for the design of cement stabilized layer

Some of the input parameters used in the design of cement-treated base layer of the semi-rigid pavement is chemically stabilized base crack spacing (ft), chemically stabilized base crack transverse LTE (%), chemically stabilized base crack fatigue LTE (%): layer thickness (in), poisson’s ratio, unit weight (pcf), elastic/resilient modulus (psi), minimum elastic/resilient modulus (psi), modulus of rupture (psi), thermal conductivity (BTU/hr-ft-deg F), and heat capacity (BTU/lb-deg F). As previously discussed, elastic modulus, modulus of rupture, thickness, and cracking spacing are an important parameter which affects the performance of the pavement. The other parameter listed before such as poisson’s ratio, unit weight, thermal conductivity is input parameters which do not affect the output performance of the pavement. These parameters are chosen as the default values suggested by the MEPDG software application and the suggested values are reasonable and in agreement with the published literature.

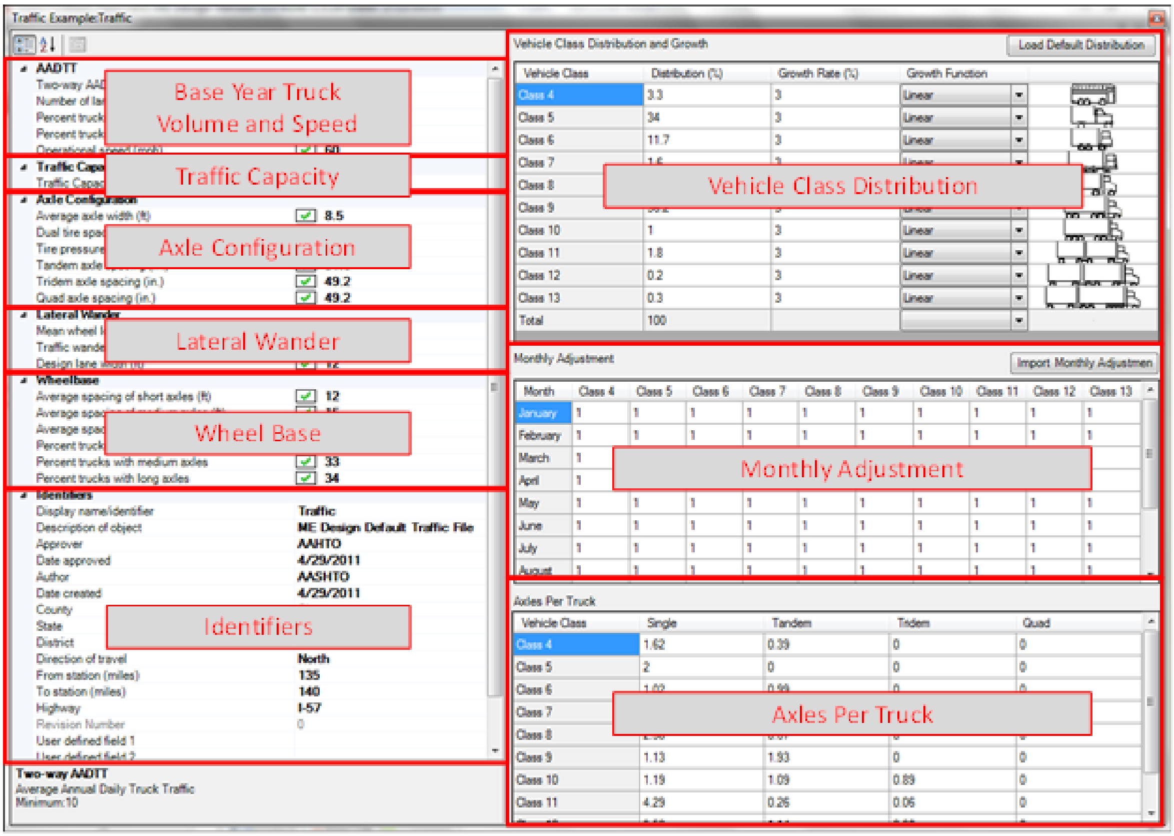

Figure 3.10: Different Parameters used in the pavement design (Hossain et al., 2017)

The equations used for the performance of pavement in MEPDG are given in Appendix II:

3.4 Motivation for Design of Experiments (DoE) Methodology in Pavement Design

In the pavement research area, much research has been focussed on changing one parameter at a different level and studying its effect on the performance of the pavement. For example, the performance of pavements is affected by the thickness. There is a significant benefit of considering the DoE over studying one factor at a time. In many cases, the use of changing one factor at a time does not lead to the optimum solution and results depend on the starting point of the solution. Alternatively, the DoE can consider many factors simultaneously and more precise result can be obtained in fewer trials (Kennedy & Krouse 1999). The application of DoE is in use in many other fields of engineering, and there are many notable uses of DoE in pavement materials (Rooholamini et al., 2018; Nassar et al., 2016; Moghaddam et al., 2015; Cai et al., 2013). The use of DoE especially to comprehensively study the factors affecting pavement design, has not been studied before with data from LTPP and MEPDG simultaneously. Table 3.6 (given in the appendix) presents the input matrix generated using the factors in DoE.

The temperature data and moisture data for the sections with dry no freeze, dry freeze, wet no freeze, and wet freeze were chosen from LTPP sections. Four sections are chosen from the LTPP dataset representing dry no freeze (New Mexico), dry freeze (Wyoming), wet no freeze (Tennessee), and wet freeze (Minnesota). The asphalt binder grade was chosen as the input parameter in the analysis. However, the binder was selected based on the local climatic conditions. The LTTPbind software application was used to calculate the local binder grade based on the climatic condition. The binder grade required for Wyoming, Tennessee, New Mexico, and Minnesota are respectively PG 52-28, PG 52-16, PG 52- 10 and PG 52-28. The responses of pavement performance for each of these zones are given in Appendix II (Tables 1-5).

The AC bottom-up fatigue cracking was another response on the pavement design using MEPDG, but from MEPDG software application the total cracking (%) was 0. Therefore, it can be concluded that bottom-up fatigue is not an issue in the design of cement-treated base pavement design. A major reason for this may be due to the strong cement layer underneath the asphalt layer. This prevents bending of the asphalt that propagates cracks. Furthermore, the IRI (in/mile), the total permanent deformation (in), fatigue cracking (bottom up- reflective), transverse cracking (%), asphalt thermal cracking (ft/mile), asphalt permanent deformation (in), and top-down cracking are reported in Figure 3.11-17 below. The limit for each of these parameters has been marked on the Figures to better represent the output of these design factors.

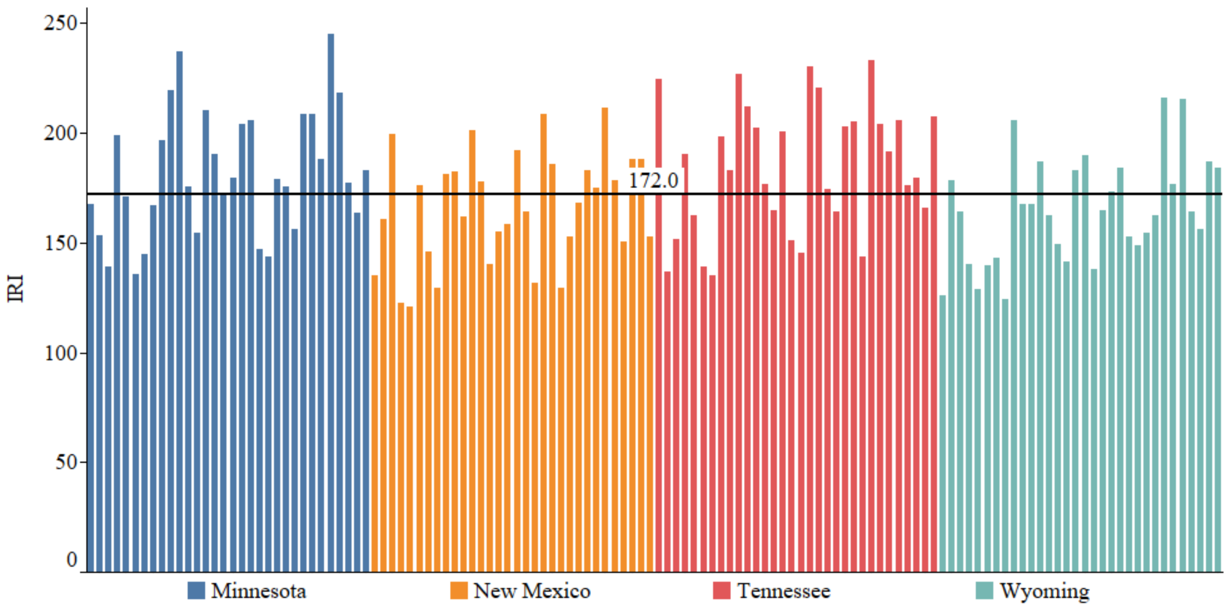

Figure 3.11:Pavement Response, IRI (in/mile) based on the different input factors through MEPDG

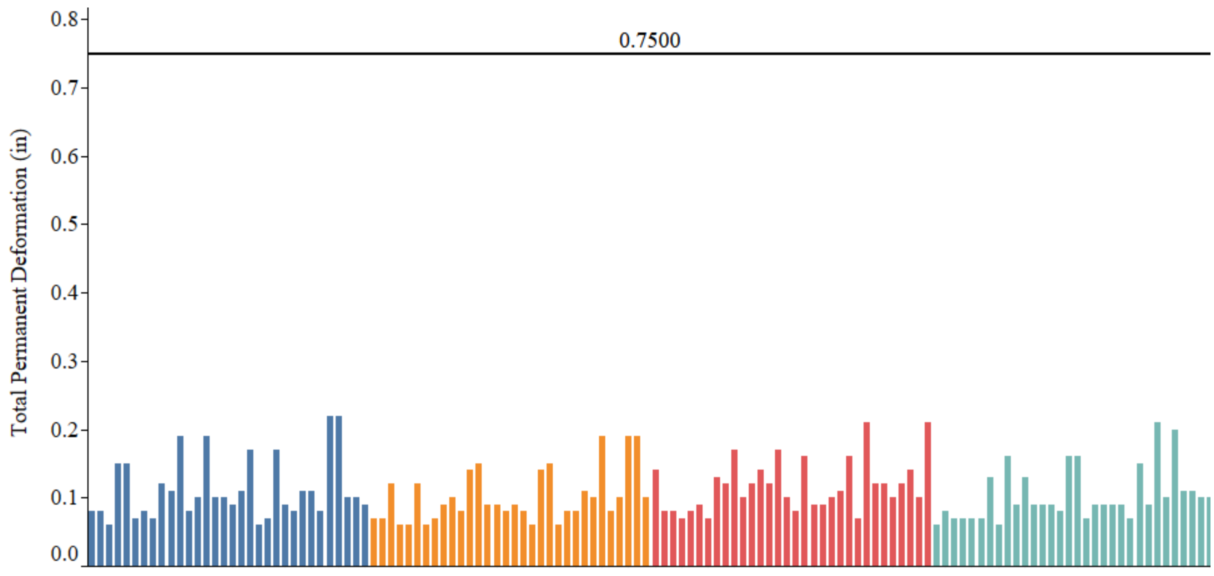

Figure 3.12:Pavement response, total permanent deformation (in) based on the different input factors through MEPDG

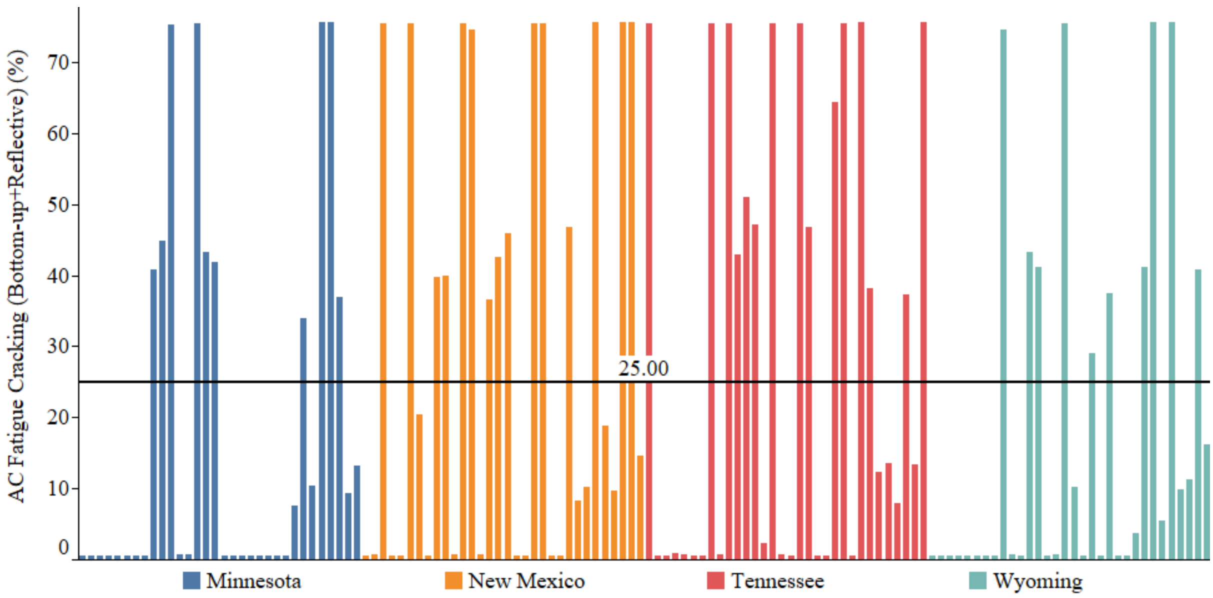

Figure 3.13:Pavement response, fatigue cracking (bottom Up + reflective) based on the different input factors through MEPDG

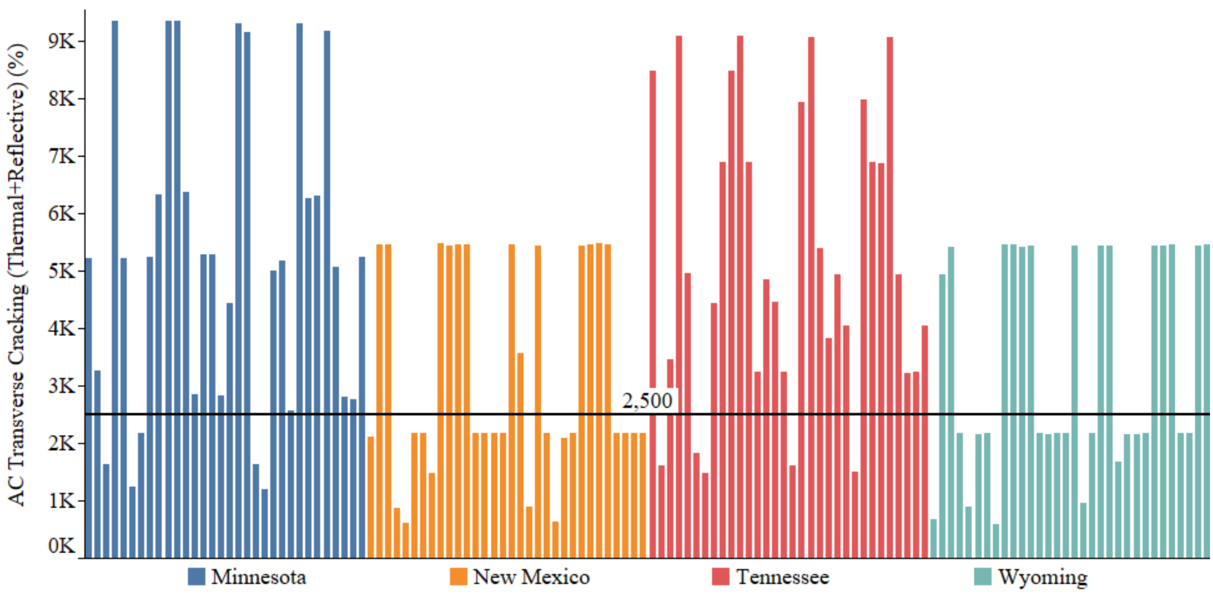

Figure 3.14:Pavement response, transverse cracking (%) based on the different input factors through MEPDG

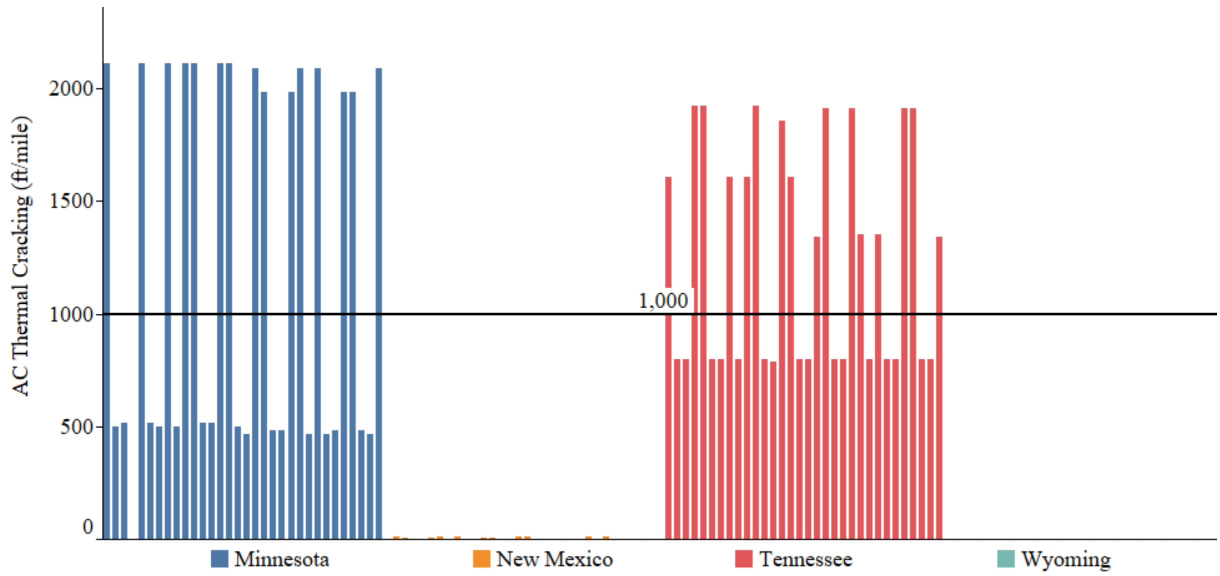

Figure 3.15:Pavement response, asphalt thermal cracking (ft/mile) based on the different input factors through MEPDG

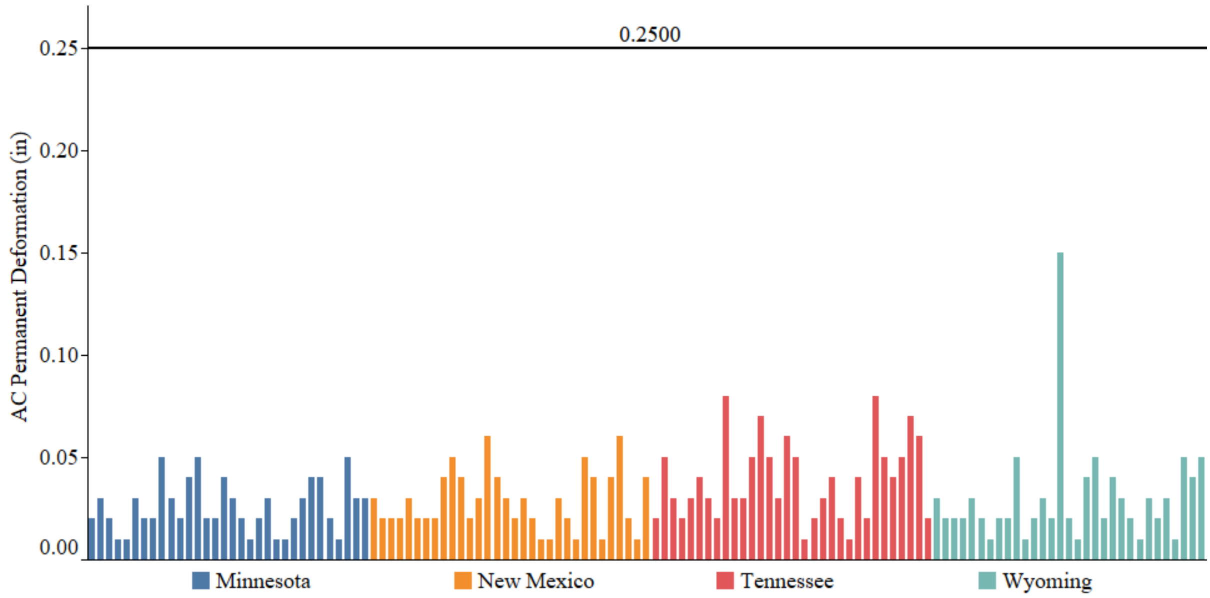

Figure 3.16: Pavement response, asphalt permanent deformation (in) based on the different input factors through MEPDG

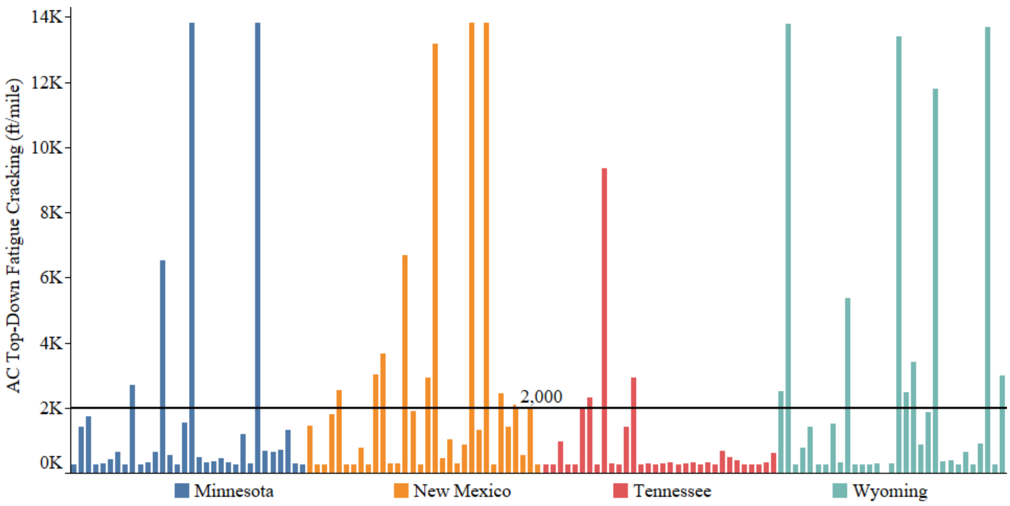

Figure 3.17: Pavement response top-down cracking based on the different input factors in MEPDG

The AC total fatigue cracking consists of bottom-up fatigue cracking and reflective cracking. However, the asphalt bottom-up cracking in the cement-treated base is negligible and approaches zero in the MEPDG analysis. Therefore, it can be concluded that reflective cracking is the most common cause of AC total fatigue cracking. This is one of the most common causes of failure in cement-treated base/semi-rigid pavement. According to the analysis of the design of the experiment, except for the traffic, crack spacing, and elastic modulus, other factors do affect the reflective cracking in pavement such as asphalt thickness, cement-treated base layer thickness, speed, subgrade type, and temperature. Figure 3.18 shows the schematic way the reflective cracking affects the pavement.

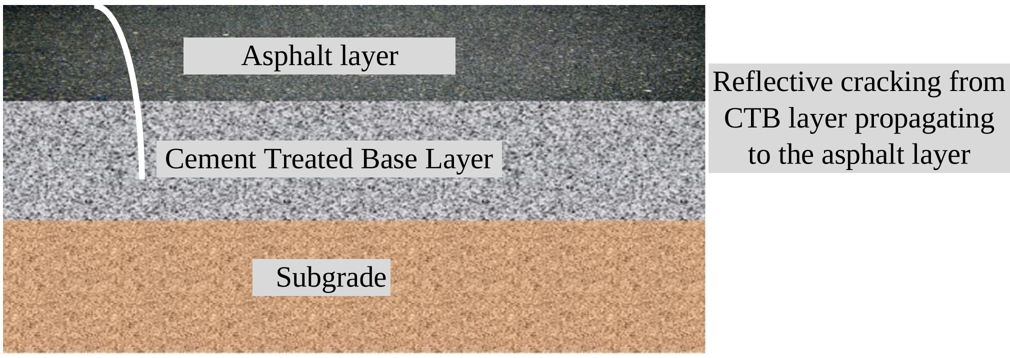

Figure 3.18: Crack propagation from CTB Layer to asphalt layer

One common way to discontinue the reflective cracking from cement-treated base layer to the asphalt layer is to add an aggregate interlayer. The aggregate interlayer absorbs the crack arising from cement treated base layer. Other methods such as fabric geotextile or the application of seal on the cement-treated layer are also prevalent. However, the addition of aggregate interlayer will lead to the generation of vertical compressive strain in the layer as this layer is placed between two strong layers namely asphalt and cement treated base layer and will eliminate the tensile strain in the layer as given in Figure 3.19 below.

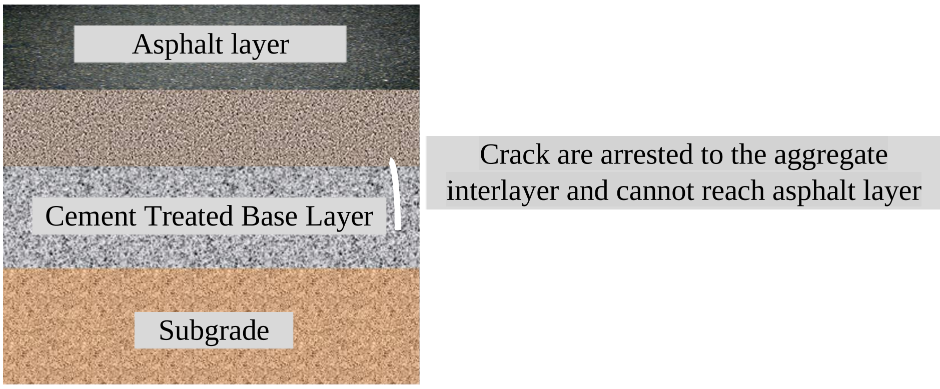

Figure 3.19: Arrest of crack in aggregate interlayer in inverted pavement

The above pavement system in literature is named an inverted pavement system. This type of design is mostly used in South Africa, and some European Countries under the title of up-side down pavement. In the U.S. some states have tried this type of pavement based on the South African experience and some states name this pavement system as stone interlayer pavement. Unfortunately, the same design software, MEPDG, used for the cement-treated base layer pavement does not work for the inverted pavement. Any structure as shown in above Figure 3.19, is not supported in the MEDPG software. There were some proposals during the last five years to conduct research on this pavement in the U.S., however, the present research does not include that literature as a result is still not in the public domain. The factors affecting this pavement design system have been studied with the help of different pavement design software, which can accommodate this pavement system.

3.5 Summary

The semi-rigid pavement system from the LTPP dataset was studied and presented in this chapter. The summary of this chapter is as follows:

- Different factors affecting the design of pavement were studied and finalized based on the LTPP data and MEPDG. The pavement response in terms of distresses was analyzed and presented in this chapter.
- For all the climatic regions, the cement-treated sections are safe in rutting (asphalt and total permanent deformation).
- The asphalt fatigue (bottom-up + reflective) and asphalt transverse cracking (thermal + reflective) is the main cause of distress in the pavement.
- Since bottom-up cracking is almost close to zero and thermal cracking is only found in two climatic regions of Minnesota and Tennessee. Reflective cracking appeared to be a common problem for all climatic regions, however, a solution to overcome reflective cracking has been proposed in terms of an inverted pavement system.

CHAPTER 4: DESIGN OF EXPERIMENT ANALYSIS

4.1 Scope and Objective of this Chapter

The previous chapter discussed the semi-rigid pavement performance using MEDPG. The major distress occurring due to the use of semi-rigid pavement is reflective cracking apart from other types of distress. Different solutions have been proposed previously and an inverted pavement system has been selected and studied in overcoming such problems. The design of experiment software (DoE) was used for this purpose.

The overall goal of this chapter is to determine the significant factors that affect the distress for both cement-treated section and inverted pavement system and develop a regression model to predict the same.

4.2 Phase 1: Factors Affecting Design of Cement Treated Base

Different output namely, terminal IRI (in/mile), total rutting (all layers and subgrade), AC rutting, AC total fatigue cracking (bottom up+ reflective) (%), AC thermal cracking (ft/mile), and AC top-down fatigue cracking (ft/mile) are selected as response variable. Each of the response parameters are used in design of experiment. A separate model is proposed for each response. Each model consists of assumptions, ANOVA for the significant factors, fit statistics, design equation and optimization of performance parameters wherever applicable.

4.2.1 Total permanent deformation

The response parameter total permanent deformation was studied as the function of different input parameters. As the most significant factor affecting pavement distresses, permanent deformation has been reported here. The assumption of the model is checked and is met in term of normality plot of the residuals, residuals versus predicted, residuals versus run, and box-cox transform. The box- cox transformation suggests the inverse square root transformation.

From the Figure 4.1, it is clear that all the assumptions of the model are met. The ANOVA for the model is given in Table 4.1.

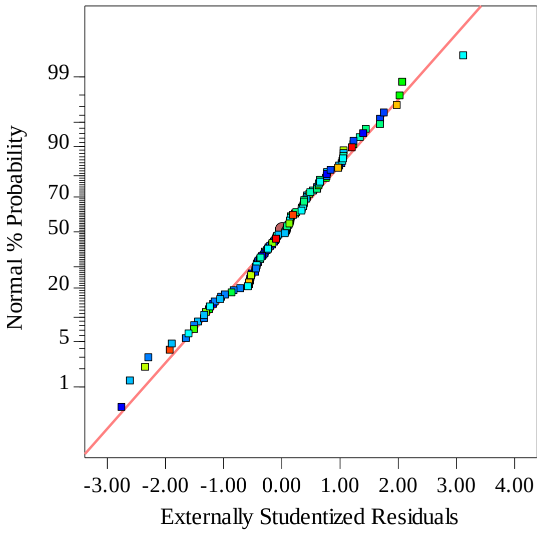

a) Normal plot of residuals for dataset

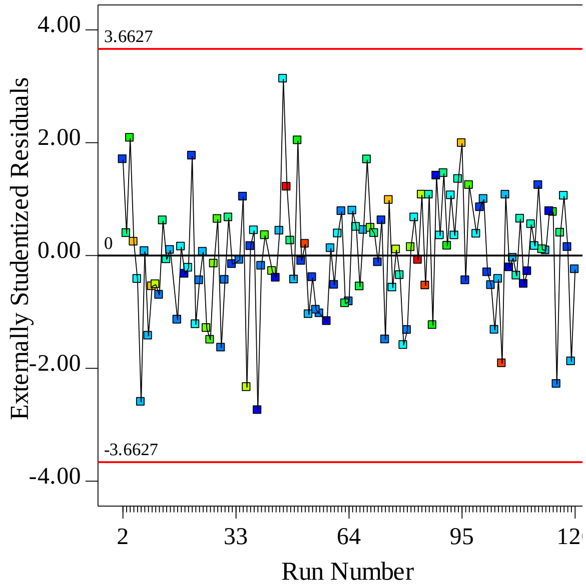

b) Residuals versus run residuals for dataset

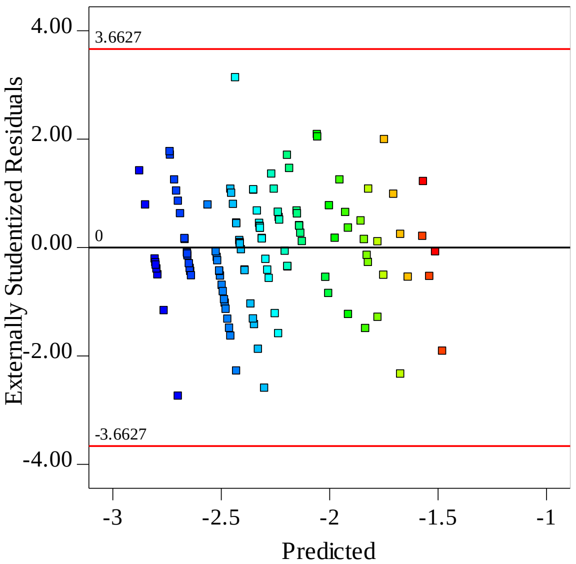

c) Residuals versus predicted for dataset

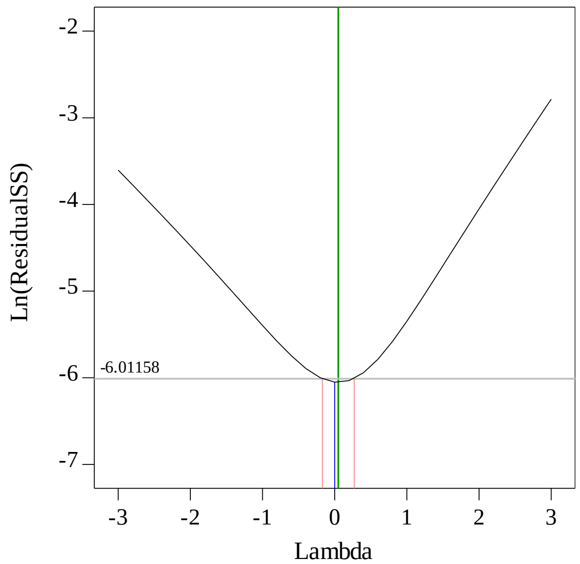

d) Box-Cox Plot for power transform

Figure 4.1: Assumption of the model for the response total permanent deformation

Table 4.1: ANOVA for response (Total Permanent Deformation)

Source	Sum of Squares	df	Mean Square	F-value	p-value	% Contribution
Model	30.96	13	2.38	115.34	< 0.0001	
A-Asphalt thickness	7.58	1	7.58	367.37	< 0.0001	22.9
B-Cement thickness	10.96	1	10.96	530.86	< 0.0001	33.13
C-Modulus of rupture	0.1088	1	0.1088	5.27	0.0236	0.33
E-Speed	0.3498	1	0.3498	16.95	< 0.0001	1.05
G-Traffic	6.47	1	6.47	313.53	< 0.0001	19.57
H-Subgrade	1.22	1	1.22	59.23	< 0.0001	3.69

Source	Sum of Squares	df	Mean Square	F-value	p-value	% Contribution
J-Temperature	0.8855	1	0.8855	42.9	< 0.0001	2.67
AB	1.92	1	1.92	93.21	< 0.0001	5.818
AG	0.488	1	0.488	23.64	< 0.0001	1.475
AH	0.1666	1	0.1666	8.07	0.0054	0.504
BE	0.1984	1	0.1984	9.61	0.0025	0.599
EJ	0.2210	1	0.2210	10.71	0.0014	0.668
HJ	0.1908	1	0.1908	9.25	0.0030	0.577
Residual	2.23	108	0.0001			
Cor Total	33.18	121				

The Model F-value of 187.97 implies the model is significant. There is only a 0.01% chance that an F-value this large could occur due to noise**.** P-values less than 0.0500 indicate model terms are significant. In this case, A, B, C, E, G, H, J, AB, and AH are significant model terms. Values greater than 0.1000 indicate the model terms are not significant.

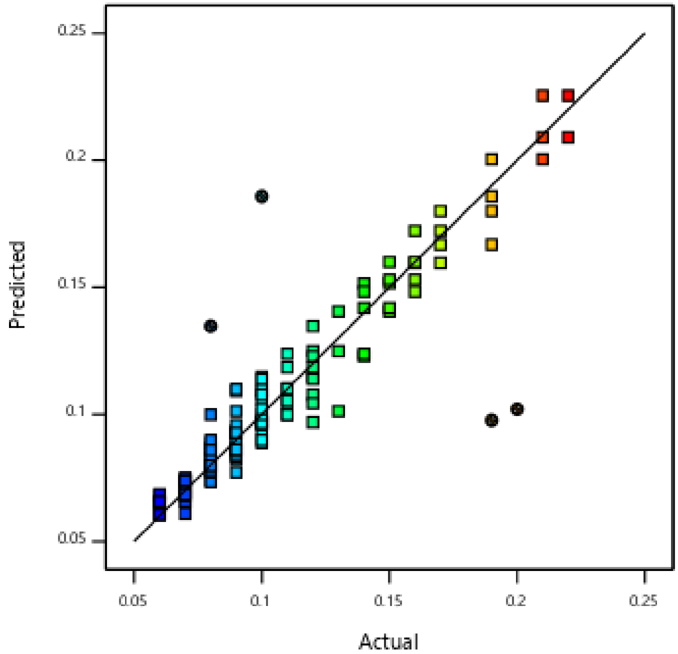

Figure 4.2: The predicted versus actual response for permanent deformation

The predicted versus the actual values from the model are given in Figure 4.2 below and it can be seen that they are close to the line of the equality. Also, the fit statistics of the model are given in Table 4.2.

The most important factors contributing to the total permanent deformation in term of percentage are asphalt thickness (23%), cement thickness (33%), traffic (19.57%), subgrade (3.69%), and interaction of cement and asphalt thickness (5.8%).

Table 4.2: Fit statistics and model comparison statistics

Std. Dev.	0.0102	**R^2**	0.9328
Mean	0.1079	**Adjusted R^2**	0.9247
C.V. %	9.49	**Predicted R^2**	0.9142
		Adeq Precision	41.966

The Predicted R^2 of 0.9142 is in reasonable agreement with the Adjusted R^2 of 0.9247 i.e., the difference is less than 0.2. Adeq Precision measures the signal to noise ratio. A ratio greater than 4 is desirable. The ratio of 41.966 indicates an adequate signal. This model can be used to navigate the design space.

The numeric design equation with categoric factors (subgrade- fine and temperature; freeze) is given below:

$$\begin{aligned}\text{Total Permanent Deformation} \\ &= +0.222467\ - 0.000420\ \mathrm{A}\ -\ 0.000394\mathrm{B}\ -\ 0.000034\mathrm{C}\ - 0.000196\ \mathrm{E} \\ &+ 0.000022\ \mathrm{G} \\ &+\ 1.06357 \times 10^{-06}\ \ \mathrm{AB} \ldots \ldots \ldots\ldots\ldots\ldots\ldots\ldots \text{Equation 4.1}\end{aligned}$$

The numeric design equation with categoric factors (subgrade- fine and temperature; no freeze) is given below:

$$\begin{aligned}\text{Total Permanent Deformation} \\ &= +0.235466\ - 0.000420\ \mathrm{A}\ -\ 0.000394\mathrm{B}\ -\ 0.000034\mathrm{C}\ - 0.000196\ \mathrm{E} \\ &+ 0.000022\ \mathrm{G} \\ &+\ 1.06357 \times 10^{-06}\ \ \mathrm{AB} \ldots\ldots\ldots\ldots\ldots\ldots\ldots\ldots \text{Equation 4.2}\end{aligned}$$

The numeric design equation with categoric factors (subgrade- coarse and temperature; freeze) is given below:

$$\text{Total Permanent Deformation} = +0.196986 - 0.000348\ \text{A} - 0.000394\text{B} - 0.000034\text{C} - 0.000196\ \text{E} + 0.000022\ \text{G} + 1.06357 \times 10^{-06}\ \text{AB} \ldots\ldots \text{Equation 4.3}$$

The numeric design equation with categoric factors (subgrade- coarse and temperature; no freeze) is given below:

$$\text{Total Permanent Deformation} = +0.209985 - 0.000348\ \text{A} - 0.000394\text{B} - 0.000034\text{C} - 0.000196\ \text{E} + 0.000022\ \text{G} + 1.06357 \times 10^{-06}\ \text{AB} \ldots\ldots \text{Equation 4.4}$$

After obtaining the critical parameter affecting the permanent deformation of the pavement, the conditions leading to the maximum and minimum total permanent deformation in the layer have been studied. The result of the optimized factors for minimum and maximum factors are given below in Figure 4.3 and 4.4, respectively.

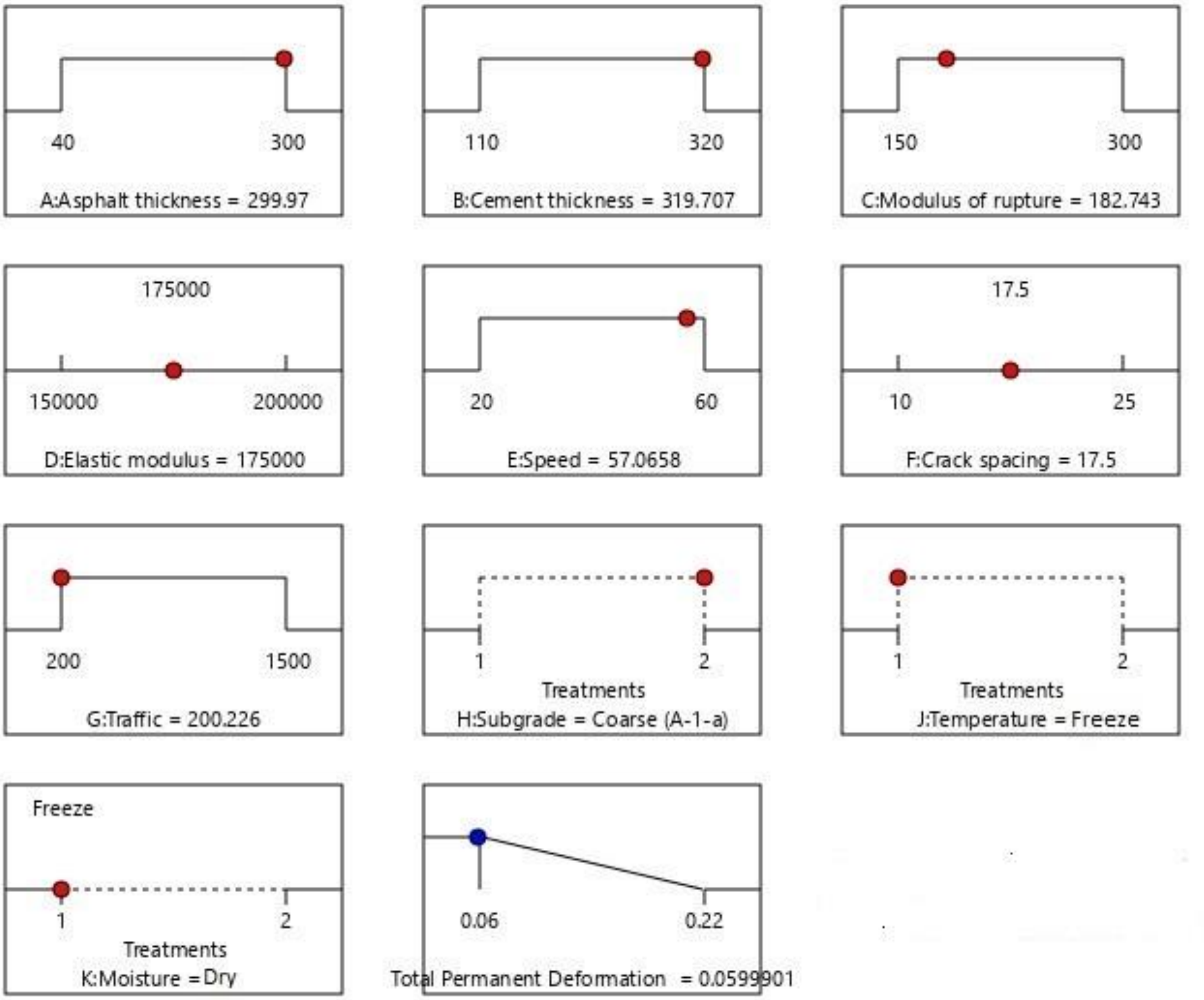

Figure 4.3: The optimized factors level based on minimum total permanent deformation

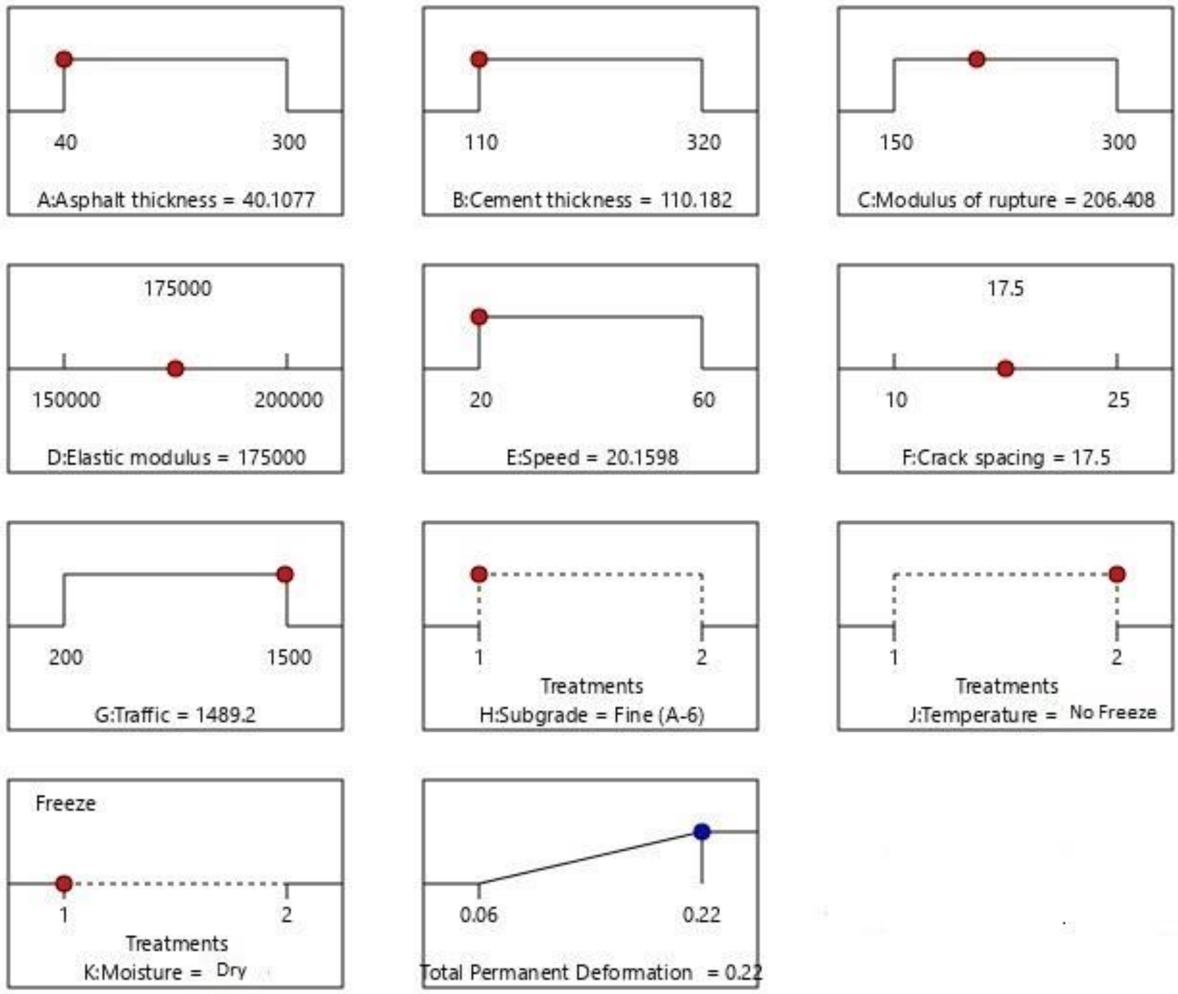

Figure 4.4: The factors level based on optimized maximum total permanent deformation

4.2.2 IRI

The response parameter IRI was studied as the function of different input parameter. The most significant factors affecting the pavement distress, IRI has been reported here. The assumption of the model is checked and is met in term of normality plot of the residuals, residuals versus predicted, residuals versus run, and box-cox transform. The assumption for box cox transformation suggests the inverse square root transformation and given in Figure 4.5.

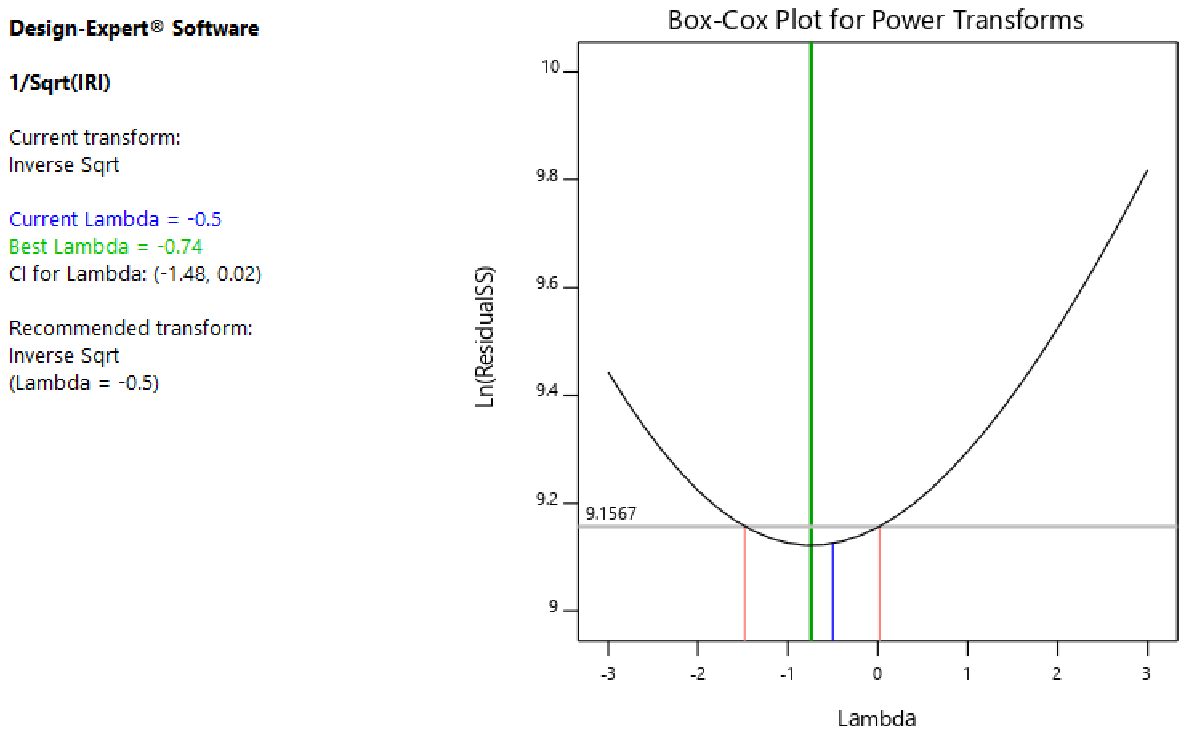

Figure 4.5: Assumption of the model for response of IRI

The ANOVA for the model is given in Table 4.3.

Table 4.3: ANOVA for response, IRI

Source	Sum of Squares	df	Mean Square	F-value	p-value	% Contribution
Model	0.0045	15	0.0003	73.8	< 0.0001	
A-Asphalt thickness	0.0016	1	0.0016	386.12	< 0.0001	30.89
B-Cement thickness	0.0004	1	0.0004	103.02	< 0.0001	9.029
C-Modulus of rupture	0.0001	1	0.0001	14.73	0.0002	1.431
F-Crack spacing	0.0005	1	0.0005	124.62	< 0.0001	10.857
G-Traffic	0.0008	1	0.0008	196.06	< 0.0001	15.2778
H-Subgrade	0.0003	1	0.0003	70.58	< 0.0001	5.35
J-Temperature	0.0005	1	0.0005	115.04	< 0.0001	9.98
AG	0.0002	1	0.0002	45.47	< 0.0001	4.122
AH	0	1	0	4.45	0.0371	0.494
AJ	7.94E-06	1	7.94E-06	1.95	0.1652	0.258
BF	0	1	0	4.55	0.0351	0.327
CH	0	1	0	7.78	0.0062	0.748
FG	0	1	0	6.32	0.0134	0.583
GH	0.0001	1	0.0001	14.04	0.0003	1.305
HJ	0	1	0	3.28	0.0729	0.2138
Residual	0.0005	111	4.07E-06			
Cor Total	0.005	126				

The Model F-value of 73.80 implies the model is significant. There is only a 0.01% chance that such F-value could occur due to noise. P-values less than 0.0500 indicate model terms are significant. In this case A, B, C, F, G, H, J, AG, AH, BF, CH, FG, and GH are significant model terms. Values greater than 0.1000 indicate the model terms are not significant. The fit statistics of the model is given below in Table 4.4.

The most important factors contributing to the IRI are asphalt thickness (31%), cement thickness (9%), modulus of rupture (1.4%), crack spacing (10.85%), traffic (15.27%), subgrade (5.35%), and temperature (10%).

Table 4.4: Fit statistics for response IRI

Std. Dev.	0.002	**R^2**	0.9089
Mean	0.0765	**Adjusted R^2**	0.8965
C.V. %	2.64	**Predicted R^2**	0.8805
		Adeq Precision	38.4606

The Predicted R^2 of 0.8805 is in reasonable agreement with the Adjusted R^2 of 0.8965; i.e. the difference is less than 0.2. Adeq precision measures the signal to noise ratio. A ratio greater than 4 is desirable. The ratio of 38.461 indicates an adequate signal.

The design equation for the model is given below.

$$1/\mathrm{Sqrt(IRI)} = +0.0765 + 0.0035\,A + 0.0018\,B + 0.0007C + 0.0020F - 0.0025\,G + 0.0015H - 0.0019J - 0.0012\,AG + 0.0004\,AH + 0.0003AJ - 0.0004\,BF - 0.0005\,CH\,FG + 0.0005\,FG - 0.0007\,GH - 0.0003\,HJ \ldots\ldots \text{Equation 4.5}$$

Where

A-Asphalt thickness

B-Cement thickness

C-Modulus of rupture

F-Crack spacing

G-Traffic

H-Subgrade

J-Temperature

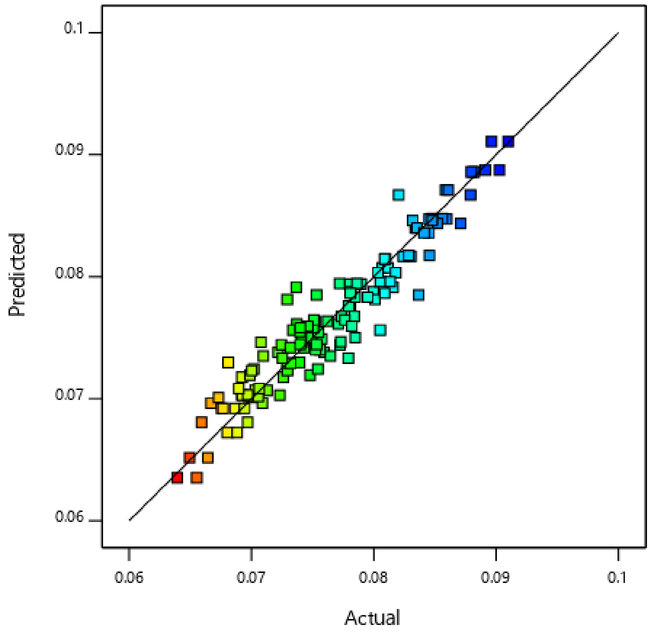

Figure 4.6: Predicted versus actual IRI for the model

The predicted versus the actual values from the model are given in Figure 4.6 and it can be seen that they are close to the line of the equality. After obtaining the critical parameter affecting the IRI of the pavement, the conditions leading to the maximum and minimum IRI in the pavement have been studied. The result of the optimized factors for minimum and maximum factors are given below in Figure 4.7 and Figure 4.8 respectively.

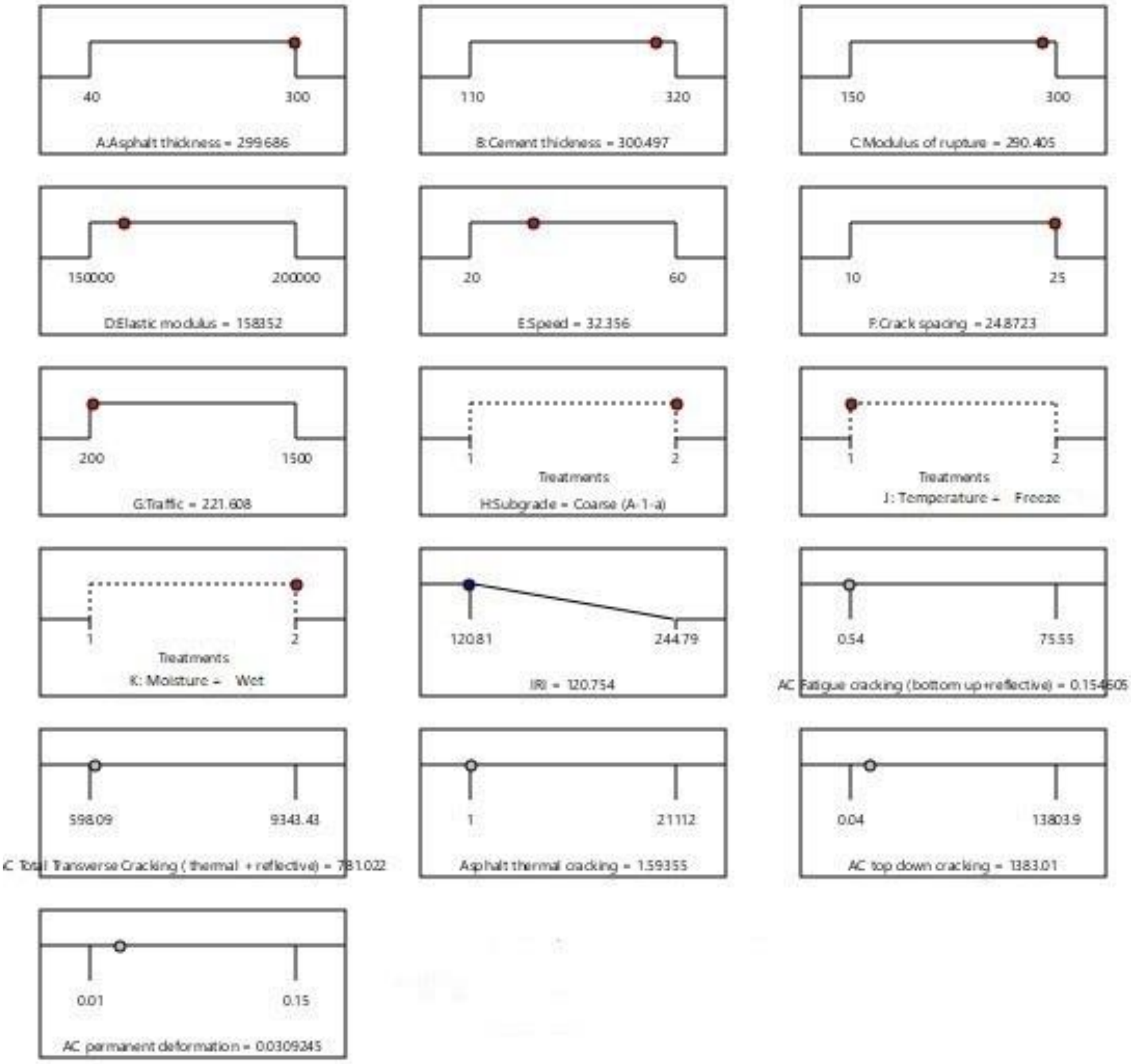

Figure 4.7: Optimized value of factor for the minimum IRI

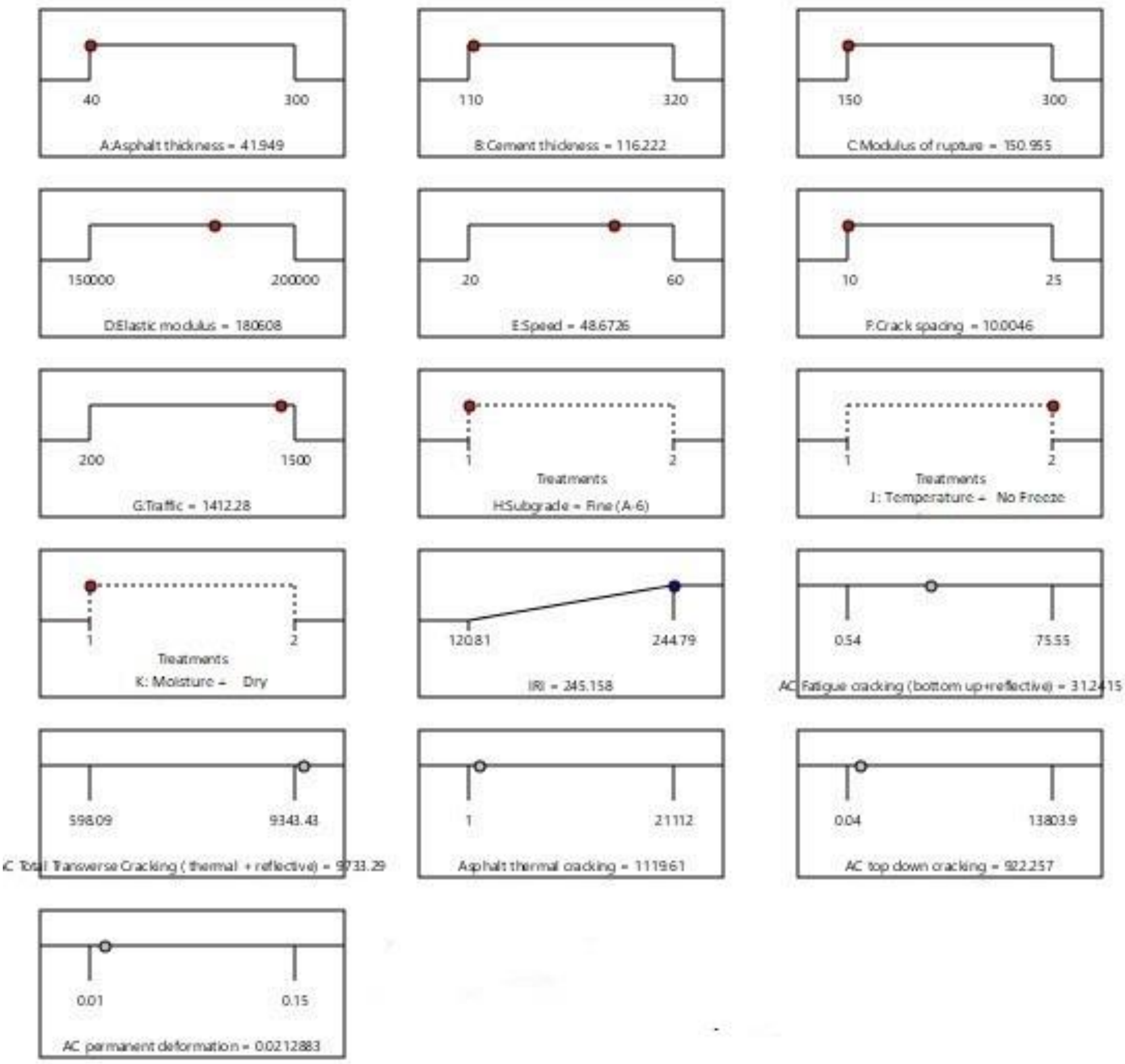

Figure 4.8:Optimized value of factor for the maximum IRI

4.2.3 AC Total Transverse Cracking (Thermal + Reflective)

The response parameter AC total transverse cracking was studied as the function of different input parameters. The most significant factors affecting the pavement distress, AC total transverse cracking has been reported here. The assumption of the model is checked and is met in terms of normality plot of the residuals, residuals versus predicted, residuals versus run, and box-cox transform. The assumption for box cox transformation suggests the square root transformation and given in Figure 4.9.

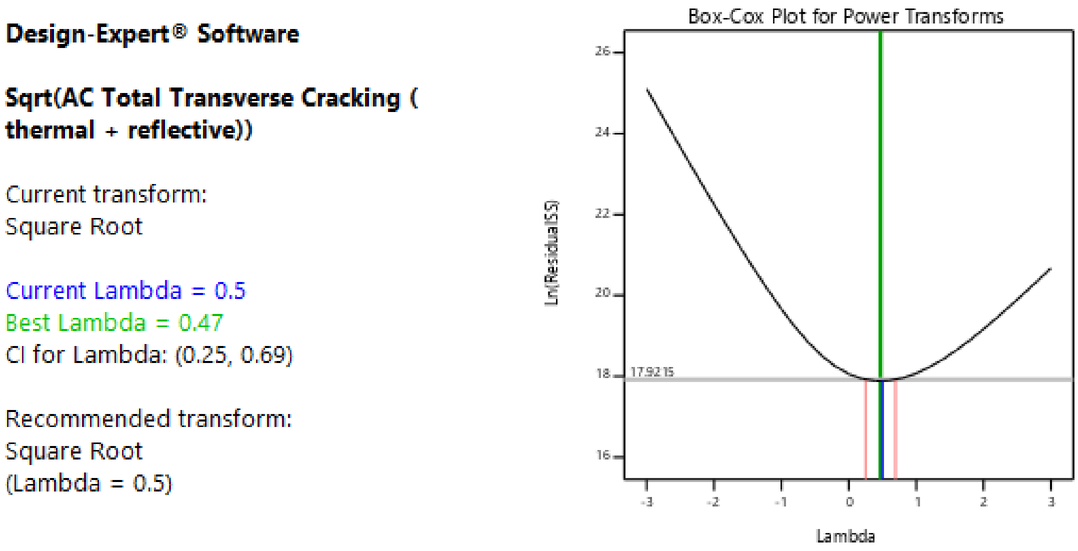

Figure 4.9: Assumption of the model for the response AC total transverse cracking (thermal + reflective)

The ANOVA for the model is given in Table 4.5 below.

Table 4.5: Response for ANOVA AC total transverse cracking (thermal + reflective)

Source	Sum of Squares	Df	Mean Square	F-value	p-value	% Contribution
Model	40167.09	14	2868.08	71.64	< 0.0001	
A-Asphalt thickness	9522.69	1	9522.69	237.78	< 0.0001	21.6
B-Cement thickness	313.25	1	313.25	7.82	0.0061	0.71
F-Crack spacing	11739.48	1	11739.48	293.14	< 0.0001	26.62
G-Traffic	3611.33	1	3611.33	90.18	< 0.0001	8.19
H-Subgrade	170	1	170	4.24	0.0418	0.385
J-Temperature	6600	1	6600	164.8	< 0.0001	14.97
AB	825.13	1	825.13	20.6	0.0001	1.87
AF	611.08	1	611.08	15.26	0.0002	1.38
AG	3449.45	1	3449.45	86.13	< 0.0001	7.82
AJ	964.22	1	964.22	24.1	< 0.0001	2.19
BF	317.64	1	317.64	7.93	0.0058	0.72
BG	561.07	1	561.07	14.01	0.0003	1.27
FG	746.85	1	746.85	18.65	< 0.0001	1.69
GH	235.75	1	235.75	5.89	0.0169	0.53
Residual	4285.08	107	40.05			
Cor Total	44452.17	121				

The Model F-value of 64.61 implies the model is significant. There is only a 0.01% chance that an F-value this large could occur due to noise**.** P-values less than 0.0500 indicate model terms are significant. In this case A, B, F, G, H, J, AB, AF, AG, AJ, BF, BG, CH, and FG are significant model terms. Values greater than 0.1000 indicate the model terms are not significant. The fit statistics for the model are given in Table 4.6.

The most important factor contributing to the total AC transverse cracking in term of percentage are asphalt thickness (21.6%), crack spacing (26.62%), traffic (8.19%), and temperature (14.97%).

Table 4.6: Fit Statistics for the response AC transverse cracking

Std. Dev.	6.38	**R^2**	0.9038
Mean	62.4	**Adjusted R^2**	0.8898
C.V. %	10.22	**Predicted R^2**	0.8719
		Adeq Precision	32.0344

The Predicted R^2 of 0.8719 is in reasonable agreement with the Adjusted R^2 of 0.8898; i.e. the difference is less than 0.2. Adeq precision measures the signal to noise ratio. A ratio greater than 4 is desirable. The ratio of 32.034 indicates an adequate signal.

The design equation with categoric variables subgrade (fine) and temperature (freeze) is given below.

$$\begin{aligned}
&\mathrm{Sqrt(AC\ Total\ Transverse\ Cracking\ (\ thermal\ +\ reflective))} \\
&\quad = +107.27024 - 0.097644\,\mathrm{A} - 0.041792\,\mathrm{B} - 0.047372\,\mathrm{C} + 0.049345\,\mathrm{E} \\
&\quad - 1.60235\,\mathrm{F} - 0.001252\,\mathrm{G} - 0.000174\,\mathrm{AB} + 0.002025\,\mathrm{AE} + 0.000060\,\mathrm{AF} \\
&\quad + 0.001715\,\mathrm{BF} + 0.000028\,\mathrm{BG} - 0.000461\,\mathrm{FG} \ldots\ldots\ldots\ldots\ldots\ldots\ldots\ \text{Equation 4.6}
\end{aligned}$$

The design equation with categoric variables subgrade (fine) and temperature (no freeze) is given below.

$$\begin{aligned}
&\mathrm{Sqrt(AC\ Total\ Transverse\ Cracking\ (\ thermal\ +\ reflective))} \\
&\quad = +128.45783 - 0.138611\,\mathrm{A} - 0.041792\,\mathrm{B} - 0.047372\,\mathrm{C} + 0.049345\,\mathrm{E} \\
&\quad - 1.60235\,\mathrm{F} - 0.001252\,\mathrm{G} - 0.000174\,\mathrm{AB} + 0.002025\,\mathrm{AE} + 0.000060\,\mathrm{AF} \\
&\quad + 0.001715\,\mathrm{BF} + 0.000028\,\mathrm{BG} - 0.000461\,\mathrm{FG} \ldots\ldots\ldots\ldots\ldots\ldots\ \text{Equation 4.7}
\end{aligned}$$

The design equation with categoric variables subgrade (coarse) and temperature (freeze) is given below.

$$\text{Sqrt(AC Total Transverse Cracking (thermal + reflective))}$$
$$= +85.61 - 0.097\text{ A} - 0.041792\text{ B} + 0.021264\text{ C} + 0.049345\text{ E} - 1.60235\text{ F}$$
$$+ 0.002631\text{ G} - 0.000174\text{ AB} + 0.002025\text{ AE} + 0.000060\text{ AF} + 0.001715\text{ BF}$$
$$+ 0.000028\text{ BG} - 0.000461\text{ FG}\ldots\ldots\ldots\ldots\ldots\ldots\text{Equation 4.8}$$

The design equation with categoric variables subgrade (coarse) and temperature (no freeze) is given below.

$$\text{Sqrt}\big(\text{AC Total Transverse Cracking (thermal + reflective)}\big)$$
$$= +106.79716 - 0.138611\text{A} - 0.041792\text{ B} + 0.021264\text{ C} + 0.049345\text{ E} - 1.60235\text{ F}$$
$$+ 0.002631\text{ G} - 0.000174\text{ AB} + 0.002025\text{ AE} + 0.000060\text{ AF} + 0.001715\text{ BF}$$
$$+ 0.000028\text{ BG}$$
$$- 0.000461\text{ FG}\ldots\ldots\ldots\ldots\ldots\ldots\ldots\ldots\ldots\ldots\ldots\ldots\ldots\ldots\ldots\ldots\ldots\ldots\ldots\ldots\ldots\ldots\ldots\ldots\ldots\ldots\ldots\ldots\ldots\ldots\text{Equation 4.9}$$

Where

A= Asphalt Traffic

B = Cement Thickness

C = Modulus of Rupture

E = Speed

F = Crack Spacing

G= Traffic

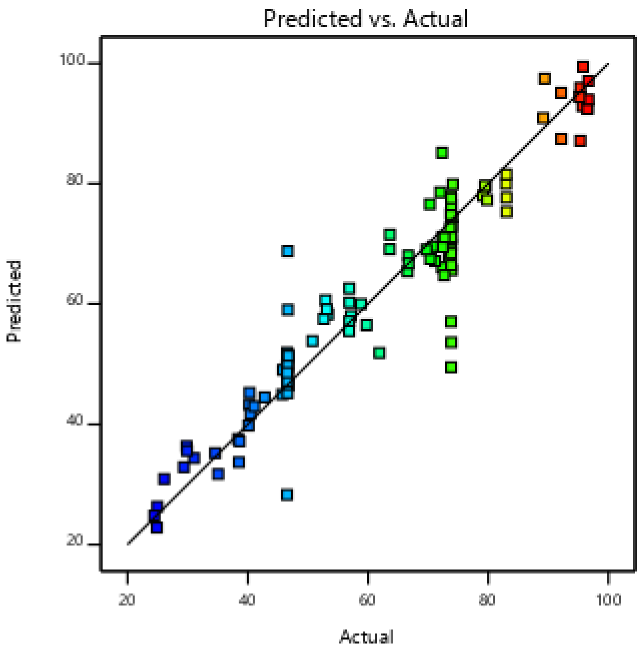

Figure 4.10: Actual verses predicted value for the response AC total transverse cracking

The predicted versus the actual values from the model are given in Figure 4.10 and it can be seen that they are close to the line of the equality.

After obtaining the critical parameter affecting the AC total Transverse Cracking (Thermal + Reflective) of the pavement, the conditions leading to the maximum and minimum AC total Transverse Cracking (Thermal + Reflective) in the layer has been studied. The result of optimized factors for minimum and maximum factors are given in Figure 4.11 and 4.12, respectively.

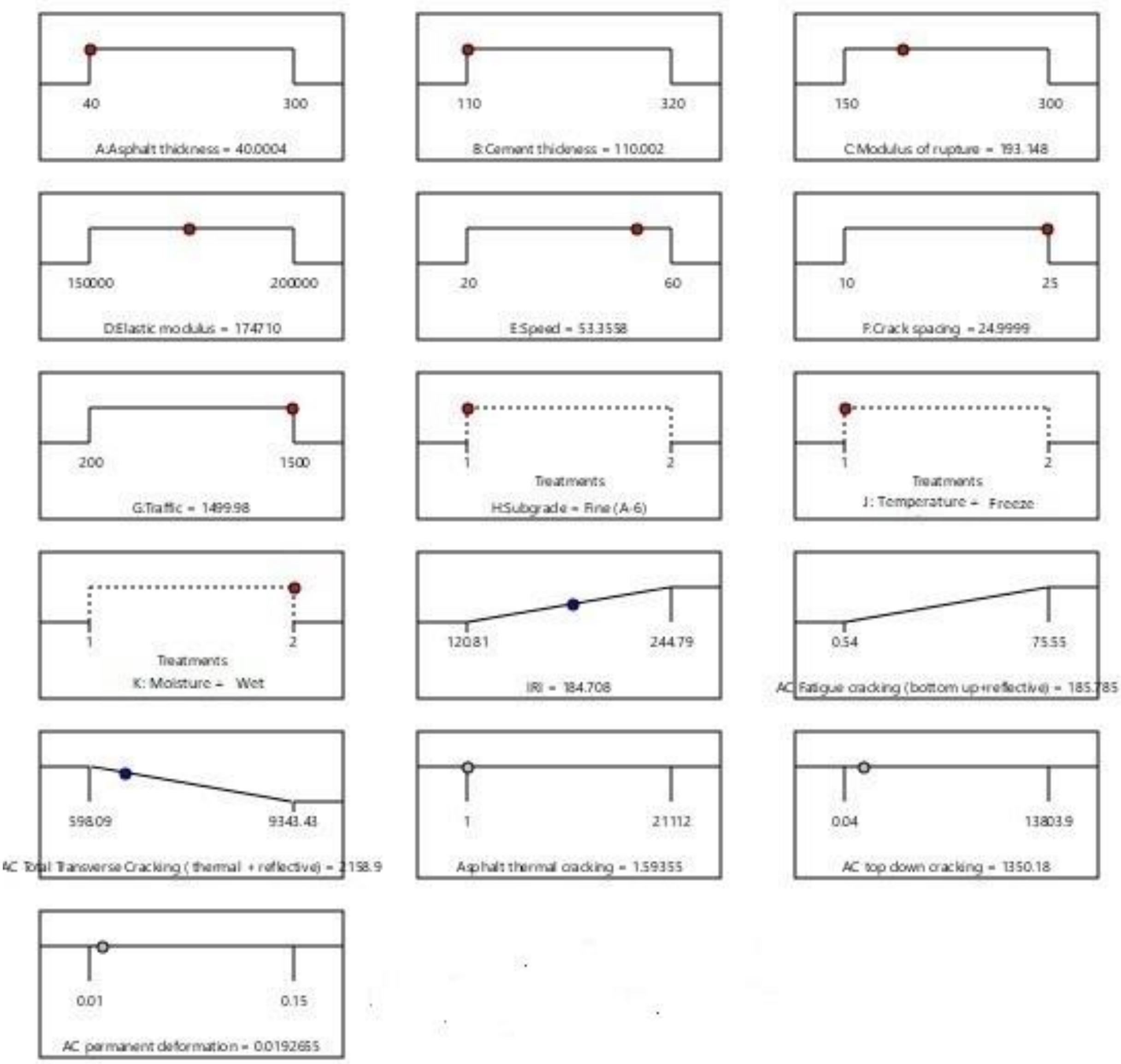

Figure 4.11: Optimized value for different factors for minimum response for AC total transverse cracking (thermal + reflective)

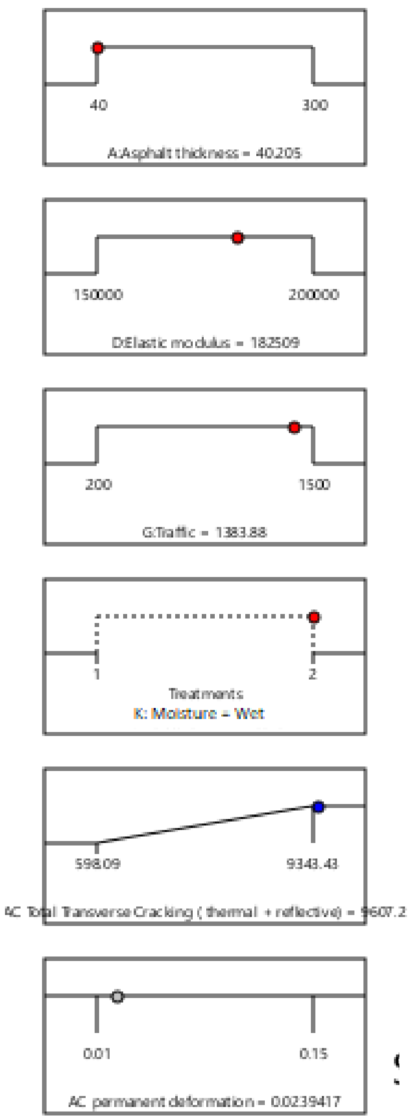

Figure 4.12: Optimized value for different factors for maximum response for AC total transverse cracking (thermal + reflective)

4.2.4 AC Top-Down Cracking

The response parameter AC top-down cracking was studied as the function of different input parameters. The most significant factors affecting the pavement distress, AC top down cracking has been reported here. The assumption of the model is checked and is met in terms of normality plot of the residuals, residuals versus predicted, residuals versus run, and box-cox transform. The assumption for box cox transformation suggests the inverse square root transformation and given in Figure 4.13.

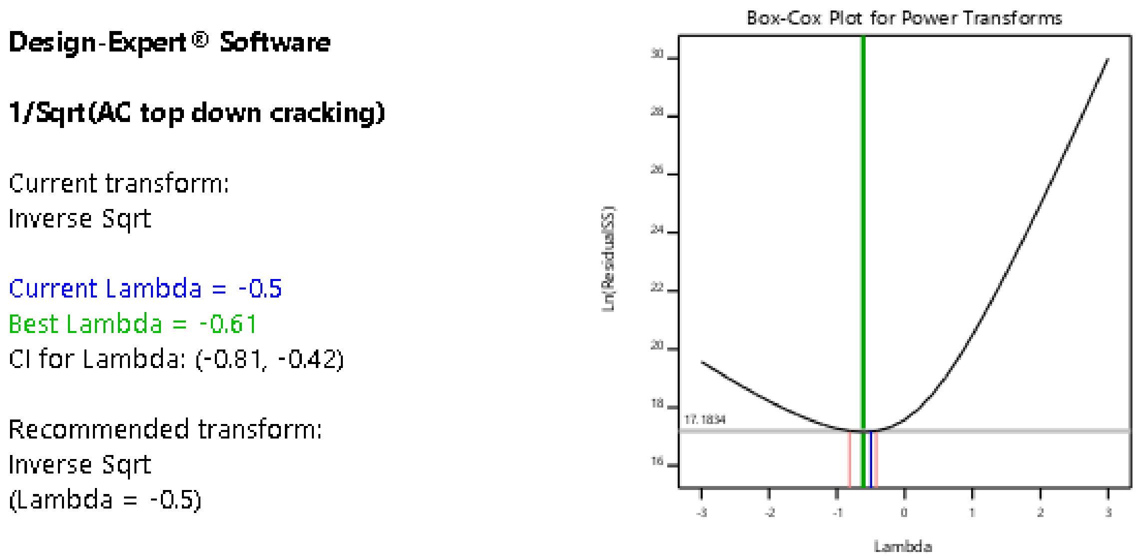

Figure 4.13: Assumption of the model for the response AC top-down fatigue cracking

From the above Figure 4.13, it is clear that all the assumption of the model are met. The ANOVA for the model is given in Table 4.7 below.

Table 4.7: ANOVA for response, AC top-down cracking

Source	Sum of Squares	df	Mean Square	F-value	p-value	% Contribution
Model	0.0271	12	0.0023	14.63	< 0.0001	
A-Asphalt thickness	0.0128	1	0.0128	83.21	< 0.0001	28.5867
B-Cement thickness	0.0009	1	0.0009	5.78	0.0179	1.986
C-Modulus of rupture	0.0008	1	0.0008	5.20	0.0245	1.788
E-Speed	0.0008	1	0.0008	5.04	0.0268	1.731
H-Subgrade	0.0005	1	0.0005	3.16	0.0784	1.084
J-Temperature	0.0021	1	0.0021	13.67	0.0003	4.69
AE	0.0005	1	0.0005	3.49	0.0644	1.198
AH	0.0034	1	0.0034	21.99	< 0.0001	7.55
BH	0.0008	1	0.0008	5.32	0.0229	1.829
CE	0.0010	1	0.0010	6.52	0.0120	2.24
CH	0.0019	1	0.0019	12.40	0.0006	4.26
HJ	0.0019	1	0.0019	12.37	0.0006	4.25
Residual	0.0168	109	0.0002			
Cor Total	0.0439	121				

The Model F-value of 14.44 implies the model is significant. There is only a 0.01% chance that an F-value this large could occur due to noise. P-values less than 0.0500 indicate model terms are significant. In this case A, B, C, E, H, J, AE, AH, BH, CE, CH, and HJ are significant model terms. Values greater than 0.1000 indicate the model terms are not significant. The fit statistics of the model is given in Table 4.8.

The most important factor contributing to the total permanent deformation in term of percentage are asphalt thickness (28.58%), temperature (4.69%), interaction between asphalt thickness and subgrade traffic (19.57%), subgrade (3.69%), interaction of asphalt thickness and subgrade (7.55%), interaction between modulus of rupture and subgrade, and interaction between subgrade and temperature.

Table 4.8: Fit statistics of the model response, AC top-down cracking

Std. Dev.	0.0126	**R^2**	0.6169
Mean	0.0429	**Adjusted R^2**	0.5747
C.V. %	29.41	**Predicted R^2**	0.5210
		Adeq Precision	13.5727

The Predicted R^2 of 0.521 is in reasonable agreement with the Adjusted R^2 of 0.5747; i.e. the difference is less than 0.2. Adeq Precision measures the signal to noise ratio. A ratio greater than 4 is desirable. The ratio of 13.57 indicates an adequate signal.

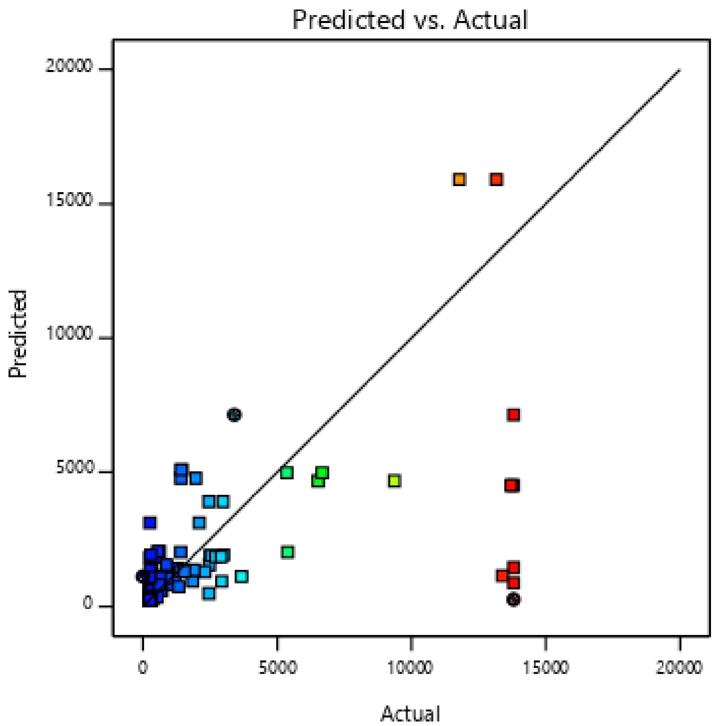

Figure 4.14: Predicted versus actual value for the model response

The predicted versus the actual values from the model are given in Figure 4.14 above and it can be seen that they are approximately close to the line of the equality.

After obtaining the critical parameter affecting the AC top-down cracking of the pavement, the conditions leading to the maximum and minimum total AC top-down cracking in the layer have been studied. The result of optimized factors for minimum top-down cracking is given in Figure 4.15.

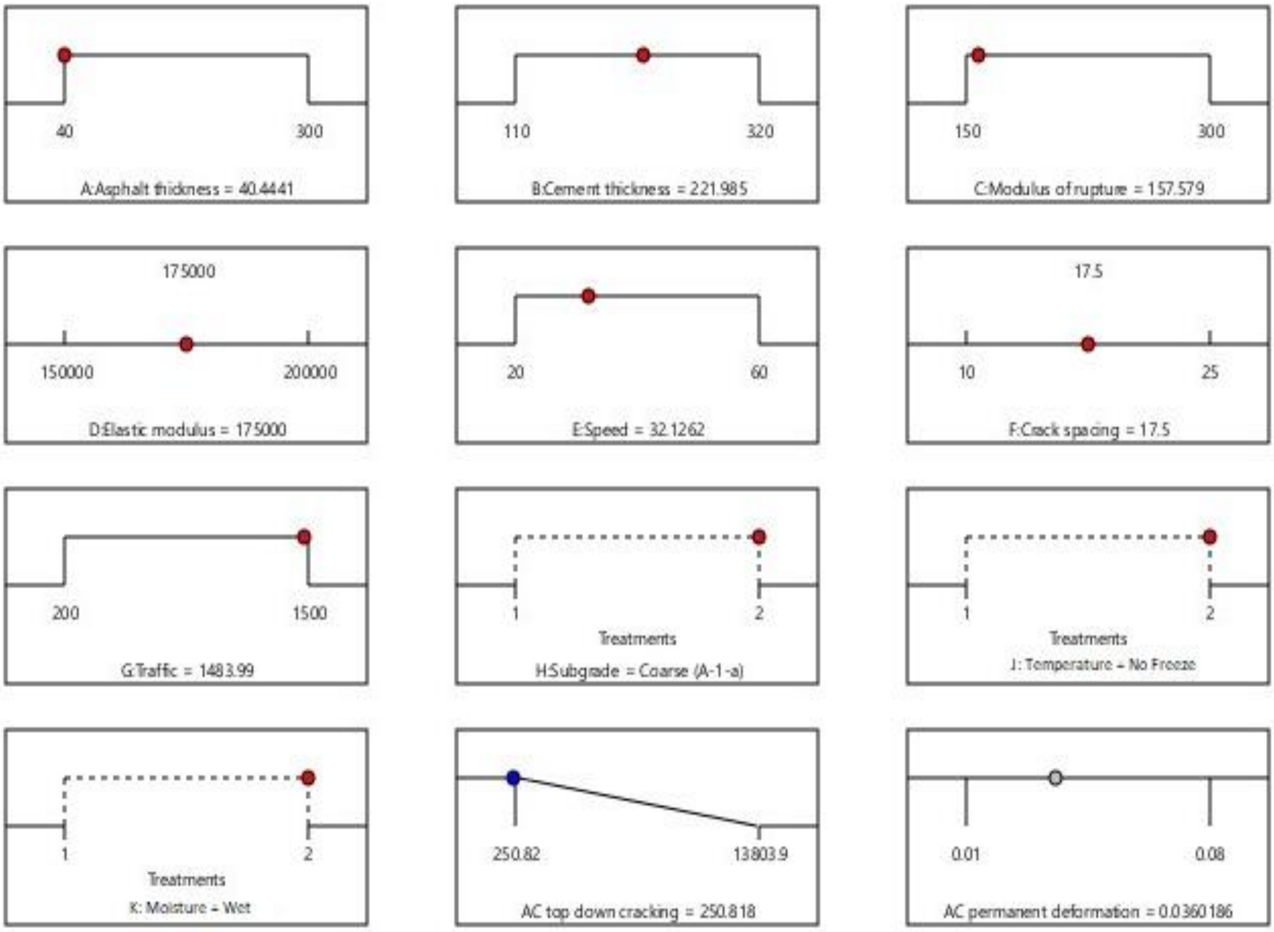

Figure 4.15: Optimized Factors for the minimum value of asphalt top-down cracking

4.2.5 AC Permanent Deformation

The response parameter AC permanent deformation was studied as the function of different input parameters. The most significant factors affecting the pavement distress, AC permanent deformation has been reported here. In terms of checking and meeting the assumptions of the model, residuals are normalized, compared to predictions, compared to runs, and standardized using the box-cox transform. According to this assumption, there will be no transformation for box cox. Figure 4.16 confirms this assumption

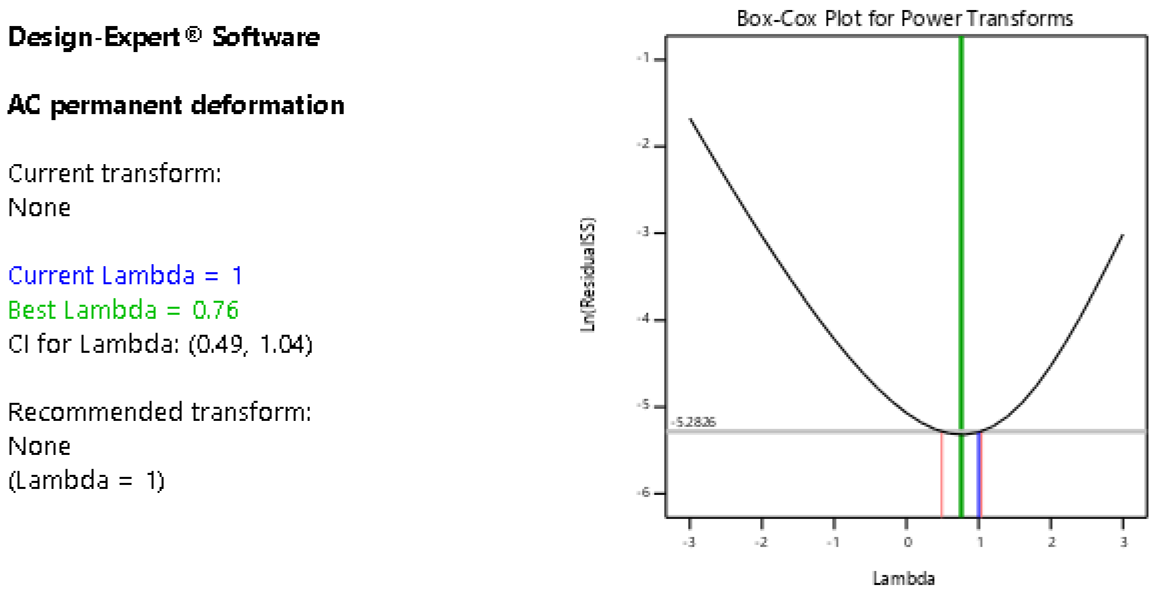

Figure 4.16: Assumption of the model for the AC permanent deformation

From the above Figure 4.16, it is clear that all the assumptions of the model are met. The ANOVA for the model is given in Table 4.9 below.

Table 4.9: ANOVA for response, AC permanent deformation

Source	Sum of Squares	df	Mean Square	F-value	p-value	% Contribution
Model	0.0258	15	0.0017	43.65	< 0.0001	
A-Asphalt thickness	0.0076	1	0.0076	194.02	< 0.0001	25.72
B-Cement thickness	0.0022	1	0.0022	56.80	< 0.0001	7.53
E-Speed	0.0023	1	0.0023	58.36	< 0.0001	7.73
G-Traffic	0.0062	1	0.0062	158.24	< 0.0001	20.98
J-Temperature	0.0008	1	0.0008	20.90	<0.0001	2.77
K-Moisture	0.0022	1	0.0022	55.42	< 0.0001	7.34
AB	0.0001	1	0.0001	3.39	0.00685	0.44
AE	0.0004	1	0.0004	11.36	0.0010	1.5
AG	0.0005	1	0.0005	12.5	0.0006	1.65
AJ	0.0007	1	0.0007	18.05	<0.0001	2.39
AK	0.0005	1	0.0005	12.65	0.0006	1.67
BG	0.0003	1	0.0003	8.52	0.0043	1.13
GJ	0.0002	1	0.0002	5.29	0.0234	0.7
GK	0.0006	1	0.0006	15.46	0.0002	2.05
JK	0.0007	1	0.0007	17.15	<0.0001	2.27
Residual	0.0057	106	0.0001			
Cor Total	0.0312	121				

The Model F-value of 32.82 implies the model is significant. There is only a 0.01% chance that an F-value this large could occur due to noise. P-values less than 0.0500 indicate model terms are significant. In this case, A, B, E, G, J, K, AE, AG, AJ, AK, GK, and JK are significant model terms. Values greater than 0.1000 indicate the model terms are not significant. The fit statistics of the model is given in Table 4.10.

The most important factor contributing to the total permanent deformation in term of percentage are asphalt thickness (25.72%), cement thickness (7.53%), speed (7.73%), traffic (20.98%), and moisture (7.34%).

Table 4.10: Fit statistics for the response, AC permanent deformation

Std. Dev.	0.0072	**R^2**	0.8607
Mean	0.0302	**Adjusted R^2**	0.8410
C.V. %	23.88	**Predicted R^2**	0.8141
		Adeq Precision	29.9901

The Predicted R^2 of 0.8141 is in reasonable agreement with the Adjusted R^2 of 0.8410; i.e. the difference is less than 0.2. Adeq precision measures the signal to noise ratio. A ratio greater than 4 is desirable. The ratio of 29.99 indicates an adequate signal. This model can be used to navigate the design space.

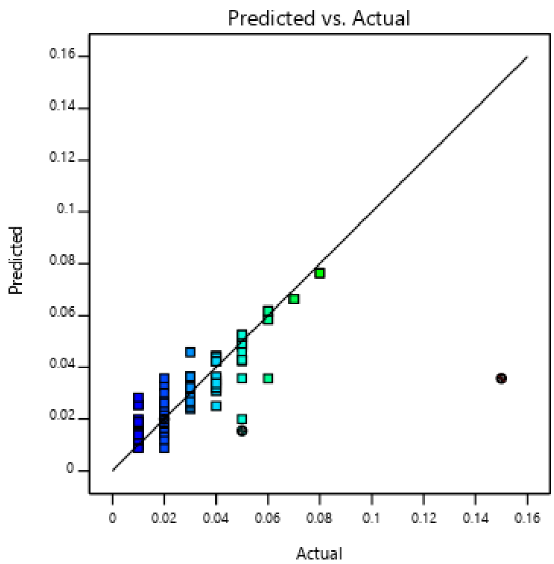

Figure 4.17: Actual versus predicted value for the response

The actual versus predicted values are close to the line of equality as given in Figure 4.17. After obtaining the critical parameter affecting the AC permanent deformation of the pavement, the conditions leading to the maximum and minimum total permanent deformation in the layer have been studied. The result of the optimized factors for minimum and maximum factors are given below in Figure 4.18 and 4.19 respectively.

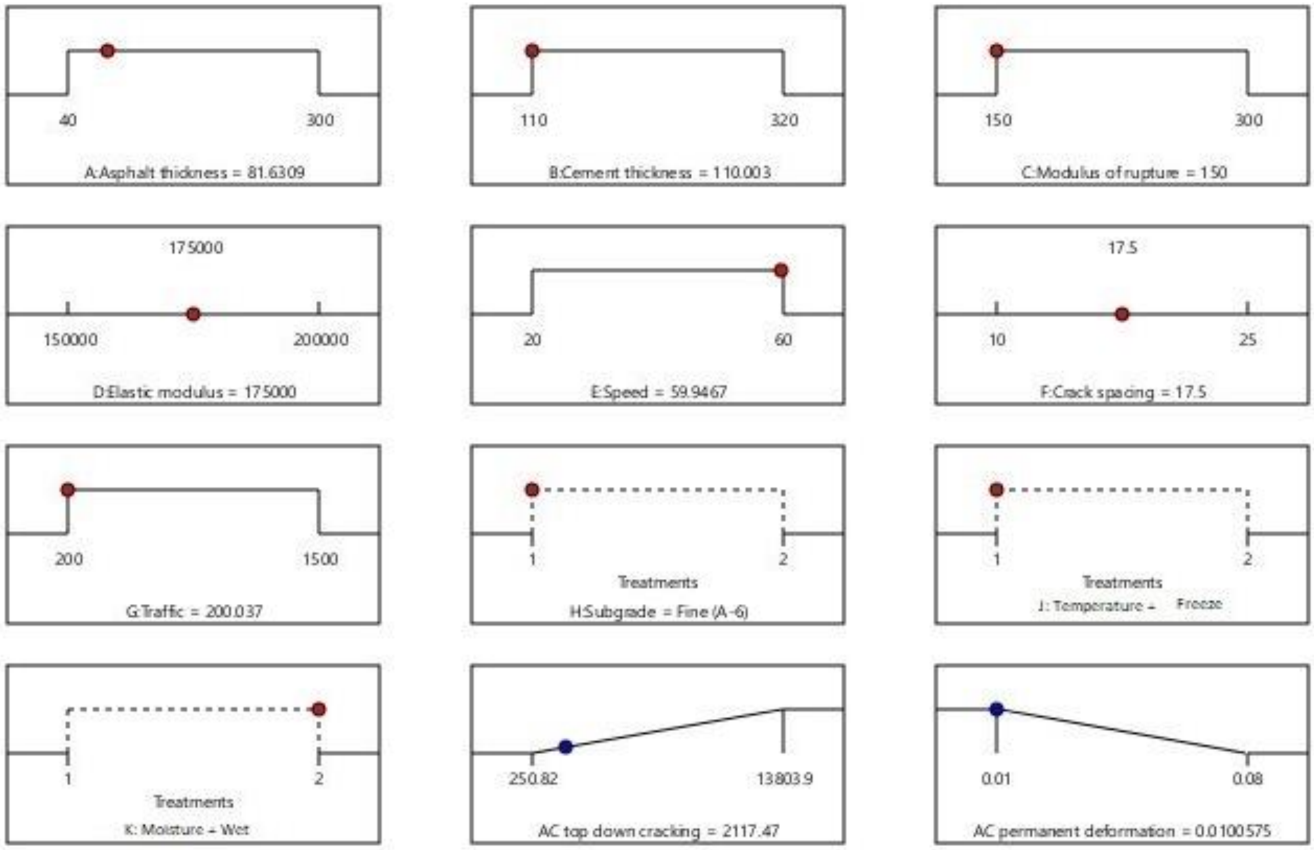

Figure 4.18: Optimized factors for the minimum value of asphalt permanent deformation

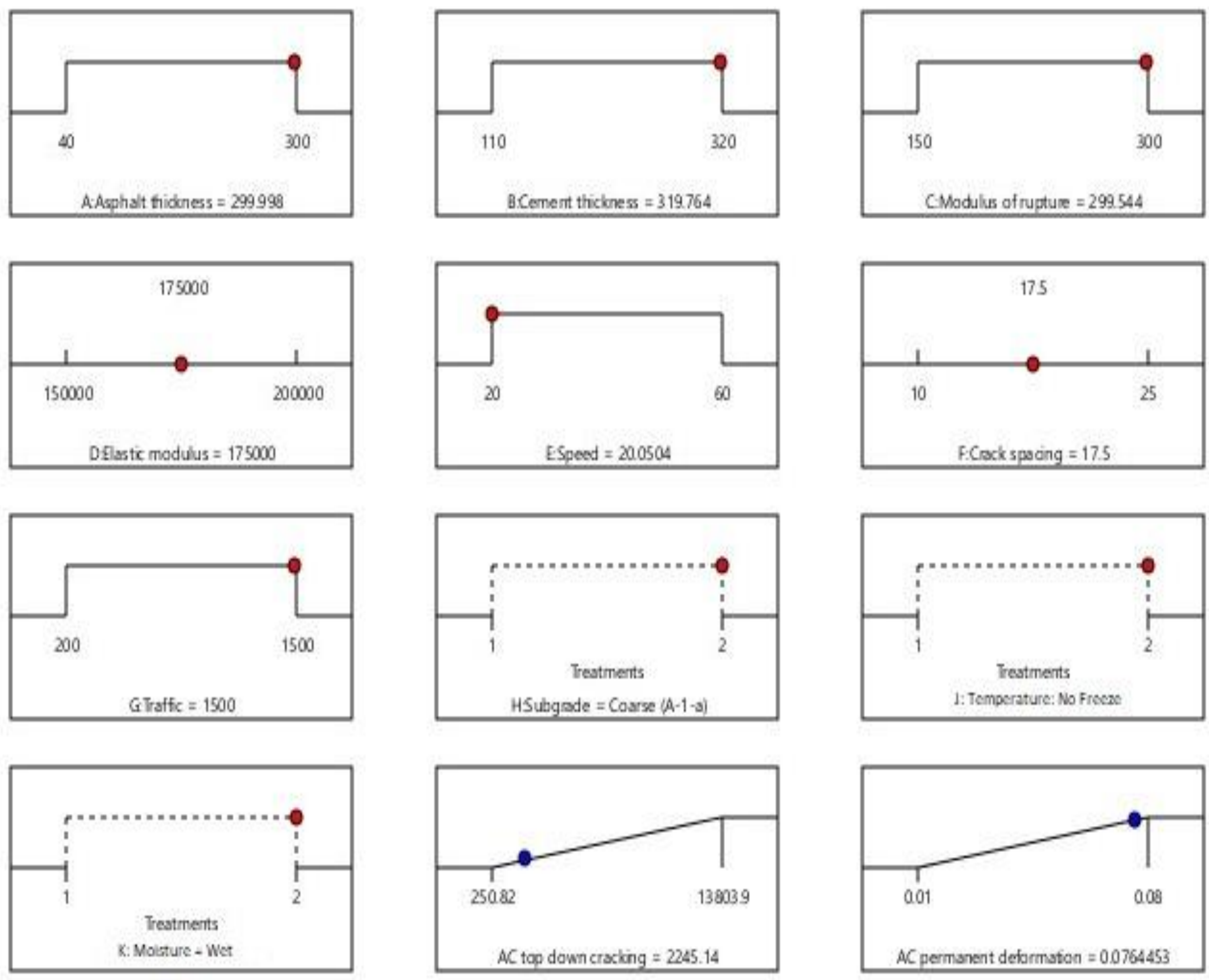

Figure 4.19: Optimized factors for the maximum value of asphalt permanent deformation

4.2.6 AC Thermal Cracking

The response parameter AC thermal cracking was studied as the function of different input parameters. The most significant factors affecting the pavement distress, AC thermal cracking has been reported here. The assumption of the model is checked and is met in terms of normality plot of the residuals, residuals versus predicted, residuals versus run, and box-cox transform. The assumption for box cox transformation suggests log transformation and given in Figure 4.20.

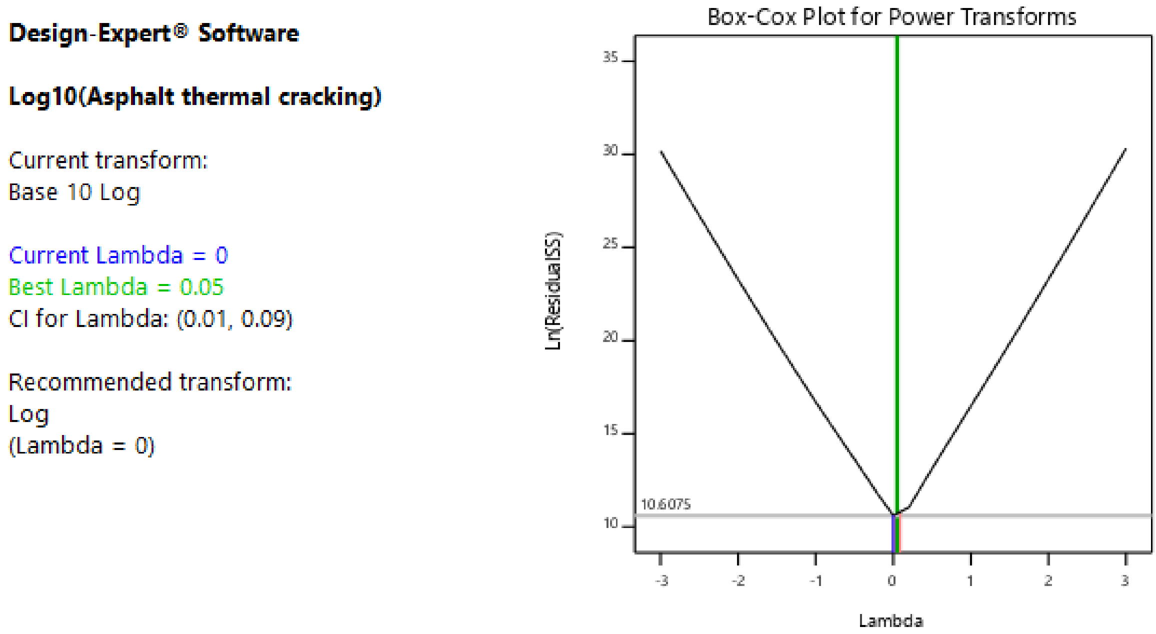

Figure 4.20: Assumption of the model for the response thermal cracking

From the above Figure 4.20, it is clear that all the assumptions of the model are met. The ANOVA for the model is given in Table 4.11.

Table 4.11: ANOVA for response thermal cracking

Source	Sum of Squares	df	Mean Square	F-value	p-value	% Contribution
Model	241.48	1	241.48	2698.6	< 0.0001	95.54
J-Temperature	241.48	1	241.48	2698.6	< 0.0001	
Residual	10.74	120	0.0895			
Cor Total	252.22	121				

The Model F-value of 252.22 implies the model is significant. There is only a 0.01% chance that an F-value this large could occur due to noise. P-values less than 0.0500 indicate model terms are significant. In this case, J is significant model term. Values greater than 0.1000 indicate the model terms are not significant. The fit statistics of the model is given in Table 4.12

Table 4.12: Fit statistics for the response thermal cracking

Std. Dev.	0.2973	**R^2**	0.9574
Mean	1.64	**Adjusted R^2**	0.9571
C.V. %	18.11	**Predicted R^2**	0.9560
		Adeq Precision	73.5052

The Predicted R^2 of 0.9828 is in reasonable agreement with the Adjusted R^2 of 0.9571, i.e., the difference is less than 0.2. Adeq precision measures the signal to noise ratio. A ratio greater than 4 is desirable. The ratio of 73.5052 indicates an adequate signal.

For temperature as freeze, the thermal cracking is given by the following equation.

$$\mathrm{Log_{10}(Asphalt\ thermal\ cracking)} = +0.209001 \quad \text{Equation 4.10}$$

For temperature as no freeze, the thermal cracking is given by the following equation.

$$\mathrm{Log_{10}(Asphalt\ thermal\ cracking)} = +3.02882 \quad \text{Equation 4.11}$$

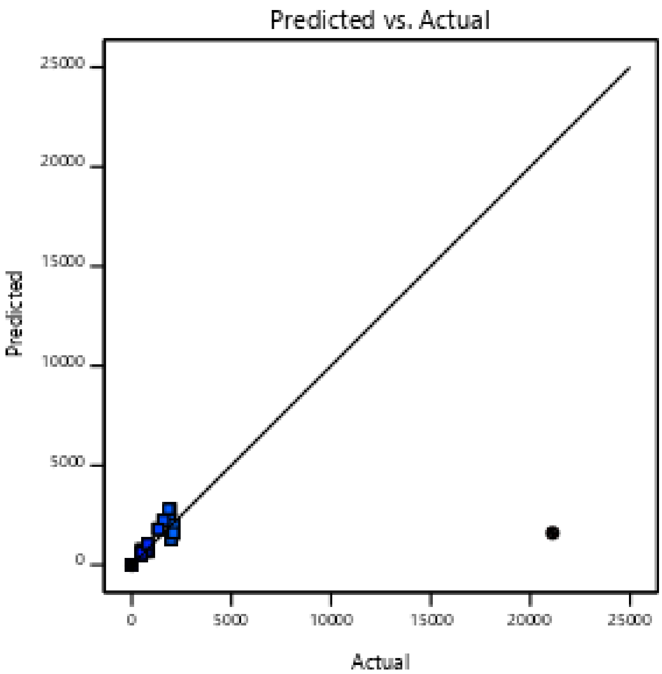

Figure 4.21: Predicted versus actual asphalt thermal cracking

The predicted versus actual values are close to the line of equality for asphalt thermal cracking, as given in Figure 4.21. After obtaining the critical parameter affecting the asphalt thermal cracking of the pavement, the conditions leading to the maximum and minimum asphalt thermal cracking in the layer has been studied. The result of the optimized factors for minimum and maximum factors are given below in Figure 4.22 and 4.23 respectively.

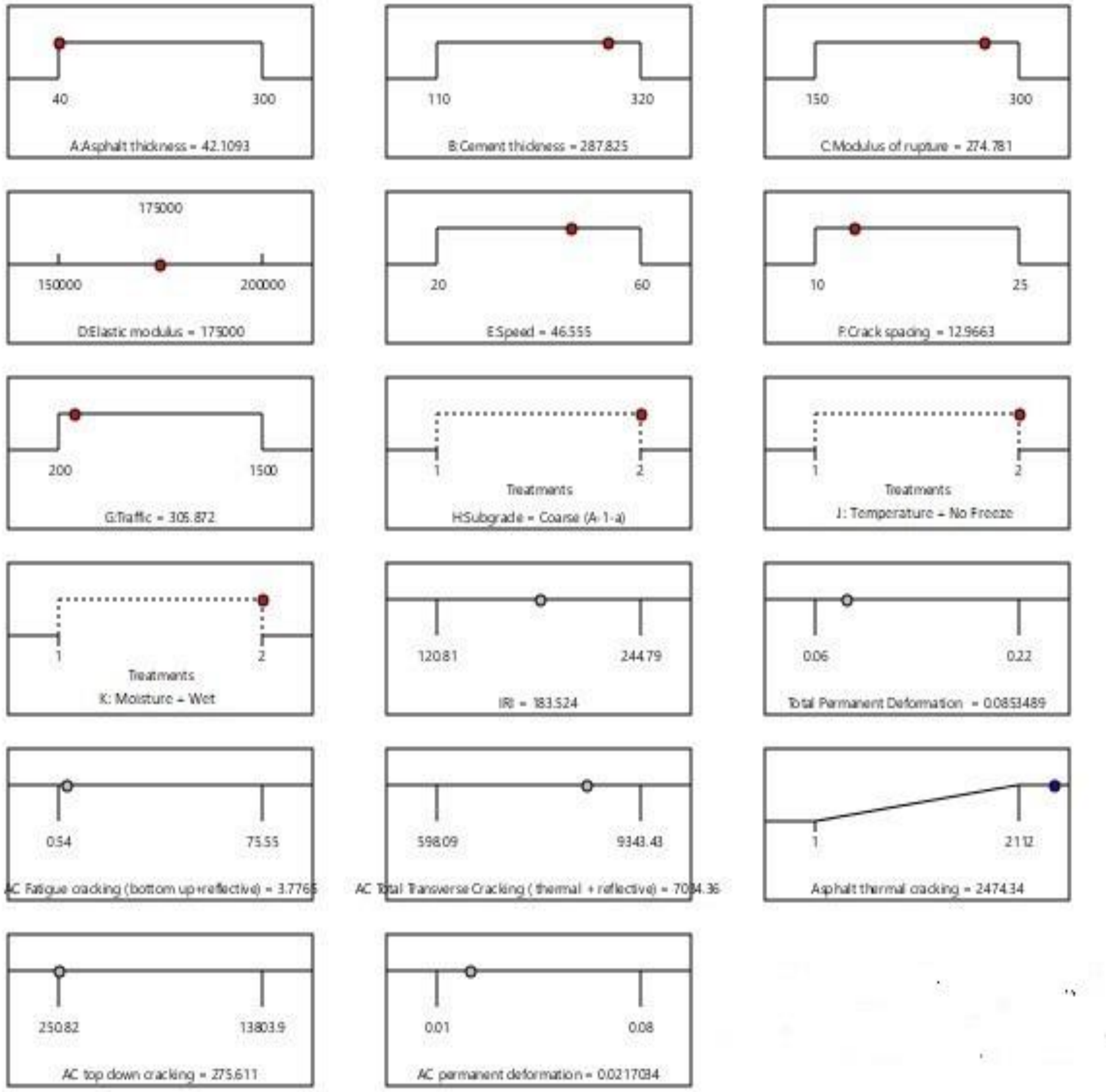

Figure 4.22: Optimized factors for the maximum value of asphalt thermal cracking

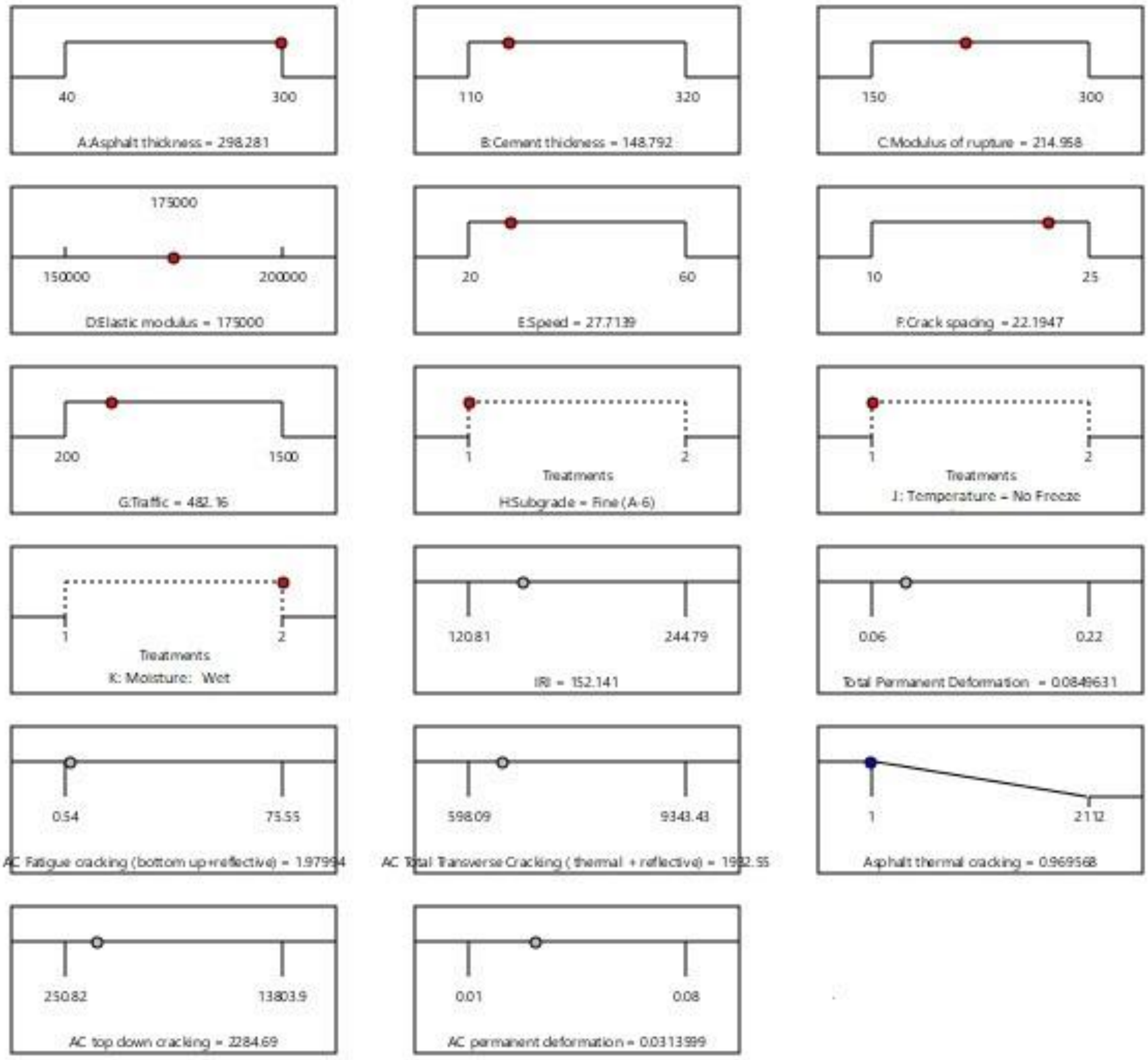

Figure 4.23: Optimized factors for the minimum value of asphalt thermal cracking

4.2.7 AC Fatigue Cracking (Bottom Up + Reflective)

The response parameter AC fatigue cracking (bottom up + reflective) was studied as the function of different input parameter. The most significant factors affecting the pavement distress, AC fatigue cracking (bottom up + reflective) has been reported here. The assumption of the model is checked and is met in term of normality plot of the residuals, residuals versus predicted, residuals versus run, and box-cox transform. The assumption for box cox transformation suggests the log transformation and given in Figure 4.24.

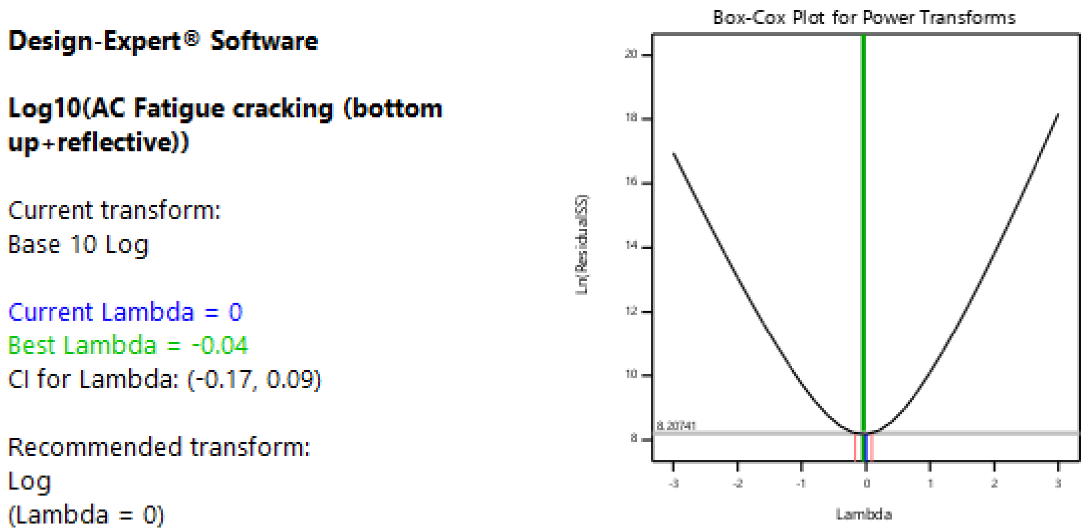

Figure 4.24: Assumption of the model for the response AC Fatigue Cracking (Bottom Up + Reflective)

Table 4.13 gives the significant factors used in the model.

Table 4.13: ANOVA for response, AC fatigue cracking (bottom-up + reflective)

Source	Sum of Squares	df	Mean Square	F-value	p-value	% Contribution
Model	85.25	16	5.33	27.62	< 0.0001	
A-Asphalt thickness	21.76	1	21.76	112.82	< 0.0001	20
B-Cement thickness	5.6	1	5.6	29.01	< 0.0001	5.52
C-Modulus of rupture	2.84	1	2.84	14.72	0.0002	2.84
G-Traffic	31.23	1	31.23	161.91	< 0.0001	29.25
H-Subgrade	2.17	1	2.17	11.26	0.0011	4.23
K-Moisture	4.62	1	4.62	23.97	< 0.0001	0.6
AB	0.5602	1	0.5602	2.9	0.0913	0.6
AG	0.9624	1	0.9624	4.99	0.0276	1.03
AK	2.78	1	2.78	14.42	0.0002	2.45
BC	4.45	1	4.45	23.09	< 0.0001	4.65
BG	0.8646	1	0.8646	4.48	0.0366	0.999
BH	1.6	1	1.6	8.3	0.0048	1.35
BK	0.8726	1	0.8726	4.52	0.0357	1
CH	0.6709	1	0.6709	3.48	0.0649	0.53
CK	0.4328	1	0.4328	2.24	0.1371	0.54
GK	2.96	1	2.96	15.35	0.0002	3.11
Residual	20.64	107	0.1929			
Cor Total	105.89	123				

The Model F-value of 27.62 implies the model is significant. There is only a 0.01% chance that an F-value this large could occur due to noise. P-values less than 0.0500 indicate model terms are significant. In this case A, B, C, G, H, K, AG, AK, BC, BG, BH, BK, and GK are significant model terms. Values greater than 0.1000 indicate the model terms are not significant. The fit statistics of the model is given Table 4.14.

The most important factor contributing to the total permanent deformation in term of percentage are asphalt thickness (20%), cement thickness (5.52%), traffic (29.25%), and subgrade (4.23%).

Table 4.14: Fit statistics of response

Std. Dev.	0.4392	**R^2**	0.8051
Mean	0.7555	**Adjusted R^2**	0.7759
C.V. %	58.13	**Predicted R^2**	0.7372
		Adeq Precision	17.3792

The Predicted R^2 of 0.7372 is in reasonable agreement with the Adjusted R^2 of 0.7759; i.e. the difference is less than 0.2. Adeq precision measures the signal to noise ratio. A ratio greater than 4 is desirable. The ratio of 17.379 indicates an adequate signal. This model can be used to navigate the design space.

The design equation for categoric factors (subgrade as fine (A-6); moisture as dry) is:

$$\mathrm{Log_{10}(AC\ Fatigue\ cracking\ (bottom\ up + reflective))} = -0.810115 - 0.004027\,\mathrm{A} + 0.005494\,\mathrm{B} + 0.004941\,\mathrm{C} + 0.001101\,\mathrm{G} + 4.93597\times10^{-6}\,\mathrm{AB} + 1.04510\times10^{-6}\,\mathrm{AG} - 0.000024\,\mathrm{BC} - 1.22761\times10^{-6}\,\mathrm{BG} \quad \text{Equation 4.12}$$

The design equation for categoric factors (subgrade as fine (A-6); moisture as wet) is:

$$\mathrm{Log_{10}(AC\ Fatigue\ cracking\ (bottom\ up + reflective))} = +1.07773 - 0.006339\,\mathrm{A} + 0.003888\,\mathrm{B} + +0.003358\,\mathrm{C} + 0.000623\mathrm{G} + 4.93597\times10^{-6}\,\mathrm{AB} + 1.04510\times10^{-6}\,\mathrm{AG} - 0.000024\,\mathrm{BC} - 1.22761\times10^{-6}\mathrm{BG} \quad \text{Equation 4.13}$$

The design equation for categoric factors (subgrade as coarse (A-1); moisture as dry) is:

$$\mathrm{Log_{10}(AC\ Fatigue\ cracking\ (bottom\ up + reflective))} = 0.165766 - 0.004027\,\mathrm{A} + 0.003322\,\mathrm{B} + +0.002973\,\mathrm{C} + 0.001101\,\mathrm{G} + 4.93597\times10^{-6}\,\mathrm{AB} + 1.04510\times10^{-6}\,\mathrm{AG} -$$

$0.000024\ \mathrm{BC}\ - 1.22761 \times$

$10^{-6}\ \mathrm{BG}$.. Equation 4.14

The design equation for categoric factors (subgrade as coarse (A-1); moisture as wet) is:

$\mathrm{Log}_{10}(\mathrm{AC\ Fatigue\ cracking\ (bottom\ up + reflective)}) = +1.72208 - 0.006339\ \mathrm{A} +$

$0.001717\mathrm{B} + +0.001390\ \mathrm{C} + 0.000623\ \mathrm{G} + 4.93597 \times 10^{-6}\ \mathrm{AB} + 1.04510 \times 10^{-6}\mathrm{AG} -$

$0.000024\ \mathrm{BC}\ - 1.22761 \times$

$10^{-6}\ \mathrm{BG}$.. Equation 4.15

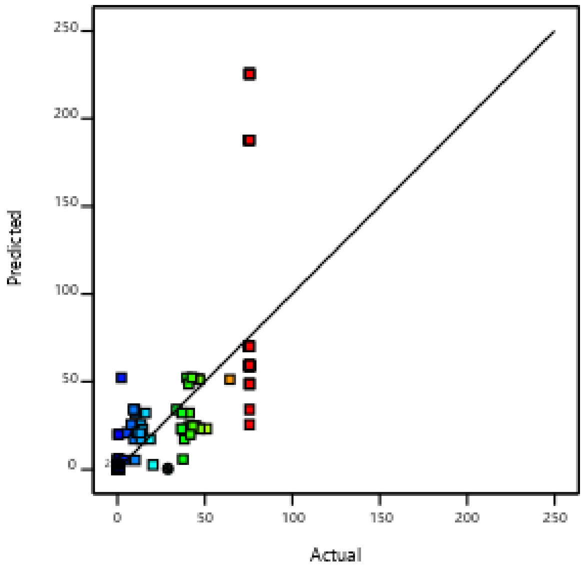

Figure 4.25: Predicted versus actual AC fatigue cracking (bottom up + reflective)

The predicted versus actual values are close to the line of equality for AC fatigue cracking as given in Figure 4.25. After obtaining the critical parameter affecting the AC fatigue cracking of the pavement, the conditions leading to the maximum and minimum asphalt thermal cracking in the layer have been studied. The result of the optimized factors for minimum and maximum factors are given below in Figure 4.26 and 4.27, respectively.

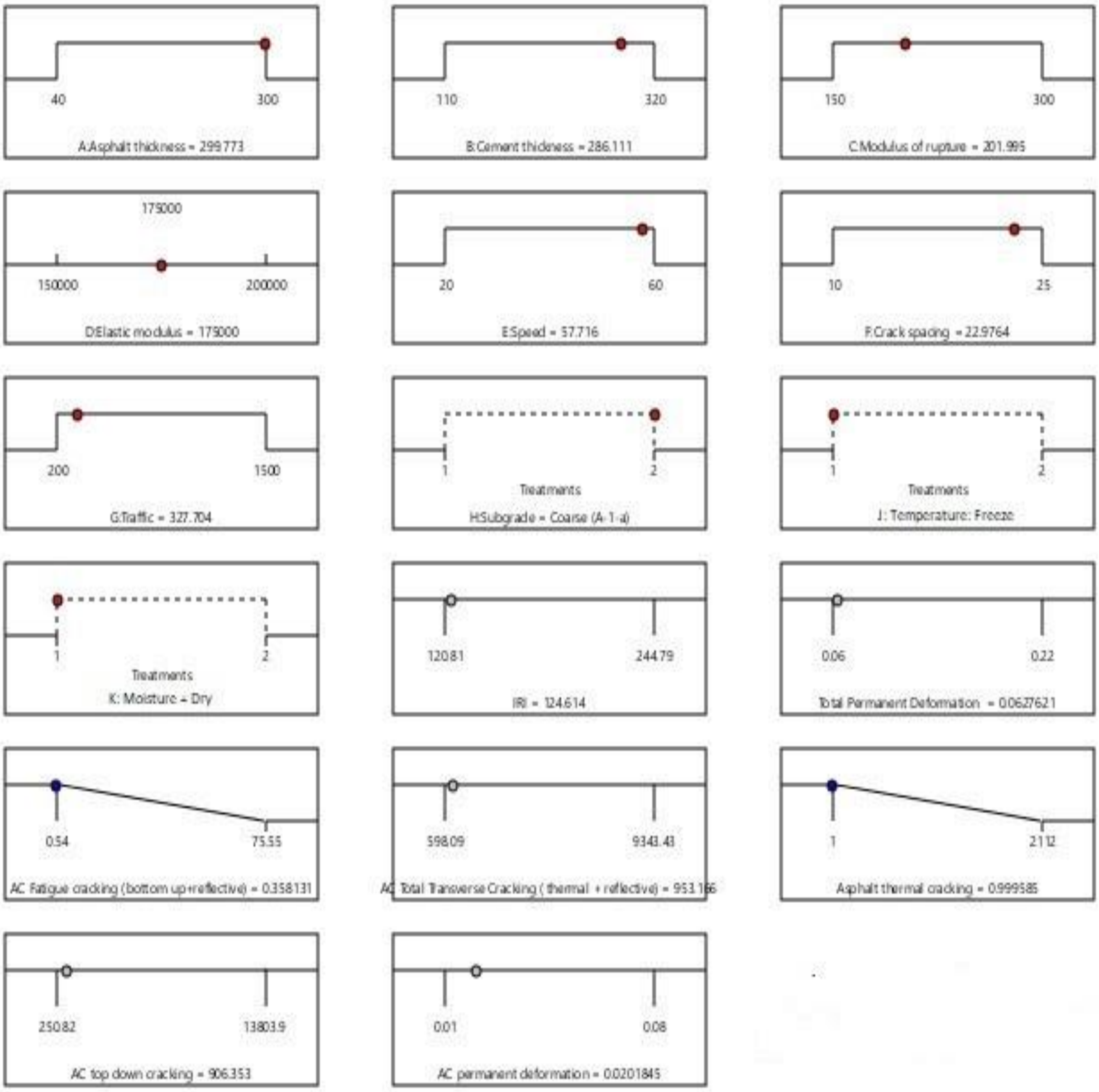

Figure 4.26: Optimized factor for minimum AC cracking (bottom up + reflective cracking)

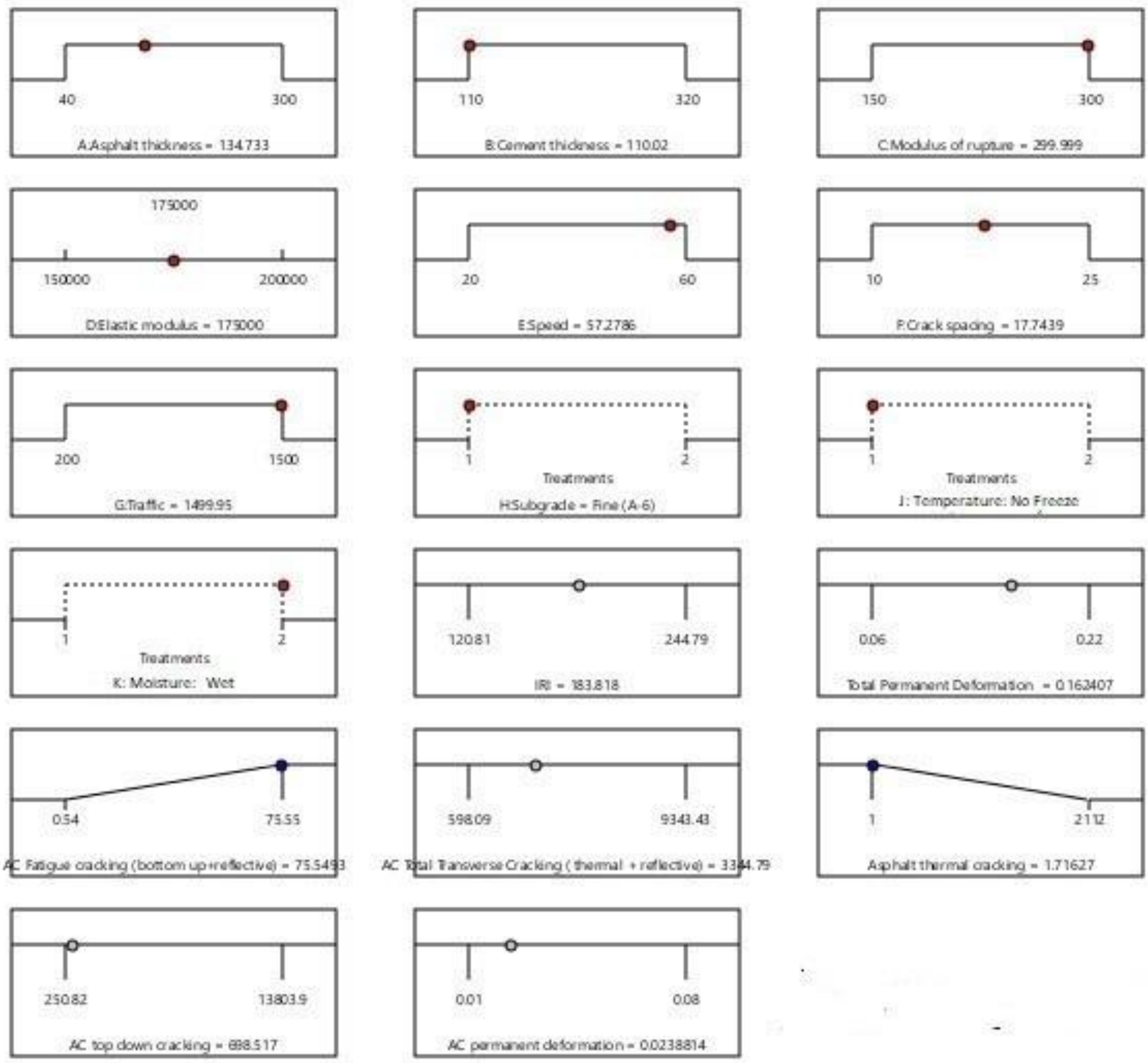

Figure 4.27: Optimized factor for maximum ac cracking (bottom up + reflective cracking)

4.2.8 Optimization of the pavement response based on the design limit of MEPDG.

The Table 3.5 suggest the distress limit that can be used to design the semi rigid pavement using MEDPG. The optimization of the factors used in the design can be achieved by limiting the pavement response to a limit taken in initial design. For example, the IRI terminal value is 172 in/mile. Figure 4.28, 4.29, 4.30, 4.31 and 4.32 denotes the optimized factors value for AC fatigue cracking (bottom up- + reflective), AC total cracking (thermal + reflective), AC thermal cracking, AC top down cracking, and IRI respectively.

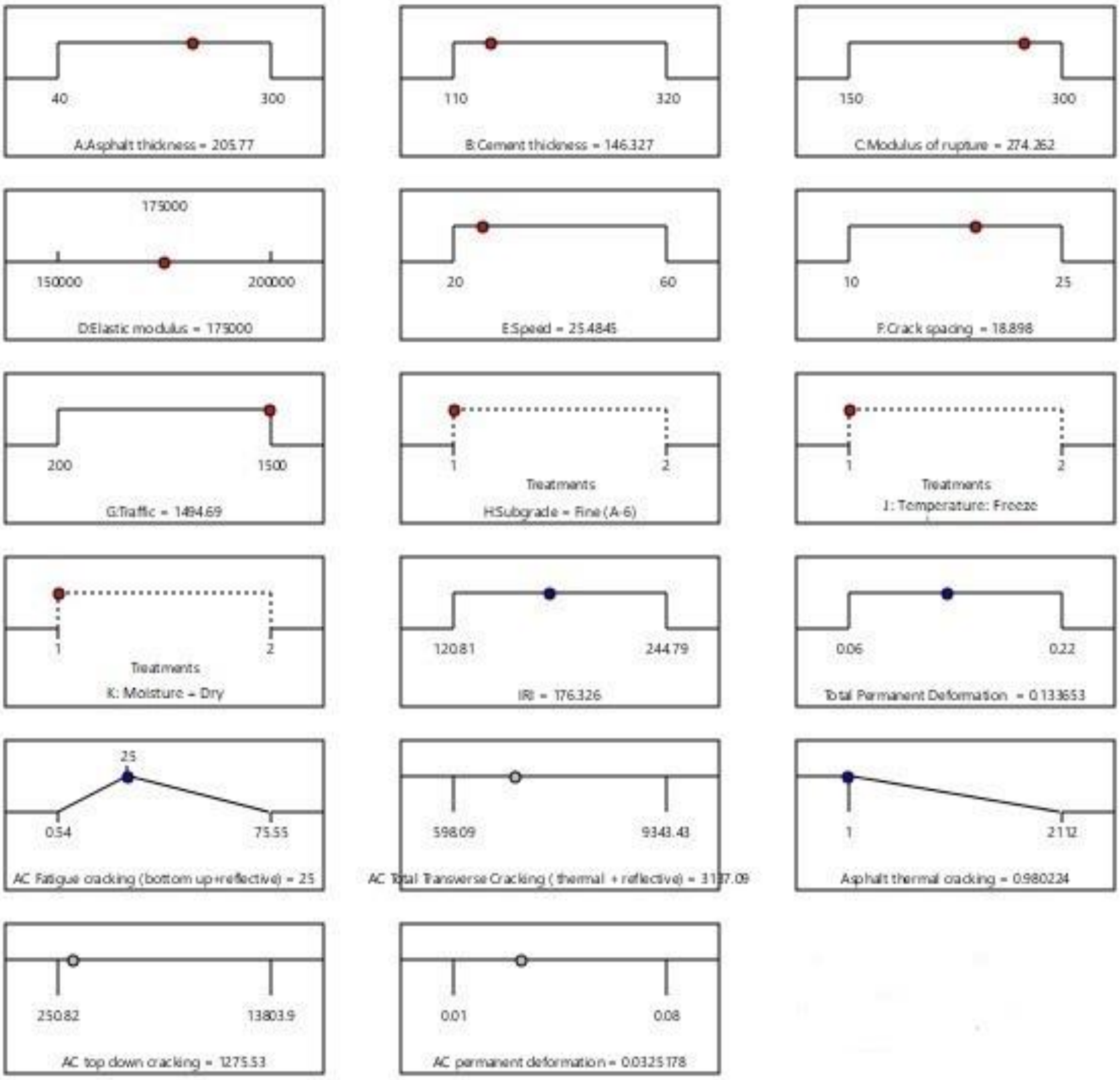

Figure 4.28: Optimized value of factors for the limit of MEPDG response, AC fatigue cracking (bottom up + reflective cracking)

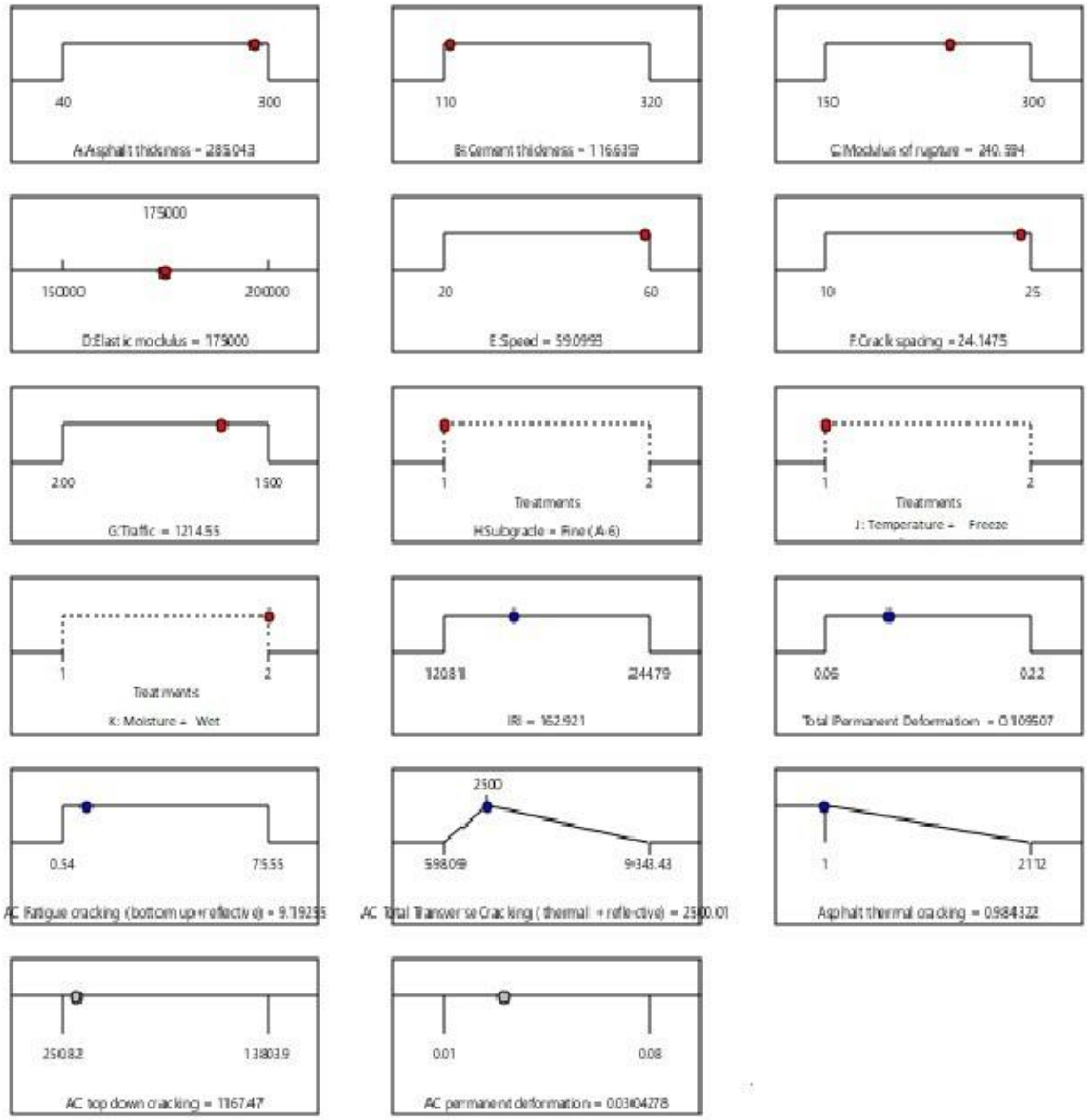

Figure 4.29: Optimized value of factors for the limit of MEPDG response, AC total cracking (thermal + reflective cracking)

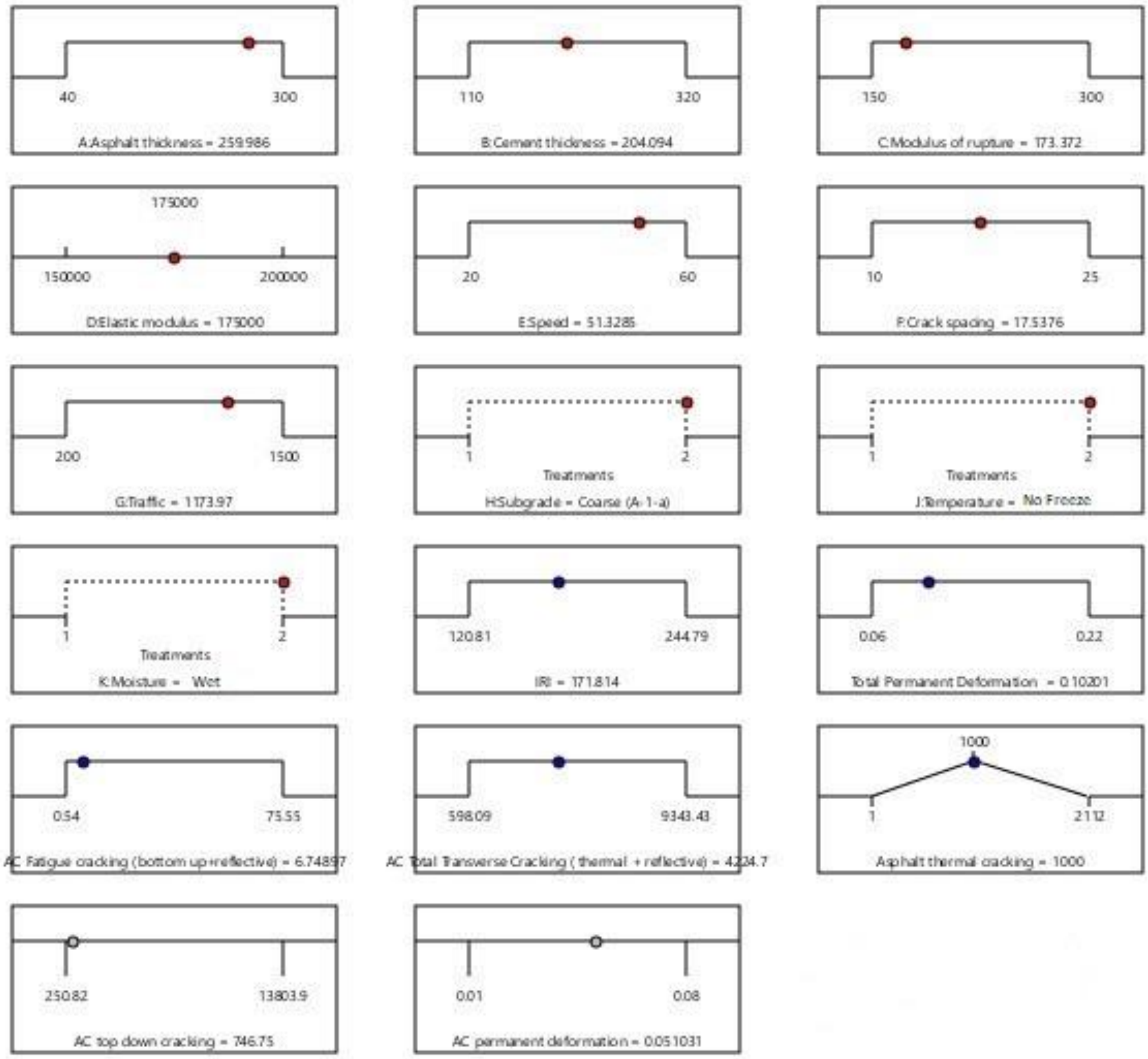

Figure 4.30: Optimized value of factors for the limit of MEPDG response, AC thermal cracking

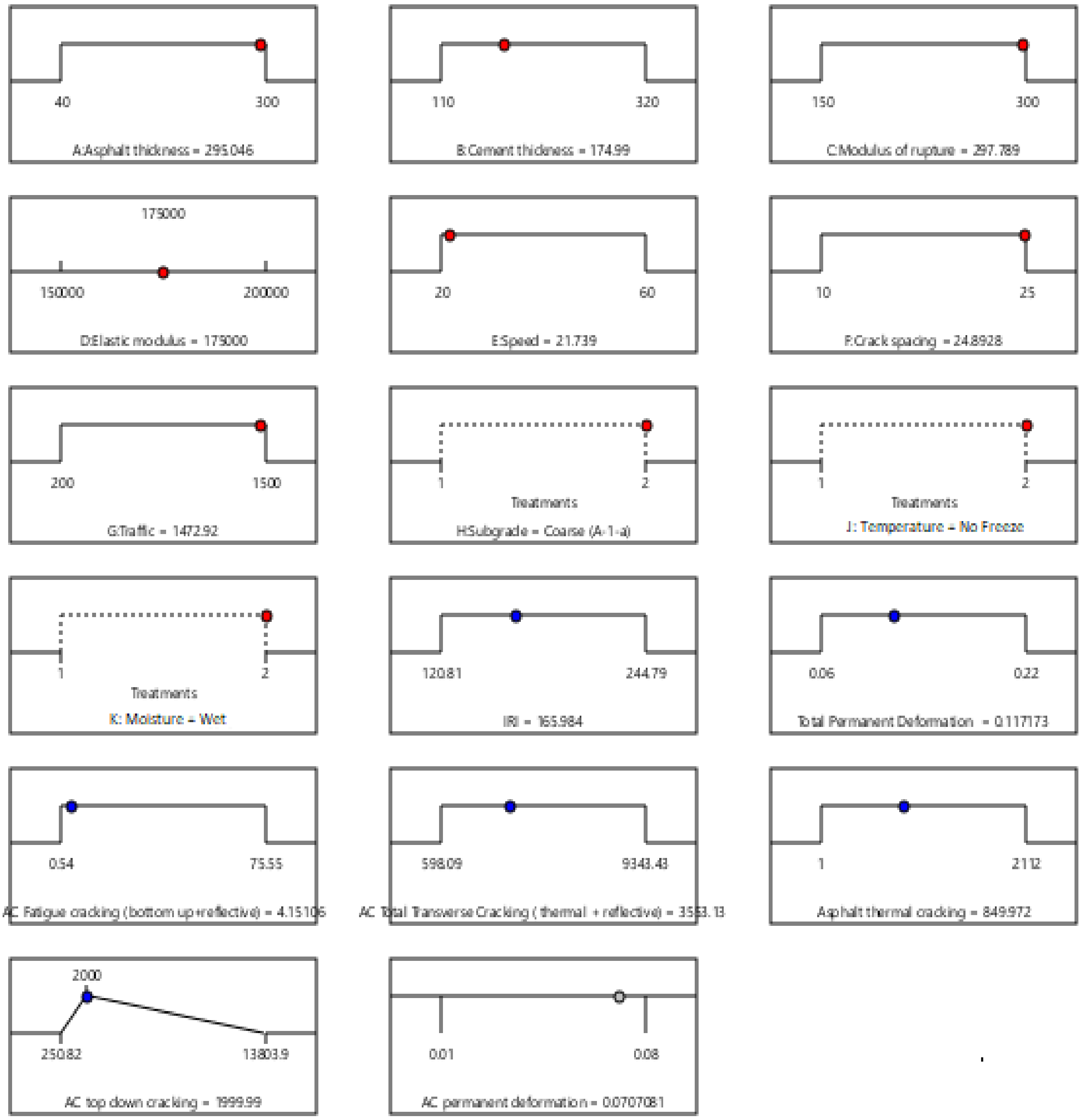

Figure 4.31:Optimized value of factors for the limit of MEPDG response, AC top-down cracking

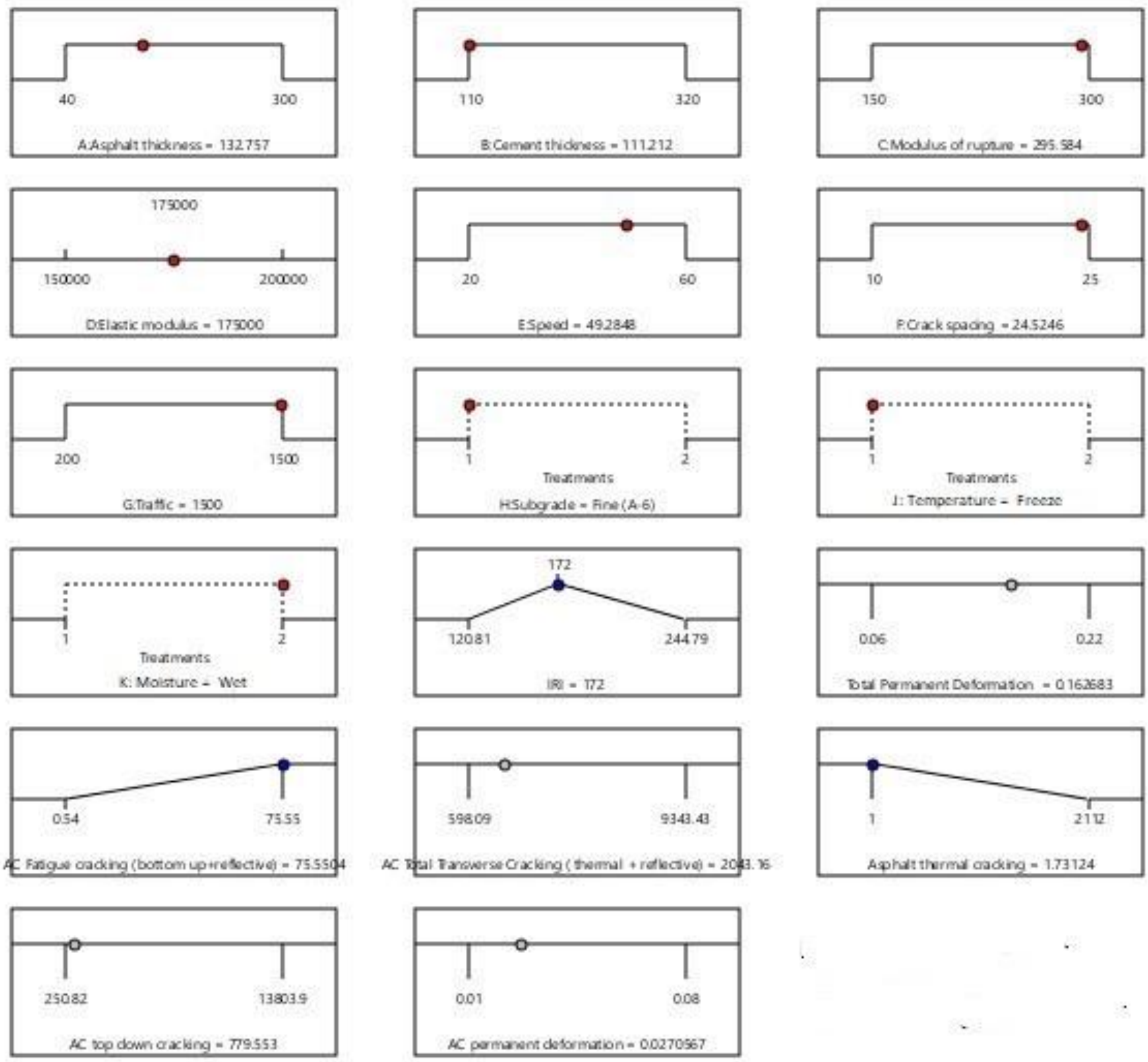

Figure 4.32: Optimized value of factors for the limit of MEPDG response, IRI

Furthermore, the optimized thickness of cement treated layers in the pavement in different climatic regions and subgrade conditions is given in Appendix III.

4.3 Phase 2: Factors Affecting Design of Inverted Pavement System

In the present case, it has been attempted to understand whether the use of a crack relief layer has any structural effect on the performance of the pavement in terms of strain/stress.

Inverted pavement is a pavement system where the supporting layer has higher stiffness than the top layer (Lewis et al., 2012). The pioneer of this pavement system, South Africa (De Beer,1996) defined this system as “a structural pavement system, where the static modulus of the unbound base layer is lower compared with the supporting (mainly lightly cementitious) subbase layers. Unbound base layer (crushed rock) of extremely high bearing capacity is usually covered with 12 mm to 50 mm asphalt layer for sealing and functional properties” (Tutumluer 2013). The pavement crust composition varies based on traffic and subgrade conditions. Though this pavement system is known by different names in different places such as inverted G1 base pavement (South Africa), stone interlayer pavement (Louisiana), upside-down pavement, sandwich pavement (Lewis et. al., 2012), the basic design principle remains the same. The construction cost of an inverted pavement has been reported to be 22.3 % cheaper than the conventional flexible pavement. The performance of this pavement has been found to be equivalent or better than the other systems (Tutumluer, 2013). From the field performance, the performance of inverted pavement has been found better in terms of deflection measured on many road sections such as Morgon County, Louisiana and Santa Fe. Also, the surface cracking through visual inspection has been less than in conventional pavement. The economic consideration of the inverted pavement has been compared with the conventional pavement and have been at par with flexible pavement (Santamarina, 2014).

The inverted pavement consists of the asphalt layer, unbound aggregate layer, cement treated layer on a prepared subgrade. The asphalt layer acts as a seal and provides a good riding quality. It acts as a membrane rather than a beam (Papadopoulos and Santamarina, 2017). Also, there is a minimum thickness of the asphalt layer recommended to prevent cracking. Based on the research, a minimum thickness of 50 mm for asphalt layer is recommended (Papadopoulos and Santamarina, 2014). The aggregate layer is composed of good quality aggregate and it is always under compression. The compaction of this layer is by achieving 101-106% of maximum dry density, which is equal to the 86-88% of apparent density. This technique is used by South Africa to increase the packing density through slushing technique. However, the U.S. experience has shown that the performance of this pavement system is independent of whether slushing technique is used or not, based on the field performance (Lewis et. al, 2012). In India, the slushing technique is not recommended. The density of the aggregate layer constructed on the cement-stabilized layer is found to be higher than equivalent granular flexible pavement structure. For instance, the achieved density of aggregate layer over stabilized base and the unstabilized base was found to be 105% and 100%, respectively (Barksdale, 1984). In addition, the reported resilient modulus of confined aggregate layer between asphalt and cement treated base layer is more than the conventional aggregate base layer (Papadopoulos, 2014).

4.3.1 Theoretical and experimental framework

Since this design system is not readily available in the North American pavement design system, the design equation was adopted from international literature. The design equation used for various response in an inverted pavement layers consist of life in fatigue, and rutting given in equation 4.16, 4.17 and 4.18 (IRC:37-2018).

$$N_f = 2.21 * 10^{-4} \left(\frac{1}{\varepsilon_{tb}}\right)^{3.89} \left(\frac{1}{E}\right)^{0.854} \text{ .... Equation 4.16}$$

$$N_R = 4.1656 * 10^{-8} \left(\frac{1}{\varepsilon_v}\right)^{4.5337} \text{ .... Equation 4.17}$$

$$N = RF\left[\frac{\frac{11300}{E_c}^{0.0804} + 191}{\varepsilon_t}\right]^{12} \text{ .... Equation 4.18}$$

N_f = Number of cumulative standard axles to produce 20 % cracked surface area.

N_R= Number of cumulative standard axles to produce rutting of 20 mm

E= Elastic modulus of bituminous surface at 35°C

E_C= Elastic modulus of cementitious layer

ε_t = Horizontal tensile stress at the bottom of the cement treated base layer

ε_{tb} = Horizontal tensile stress at the bottom of the bituminous layer

ε_v = Vertical compressive strain at the top of subgrade

N = Number of cumulative standard axles for fatigue cracking

RF= Reliability factor

4.3.2 Input parameter in DoE

The concept of inverted pavement has been recently introduced in the Indian design code. Similar to the design of cement treated base pavement, Indian Road Congress (IRC) code was used to input the parameters. The use of IRC code was done to facilitate the comparison as equivalent pavement sections could not be found in LTPP section and MEPDG does not facilitate analysis of these pavement systems. However, efforts are underway to include these sections in MEDPG based on the research work. The number of factors for DoE has been decided based on the IRC: 37-2018. The various values used in the design of experiment are as follows:

1. Bituminous layer thickness

The code considered the minimum design thickness of 40 mm for design of 5 million standard axles with 5% CBR value and maximum value of 100 mm for a traffic of 50 million standard axle.

2. Bituminous layer modulus

The resilient modulus value is considered at two-level for viscosity grade (VG)-30 and VG - 40. The standard value of resilient modulus for VG-30 and VG-40 binder are 2000 MPa and

3000 MPa, respectively at 35 °C. These two binders are considered in the majority of the state in country (IRC: 37).

3. Aggregate layer thickness

The aggregate layer is basically used as the crack relief layer and in some cases where similar composition expect aggregate layer is called cemented stabilized pavement. Therefore, two cases are considered in present case, one with aggregate layer thickness of 100 mm and the other with no aggregate layer. The value of 100 mm is recommended (AASHTO 1993, IRC: 37- 2018 and Sha et al., 2020).

4. Aggregate layer modulus

The highest modulus considered for good quality aggregate is 450 MPa. This value is recommended by South African researchers and it is adopted in IRC: 37. However, many researchers (Biswal et al., 2020; Beriha et al., 2020; Beriha and Sahoo, 2020) have pointed out the stress dependent and cross anisotropic properties of the aggregate layer in the inverted pavement due to its proximity to bituminous layer. Therefore, anisotropy is considered at two levels such as 0.5 and 1 (representing 450 MPa modulus). The value of 0.5 represents the modulus in horizontal direction is 0.5 times in vertical direction.

5. Cement treated base layer thickness

The strongest layer in the inverted pavement design is the cemented treated base layer. The minimum thickness recommended in the IRC specification is 100 mm and maximum value is suggested up to 200 mm for a different design condition and subgrade condition as given design catalogue (IRC:37 gives different combination of thickness in form of plate 1 to 48 for CBR 5-15% and traffic 5 -50 MSA).

6. Cement treated base layer modulus

The minimum recommended modulus after 28 days curing period is 5000 MPa in IRC: 37. AASHTO 1993 has given a nomograph for the determination of elastic modulus from unconfined compressive strength (UCS) of the material. Many published specifications (AUSTROAD, 2004; IRC:37) report that the elastic modulus after 28 days is 1000-1250 times the UCS value. However, the minimum curing period in many literatures is 7 days. So, there is some discrepancy in curing period and minimum strength required time span. It is best to have both requirements at 7 days or 28 days to make it consistent for designers and practitioners Therefore, the elastic modulus of 7 days and 28 days are considered in the present case from published literature (Sounthararajah et al., 2018). The elastic modulus value at 7 and 28 days is 7475 MPa and 11525 MPa, respectively.

7. Cement treated subbase layer thickness

The present IRC specification suggests a value of a minimum and maximum value of 100 mm and 200 mm for different design compositions (IRC: 37). Therefore, these levels are considered in this phase.

8. Cement treated subbase layer modulus

The subbase can be either stabilized with cement and can also be of a granular layer. The modulus value of 600 MPa is suggested in the present IRC specification for stabilized subbase (IRC: 37). The value of 200 MPa is suggested for the granular layer.

9. CBR

The subgrade CBR varied from 5% and 15 % in the present IRC specification. However, two levels of 5% and 10% are considered in the analysis to simulate the minimum and fair subgrade condition. The corresponding modulus values for 5% and 15% subgrade are 50 MPa and 76 MPa, respectively (IRC: 37).

10. Pressure

The standard pressure considered for the design of pavements is 0.56 MPa (IRC:37). Therefore, a condition with higher pressure is also considered with a value of 0.7 MPa.

Initially, a minimum run 2^K factorial design was tried with center points. In the result, curvature was found to be significant, therefore, central composite design with one face centered point and a total of 77 runs of the software application was done as per minimum run resolution five design. Response Surface Methodology (RSM) design called Central Composite designs (CCD) are based on 2-level factorial designs, augmented with center and axial points are used to fit the model. RSM is used for the optimization of the input factors (Lye, 2020).

4.3.3 Response

The pavement responses in terms of vertical compressive strain on subgrade and horizontal tensile strain below the bituminous layer and cemented base layer are the main interests for the designer. The pavement responses were calculated from a pavement design software, named CROSSPAVE. The software application is validated with the standard result (field result) and more details about the application of software can be found in research paper by Brundaban et al., 2020. All the possible combination of input from the data set was tried using face centred CCD model. The box plot of the response data is shown in Figure 4.33.

4.3.4 Model considered in DoE

Response Surface Method

The Response surface method is “a collection of mathematical and statistical techniques that are useful for the modelling and analysis of problems in which a response of interest is influenced by several variables and the objective is to optimize the response” (Montgomery, 1997).

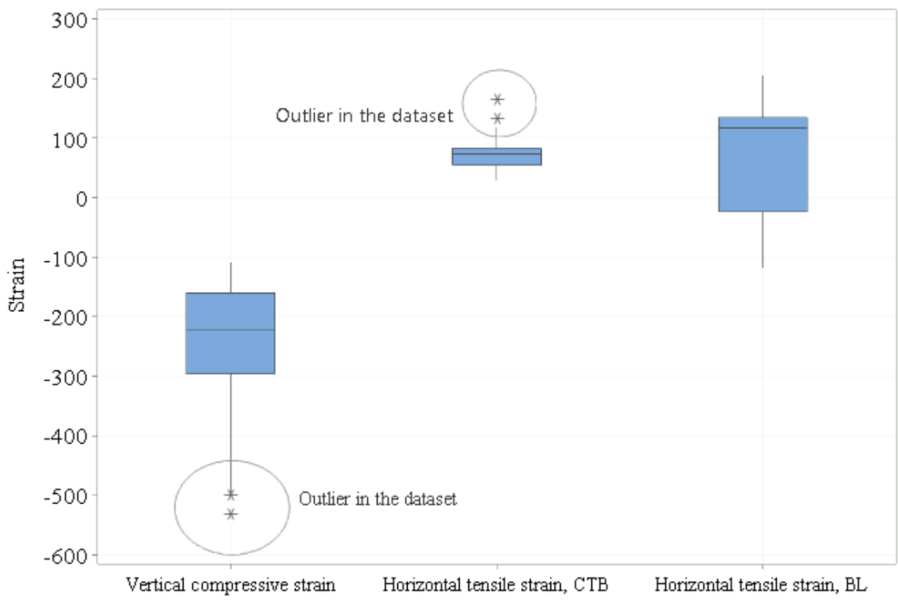

Figure 4.33: Box plot for the pavement response from CROSSPAVE

To start with, in RSM, the form of relationship between the response and the independent variable is unknown. Therefore, the following method is employed is most cases to come with a relationship between the variable (Donnelly, 1984).

- To find a suitable approximation of the true functional relationship between y and the set of independent variables. In the case of linear function between the independent variables, equation 4.19 is used to represent first-order model.
- If the curvature is significant based on the response of the system, the higher-order equation is used as given in equation 4.20.

$$y = \beta_0 + \beta_1 x_1 + \beta_2 x_2 + \cdots \ldots \ldots . + \beta_k x_k + \varepsilon \ldots \ldots \ldots \ldots \ldots \ldots \ldots \ldots \ldots \text{Equation 4.19}$$

$$y = \beta_0 + \sum_{1}^{k} \beta_i x_i + \sum_{1}^{k} \beta_{ii} x_i^2 + \sum\sum_{i<j} \beta_{ij} x_i x_j + \varepsilon \ldots \ldots \ldots \ldots \ldots \ldots \ldots \ldots \text{Equation 4.20}$$

In which β_0 is the constant term, β_i, β_{ij} and β_{ii} are the coefficients of the linear, interaction, and quadratic, respectively, and ε is the residual associated to the experiments.

There are different RSM available in DoE, such as Box Behnken Design (BBD) and Central Composite Design (CCD). The CCD has an advantage over BBD when the number of factors is more than four (Lye, 2020). Furthermore, three types of central composite designs namely circumscribed, face-centred, and inscribed, are available (El Hami and Pougnet, 2020). In the present case, face centred design with three levels and one centre point as the response factor in the design has been used from pavement software application.

4.3.5 Analysis with DoE

Three pavement responses were studied including vertical compressive strain, horizontal tensile strain below cement treated base, and horizontal tensile strain below bituminous layer. The outlier in the Figure 4.33 was excluded from the study. The input factors for DoE are given in Table 4.15.

Table 4.15: Input parameter used in the design of inverted pavement through DoE

Factor	Name	Unit-s	Type	Mini-mum	Maxi-mum	Coded Low	Coded High
A	Bituminous layer modulus	MPa	Numeric	-1	1	-1 ↔ -1.00	+1 ↔ 1.00
B	Bituminous layer thickness	mm	Numeric	-1	1	-1 ↔ -1.00	+1 ↔ 1.00
C	Aggregate interlayer modulus	MPa	Numeric	-1	1	-1 ↔ -1.00	+1 ↔ 1.00
D	Aggregate interlayer thickness	mm	Numeric	-1	1	-1 ↔ -1.00	+1 ↔ 1.00
E	Cement treated base layer, modulus	MPa	Numeric	-1	1	-1 ↔ -1.00	+1 ↔ 1.00
F	Cement treated base layer, thickness	mm	Numeric	-1	1	-1 ↔ -1.00	+1 ↔ 1.00
G	Cement treated subbase layer, modulus	MPa	Numeric	-1	1	-1 ↔ -1.00	+1 ↔ 1.00
H	Cement treated subbase layer, thickness	mm	Numeric	-1	1	-1 ↔ -1.00	+1 ↔ 1.00
J	Subgrade, modulus	MPa	Numeric	-1	1	-1 ↔ -1.00	+1 ↔ 1.00
K	Pressure	MPa	Numeric	-1	1	-1 ↔ -1.00	+1 ↔ 1.00

I. Vertical compressive strain at the top of the subgrade

First the response, vertical compressive strain is selected based on the input parameter as given in Table 4.16. Different models are available for the analysis and it is given in Table 4.16.

Table 4.16: Various available model available for response 1: vertical compressive strain

Source	Sequential p-value	Adjusted R^2	Predicted R^2	
Linear	< 0.0001	0.98	0.9745	Suggested
Quadratic	0.026	0.9969	0.7222	Suggested
Cubic				Aliased

It is clear that only two models, i.e., linear and quadratic, are suitable for the vertical compressive strain response. However, the predicted R^2 value for the linear model is better than the quadratic model. Therefore, the linear model is preferred in this analysis. The quadratic model means some terms will be of second order in the model.

The response parameter vertical compressive strain was studied as the function of different input parameters. The most significant factor affecting the pavement response, vertical compressive strain has been reported here. The assumption of the model is met and is checked in terms of normality plot of the residuals, residuals versus predicted, residuals versus run, and box-cox transform are met. The assumption for box cox transformation suggests the power transformation and given in Figure 4.34.

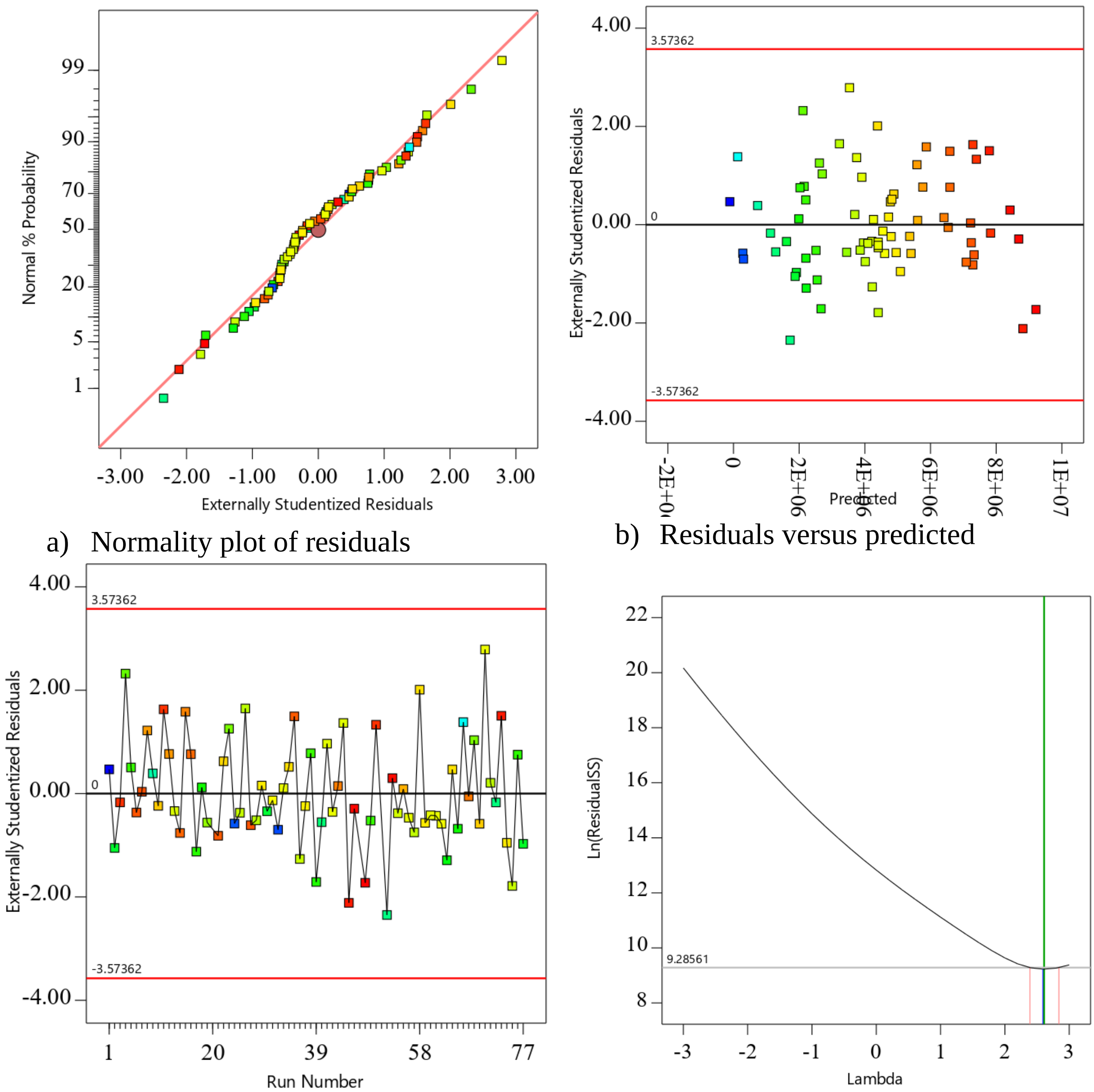

a) Normality plot of residuals
b) Residuals versus predicted
c) Residuals versus run
d) Box-cox transform

Figure 4.34: Assumptions of the model for vertical compressive strain

From the above the Figure 4.34, it is clear all the assumptions are satisfied. The same was achieved through box-cox power transform. After verifying the significant factors are selected in the model using ANOVA and are given in Table 4.17 below.

Table 4.17: ANOVA for response 1: vertical compressive strain with reduced linear model

Source	Sum of Squares	df	Mean Square	F-value	p-value
Model	3.77E+14	8	4.71E+13	447.27	< 0.0001
A-Bituminous layer modulus	2.18E+12	1	2.18E+12	20.66	< 0.0001
B-Bituminous layer thickness	5.17E+13	1	5.17E+13	491.01	< 0.0001
D-Aggregate interlayer thickness	1.11E+13	1	1.11E+13	105.01	< 0.0001
E-Cement treated base layer, modulus	8.81E+12	1	8.81E+12	83.62	< 0.0001
F-Cement treated base layer, thickness	2.65E+14	1	2.65E+14	2514.5	< 0.0001
G-Cement treated subbase layer, modulus	1.15E+12	1	1.15E+12	10.93	0.0015
H-Cement treated subbase layer, thickness	5.59E+12	1	5.59E+12	53.02	< 0.0001
J-Subgrade, modulus	1.69E+13	1	1.69E+13	160.17	< 0.0001
Residual	6.85E+12	65	1.05E+11		
Cor Total	3.84E+14	73			

The Model F-value of 447.27 implies the model is significant. There is only a 0.01% chance that an F-value this large could occur due to noise. P-values less than 0.0500 indicate model terms are significant. In this case A, B, D, E, F, G, H, and J are significant model terms. Values greater than 0.1000 indicate the model terms are not significant.

Table 4.18: Fit statistics of the model and model comparison statistics

Std. Dev.	3.25E+05	**R^2**	0.9822
Mean	4.32E+06	**Adjusted R^2**	0.98
C.V. %	7.51	**Predicted R^2**	0.9758
		Adeq Precision	82.3445
PRESS			9.31E+12
-2 Log Likelihood			2078.59
BIC			2117.33
AICc			2099.4

The Predicted R^2 of 0.9758 is in reasonable agreement with the Adjusted R^2 of 0.9800; i.e. the difference is less than 0.2. Adeq Precision measures the signal to noise ratio. A ratio greater than 4 is desirable.

The equation to determine the vertical compressive strain in the inverted pavement with factors considered in the present model is given by the equation below.

$$(\text{Vertical Compressive Strain} + 585.00)^{2.59} = 10^5(44.06 + 1.959\text{A} + 9.60\text{B} + 4.47\text{D} + 3.94\text{E} + 21.93\text{F} + 1.43\text{G} + 3.15\text{H} + 05 + 5.47\text{J}) \ldots\ldots\ldots\ldots\ldots\ldots\ldots\ldots\ldots.\ldots.\text{Equation 4.21}$$

Where A = bituminous layer modulus,

B = bituminous layer thickness,

D = aggregate interlayer modulus,

E = cement treated base layer thickness,

F = cement treated base layer modulus,

G = cement treated subbase layer modulus,

H = cement treated subbase layer thickness and

J = Subgrade respectively.

The equation in terms of actual factors can be used to make predictions about the response for given levels of each factor. Here, the levels should be specified in the original units for each factor. This equation should not be used to determine the relative impact of each factor because the coefficients are scaled to accommodate the units of each factor and the intercept is not at the center of the design space.

Furthermore, the predicted versus the actual response of the vertical compressive strain is given in Figure 4.35 below. It is clear that the predicted versus the actual value are close to the line of equality for the response (vertical compressive strain).

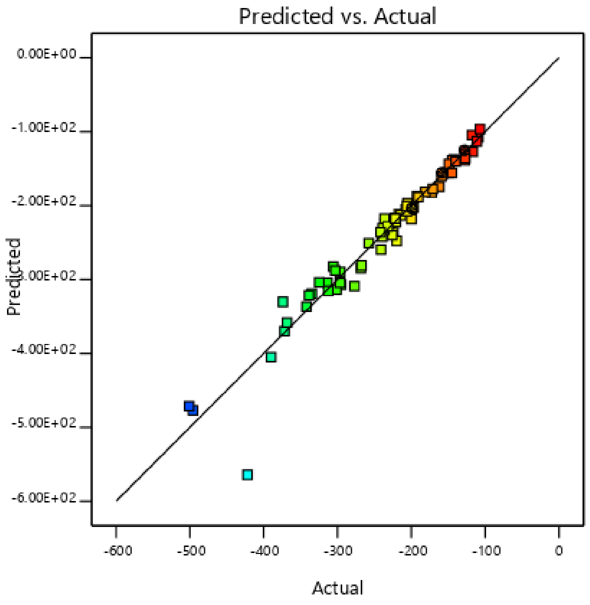

Figure 4.35: Predicted versus the actual response parameter for the design of the vertical compressive strain

II. Horizontal tensile strain below cement treated base

Different models for the pavement response horizontal tensile strain below cement treated base is studied such as linear, two factor interaction, and quadratic model as given in Table 4.19.

Table 4.19: Model suggestion for horizontal tensile strain in the inverted pavement

Source	Sequential p-value	Adjusted R^2	Predicted R^2
Linear	**< 0.0001**	**0.9311**	**0.9239**
2FI	0.9942	0.8785	-15.867
Quadratic	0.1959	0.9177	-8.936

From Table 4.19, the linear model is selected for the response, horizontal tensile strain below the bituminous layer. The assumptions of the suggested linear model is given below

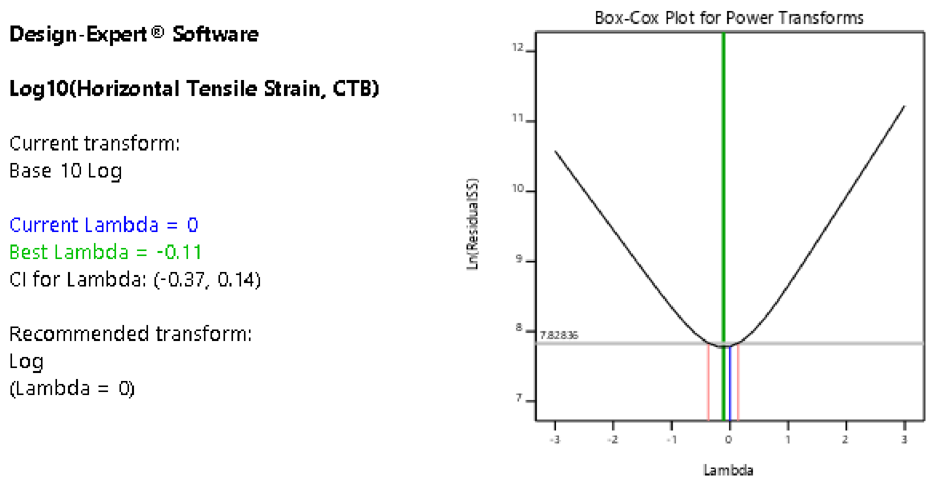

Figure 4.36: Assumption of the horizontal tensile strain in the model

All the assumptions of the model are satisfied. Furthermore, the predicted versus the actual values are close to the line of equality. The ANOVA for the model is given in Table 4.20.

Table 4.20: ANOVA for the response 2: horizontal tensile strain, CTB in inverted pavement

Source	Sum of Squares	df	Mean Square	F-value	p-value
Model	1.56	8	0.1947	126.03	< 0.0001
A-Bituminous layer modulus	0.0055	1	0.0055	3.56	0.0638
B-Bituminous layer thickness	0.2901	1	0.2901	187.74	< 0.0001
D-Aggregate interlayer thickness	0.0999	1	0.0999	64.65	< 0.0001
E-Cement treated base layer, modulus	0.104	1	0.104	67.3	< 0.0001
F-Cement treated base layer, thickness	0.8898	1	0.8898	575.91	< 0.0001
G-Cement treated subbase layer, modulus	0.0887	1	0.0887	57.39	< 0.0001
H-Cement treated subbase layer, thickness	0.0336	1	0.0336	21.76	< 0.0001

J-Subgrade, modulus	0.0207	1	0.0207	13.38	0.0005
Residual	0.1004	65	0.0015		
Cor Total	1.66	0.73			

The Model F-value of 126.03 implies the model is significant. There is only a 0.01% chance that an F-value this large could occur due to noise. P-values less than 0.0500 indicate model terms are significant. In this case, B, D, E, F, G, H, and J are significant model terms. Values greater than 0.1000 indicate the model terms are not significant. Table 4.21 gives the fit statistics of the model.

Table 4.21: Fit Statistics and model comparison statistics

Std. Dev.	0.0393	**R^2**	0.9394
Mean	1.83	**Adjusted R^2**	0.932
C.V. %	2.15	**Predicted R^2**	0.9263
		Adeq Precision	50.8342
PRESS	0.1223		
-2 Log Likelihood			-278.57
BIC			-239.84
AICc			-257.76

The Predicted R^2 of 0.9263 is in reasonable agreement with the Adjusted R^2 of 0.9320; i.e., the difference is less than 0.2. Adeq Precision measures the signal to noise ratio. A ratio greater than 4 is desirable. The ratio of 50.834 indicates an adequate signal. The equation for the response is given below.

$$\mathrm{Log}_{10}(\text{Horizontal Tensile Strain, CTB}) = +1.82 - 0.00984\,A - 0.0718\,B - 0.0425\,D - 0.0428E - 0.127\,F - 0.0397\,G - 0.0244\,H - 0.0191\,J \ldots\ldots\ldots\ldots\ldots\ldots \text{Equation 4.22}$$

where

A = bituminous layer modulus,

B = bituminous layer thickness,

D = aggregate interlayer modulus,

F = cement treated base layer modulus,

G = cement treated subbase layer modulus,

H = cement treated subbase layer thickness and

J = Subgrade modulus.

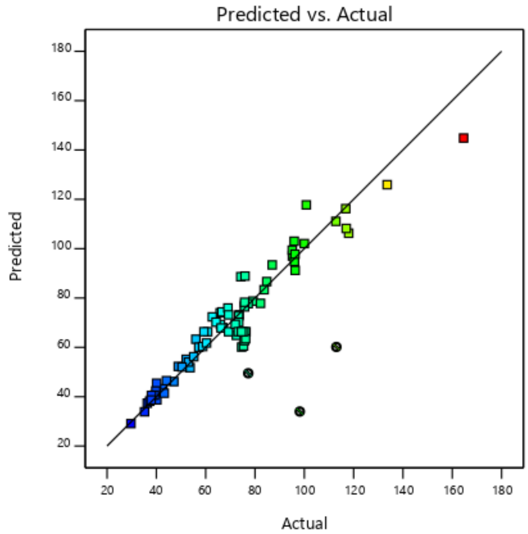

Figure 4.37: Predicted versus actual value of the response, tensile strain at the bottom of bituminous layer

III. Horizontal tensile strain below bituminous layer

The response parameter horizontal tensile strain below bituminous layer was studied as the function of different input parameters. The most significant factors affecting the pavement response, horizontal tensile strain below the bituminous layer has been reported here. The assumption of the model is checked and is met in terms of normality plot of the residuals, residuals versus predicted, residuals versus run, and box-cox transform. The assumption for box cox transformation suggests the power transformation and given in Figure 4.38.

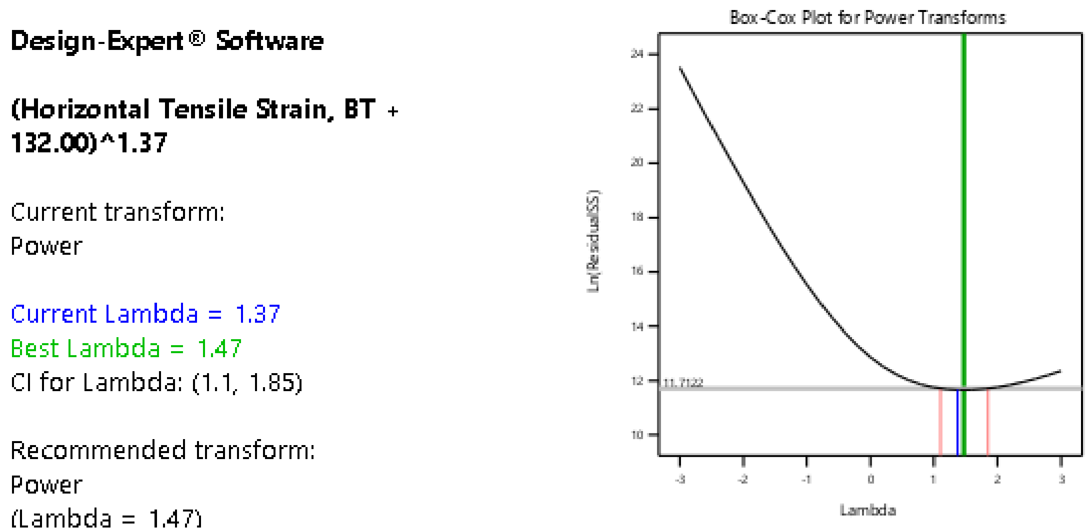

Figure 4.38: Assumption of the model for response 3, horizontal tensile strain in pavement layer

Table 4.22 represents the significant factors affecting the horizontal tensile strain in the inverted pavement.

Table 4.22: ANOVA for the response 3: horizontal tensile strain, BT in the inverted pavement

Source	Sum of Squares	df	Mean Square	F-value	p-value	
Model	4.45E+07	2	2.22E+07	169.44	< 0.0001	significant
D-Aggregate interlayer thickness	4.41E+07	1	4.41E+07	336.16	< 0.0001	
K-Pressure	5.18E+05	1	5.18E+05	3.94	0.051	
Residual	9.32E+06	71	1.31E+05			
Cor Total	5.38E+07	73				

The Model F-value of 169.44 implies the model is significant. There is only a 0.01% chance that an F-value this large could occur due to noise**.** P-values less than 0.0500 indicate model terms are significant. In this case D is a significant model term. Values greater than 0.1000 indicate the model terms are not significant. Table 4.23 gives the fit statistics of the model.

Table 4.23: Fit statistics and model comparison statistics for the response

Std. Dev.	362.32	**R^2**	0.8268
Mean	1452.1	**Adjusted R^2**	0.8219
C.V. %	24.95	**Predicted R^2**	0.8157

		Adeq Precision	26.9654
PRESS	9.92E+06		
-2 Log Likelihood	1079.04		
BIC	1091.95		
AICc	1085.38		

The Predicted R^2 of 0.8157 is in reasonable agreement with the Adjusted R^2 of 0.8219; i.e., the difference is less than 0.2. Adeq Precision measures the signal to noise ratio. A ratio greater than 4 is desirable. The equation for horizontal tensile strain in bituminous layer is given by:

$$(\text{Horizontal Tensile Strain, BT} + 132.00)^{1.37} = 1477.39 + 888.28\,\text{D} + 95.31\,\text{K} \ldots\ldots\ldots \text{Equation 4.23}$$

Where,

D = Aggregate interlayer thickness and

K = pressure respectively

The Table 4.24 gives the coefficient of the different responses in the pavement design namely, vertical compressive strain, horizontal tensile strain below cemented layer, and horizontal tensile strain below bituminous layer. Figure 4.39 and Figure 4.40 denote the optimized factors for the design of maximum vertical compressive strain and minimum compressive strain, respectively. Figure 4.41 givens the optimized factors for a tensile strain value of 72 microns in CTB. Different values of tensile strain are suggested, the value of 72 is chosen because it is approximately midway between the range of 29 micron and 120 micron.

Table 4.24: The Coefficient Table for different response considered in the model

	Intercept	**A**	**B**	**D**	**E**	**F**	**G**	**H**	**J**	**K**
(Vertical Compressive Strain + 585.00)^2.59	4.41E+06	195920	960050	447421	394145	2.19E+06	143049	315022	547470	
p-values		< **0.0001**	< **0.0001**	< **0.0001**	< **0.0001**	< **0.0001**	**0.0015**	< **0.0001**	< **0.0001**	
Log_{10}(Horizontal Tensile Strain, CTB)	1.82006	-0.00984	-0.07188	-0.04251	-0.04282	-0.12708	-0.0397	-0.02444	-0.01916	
p-values		**0.0638**	< **0.0001**	< **0.0001**	< **0.0001**	< **0.0001**	< **0.0001**	< **0.0001**	**0.0005**	
(Horizontal Tensile Strain, BT + 132.00)^1.37	1477.39			888.286						95.3088
p-values				< 0.0001						0.051

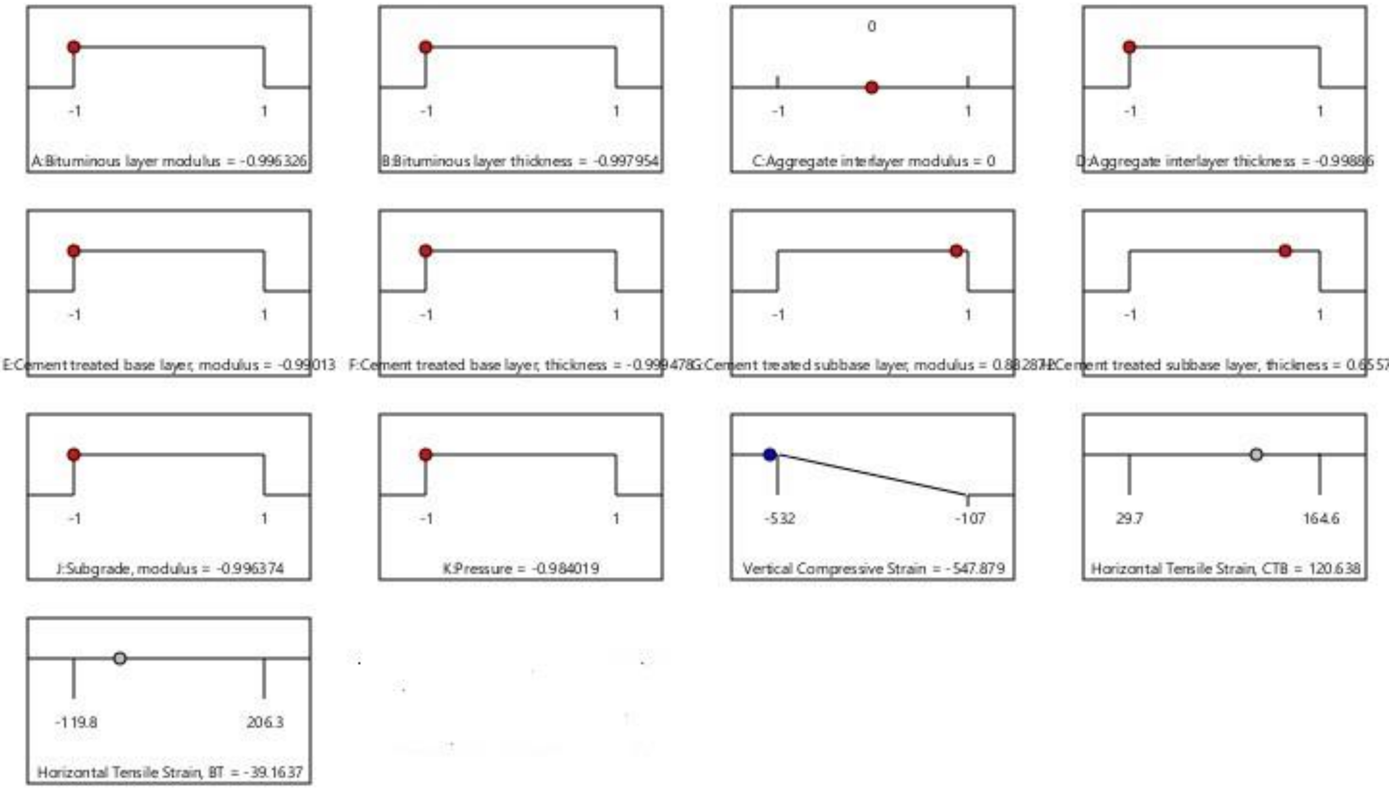

Figure 4.39: Optimized factors for the maximum vertical compressive strain

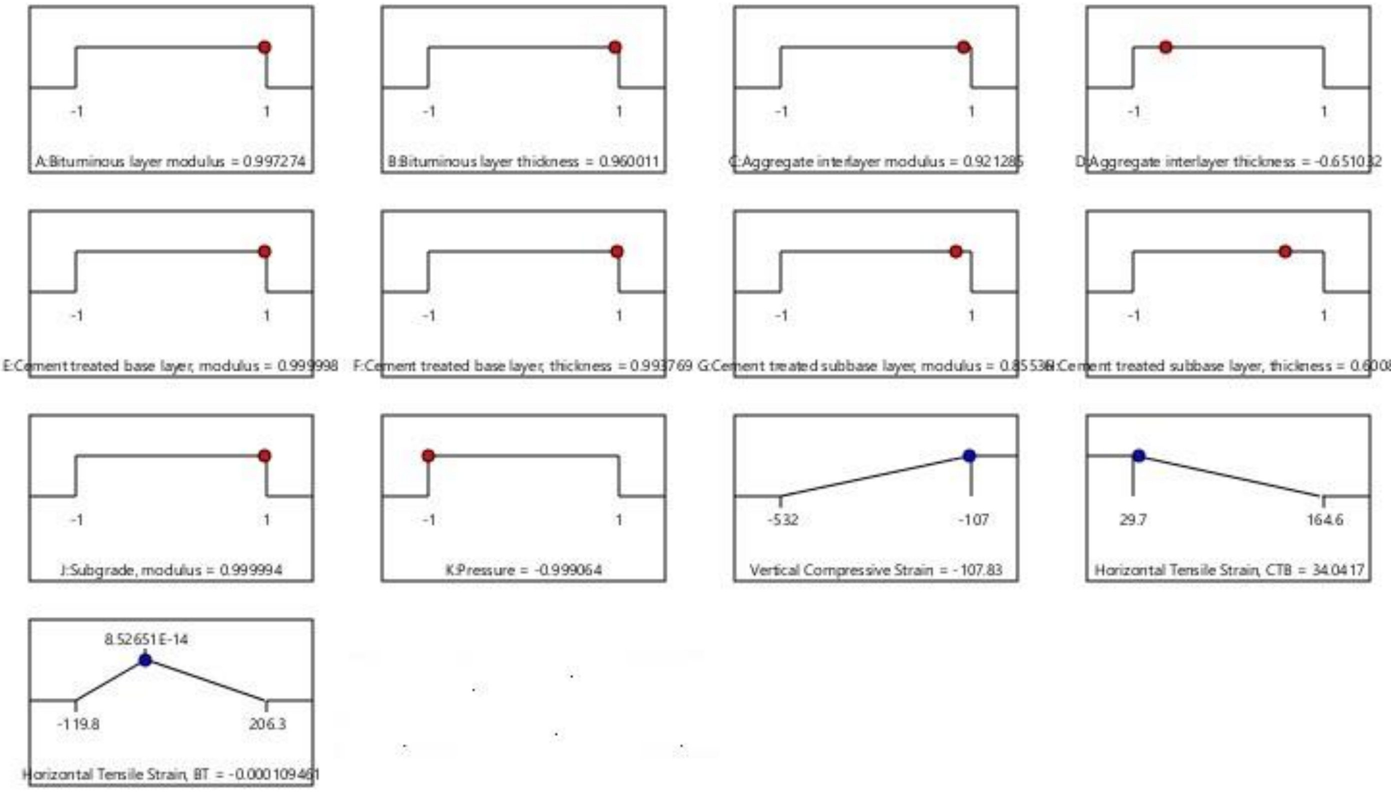

Figure 4.40: Optimized factors for the minimum vertical compressive strain

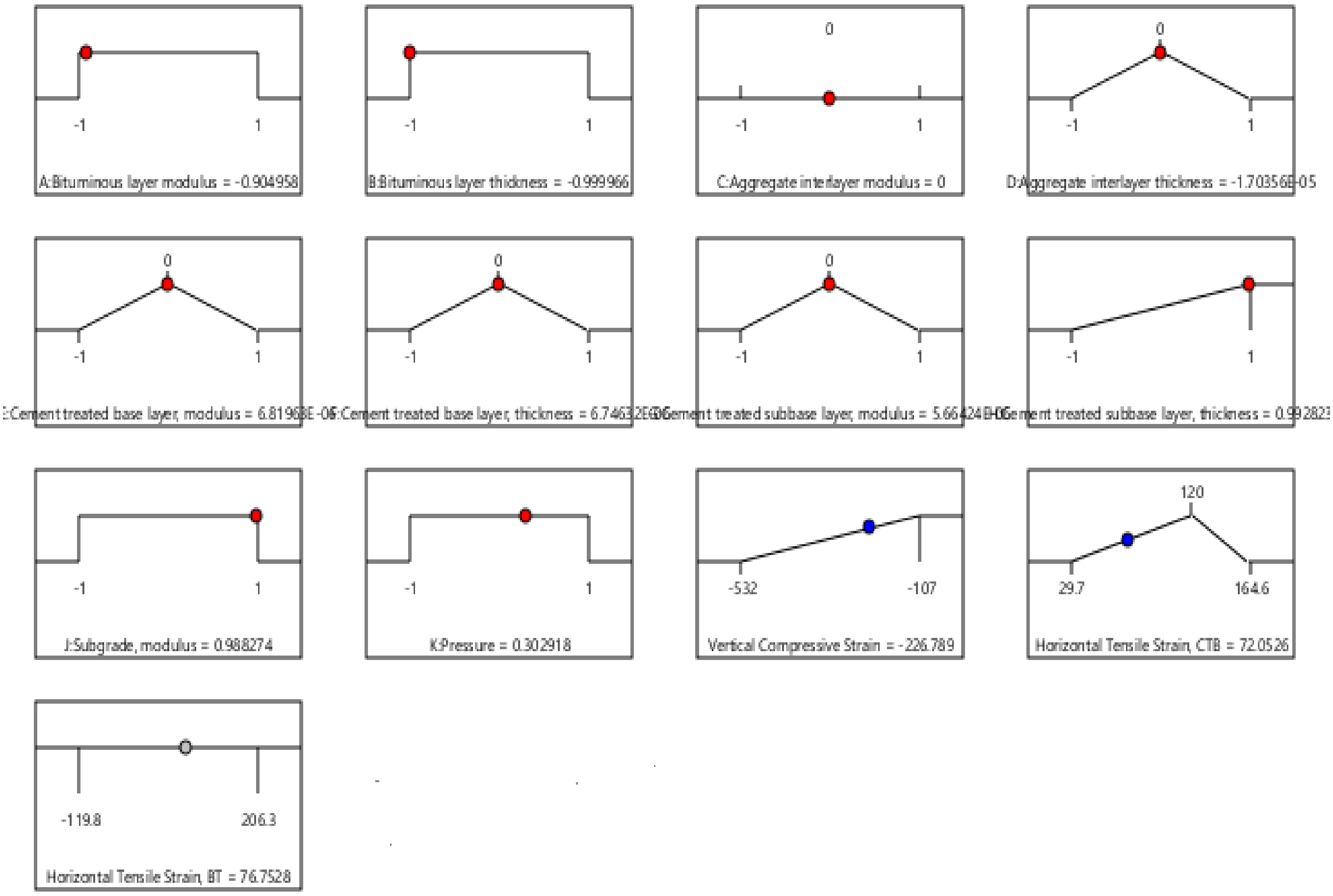

Figure 4.41: Optimized factors for the horizontal tensile strain, CTB value of 72 micron

4.4 Summary

The chapter discuss the significant factors affecting the design of cement treated pavement and inverted pavement. The significant factors were decided based on the level of significance. All the models considered here were checked for assumption, and level of prediction (R^2). The equations of the models were also presented here. Finally, the models in term distresses were optimized for different input factors quantitively.

CHAPTER 5: CONCLUSION

This thesis is focused on the performance analysis of cement treated base layer in both semi-rigid pavement and inverted pavement and the analysis has been carried out using LTPP dataset and MEPDG. Initially, the LTPP dataset was extracted for cement treated base layers and thereafter, the factors affecting the design of cement treated pavement were studied using two mechanistic empirical pavement design software application.

In the first part consisting of semi-rigid pavement, the MEPDG software was used to study seven numeric and three categoric factors for the design of the cement treated pavement for the pavement response in terms of distresses. The main factors affecting the performance of the pavement was finalized. Thereafter, optimization of pavement sections was suggested based on the different distresses.

In the second part consisting of inverted pavement, the distresses that were causing the failure of pavement in the first phase (semi-rigid pavement) namely, reflective cracking, were attempted to be mitigated through the use of an inverted pavement system. The crack propagating from the cement treat layer could not reach the asphalt layer because of the presence of an aggregate interlayer. The aggregate interlayer acts as a buffer to eliminate the tensile strain in the layer and only compressive strain is generated in the aggregate interlayer. Therefore, the cracks occurring due to tensile stresses could not reach the asphalt layer. Finally, similar to the first phase, the factors affecting the design of inverted pavement were studied using another mechanistic empirical pavement design software application namely, CROSSPAVE. The strains were considered as the response factors.

The results drawn from the two phases study involved in this thesis are summarized below:

Phase 1

- From MEPDG analysis, it can be seen that all the sections with different factors are safe in total permanent deformation and AC permanent deformation. This can be interpreted that when rutting (AC and total) in the pavement system is the critical performance factors, it may be recommended to use a cement treated base layer/semi-rigid pavement. However, other performance factors should be considered simultaneously to be able to provide safe pavement.
- The AC bottom-up fatigue cracking was another response on the pavement design using MEPDG but the total cracking (%) was zero. Therefore, it can be concluded that bottom-up fatigue is not an issue in the design of pavement with cemented treated base layer. This can be mainly because of the strong base of the cement layer; because of this layer, the bending action of asphalt slab due to which crack propagates is not possible.
- The AC total fatigue cracking is a combination of bottom-up fatigue cracking and reflective cracking. However, the asphalt bottom-up cracking in the cement treated base is negligible and almost close to zero in the MEPDG analysis. Therefore, it can be concluded that reflective cracking is the most common cause of the AC total fatigue cracking. To overcome this failure distress, the use of aggregate interlayer/ geotextile/ chip seal above the cement treated base layer should be considered.
- The minimum total permanent deformation is achieved for the condition having combination of the maximum asphalt thickness, maximum cement base layer thickness, maximum speed, minimum traffic, the subgrade condition is coarse and temperature as freeze. Similarly, the maximum total permanent deformation occurs at the minimum asphalt thickness, minimum cement base layer thickness, minimum speed, maximum

traffic, the subgrade condition is fine and temperature as no-freeze. This is quite logical to grasp as the condition for minimum and maximum permanent deformation are in two extremes.

- The asphalt thermal cracking is found more prevalent in some states (e.g., Tennessee and Minnesota), which are wet no freeze and wet freeze zone. This is an interesting result, as the thermal cracking is mainly dependent of temperatures. The dry -freeze/no freeze states have the thermal cracking, if any, within the limit as given in Figure 3.15.
- Also, the asphalt transverse cracking with the combined effect of (thermal +reflective) cracking, is showing major distresses but individually thermal cracking is mostly within the limit. Therefore, reflective cracking is the one of the major causes of failure as suggested earlier in total asphalt cracking. Therefore, the same mitigation technique as suggested for total asphalt cracking in the layer should be used to overcome the distress. The proposed idea includes addition of another layer such as crack relief aggregate interlayer between asphalt and cement treated base layer to arrest the cracking arising from cement treated layer to the asphalt layer.
- Majority of the distress can be predicted very well from the model with the R^2 value of about 90 except the AC top-down cracking, which can only predict with 50% accuracy.

Phase 2

Inverted pavement performance is primarily influenced by the pavement response critical to the design of the pavement, such as strain/stress, like the performance of cement-treated base/semi-rigid pavement. In this case, MEPDG could not generate or input pavement structure data. Therefore, a different software, Crosspave, was used to study the factors that affect pavement design with regard to strain as a response parameter. One of the new parameters that was considered in the design of inverted pavement was aggregate layer anisotropy. There are many published literatures suggesting the aggregate interlayer used in the inverted pavement has anisotropy behaviour. The following conclusions can be drawn based on the output and design of experiment analysis.

- The vertical compressive strain is affected by modulus and thickness of bituminous layer, cement treated base layer and cement treated subbase layer. Also, it is affected by subgrade modulus and aggregate interlayer thickness.
- One interesting conclusion is that vertical compressive strain, horizontal tensile strain below cement treated base and horizontal tensile strain below bituminous layer is not affected by aggregate layer modulus. Many published literatures have focussed on this layer and laid so much emphasis on the stress dependent modulus of this layer, that it has been included in the specification in many countries. The major advantage of using DoE is that it can consider many factors at the same time, which can be studied comprehensively in one go instead of studying one factor a time.
- Interestedly, the same factors affecting the response of vertical compressive strain is also affecting the horizontal tensile strain in the cement treated base layer. In both the phases the predicted R^2 value is more than 92%.
- The horizontal tensile strain in bituminous layer is affected by the aggregate interlayer thickness, and pressure.

Recommendation for Future Studies

Although, it was a comprehensive study to investigating the factors affecting the design of the semi-rigid and inverted pavement system, the following is recommended for future studies

1. MEPDG should be made more versatile to accommodate different pavement structures especially inverted pavement.
2. The study can be conducted in regions where local calibration factors are available. This would reduce the calibration bias of the equation.

3. Similar analysis should be carried for flexible, and rigid pavement while considering data from LTPP, and MEPDG software. Since, one of the issues faced during LTPP sections constructions was that all the combinations of the study couldn't be formulated, therefore, MEPDG, LTPP and Design of Experiment can solve this issue efficiently.
4. The number of runs considered here was based on fractional factorial. However, full factorial analysis can be considered to study all the terms without aliasing.
5. The effect of different load spectrum on the fatigue properties of the semi-rigid pavement should also be carried out.

APPENDIX I

Table 1:Different cement-treated sections in the LTPP dataset

State Code	Section ID	State/Province	County	GPS- Lat., Long.	Functional Class	Climatic Zone
5	5_3048	Arkansas	Arkansas	34.37233, -91.12808	Rural Principal Arterial - Other	Wet, No-Freeze
5	5_2042	Arkansas	Ashley	33.13424, -91.83836	Rural Principal Arterial - Other	Wet, No-Freeze
6	6_2002	California	Siskiyou	41.62159, -122.19969	Rural Principal Arterial - Other	Wet, No-Freeze
6	6_2004	California	Riverside	33.509, -117.15531	Rural Principal Arterial - Interstate	Dry, No-Freeze
6	6_2038	California	Del Norte	41.79421, -124.15812	Rural Principal Arterial - Other	Wet, No-Freeze
6	6_2040	California	Humboldt	40.45966, -124.0768	Rural Principal Arterial - Other	Wet, No-Freeze
6	6_2041	California	Humboldt	40.45415, -124.05378	Rural Principal Arterial - Other	Wet, No-Freeze
6	6_2051	California	Napa	38.26798, -122.29852	Urban Principal Arterial - Other Freeways or Expressways	Wet, No-Freeze
6	6_2053	California	San Mateo	37.45123, -122.27985	Rural Principal Arterial - Interstate	Wet, No-Freeze
6	6_2647	California	Tuolumne	37.84778, -120.57071	Rural Principal Arterial - Other	Wet, No-Freeze
6	6_7452	California	Lake	39.0766, -122.93076	Rural Minor Arterial	Wet, No-Freeze
6	6_7491	California	San Bernardino	34.77259, -114.58027	Rural Principal Arterial - Interstate	Dry, No-Freeze
6	6_8149	California	San Bernardino	34.8555, -114.89636	Rural Principal Arterial - Interstate	Dry, No-Freeze
6	6_8150	California	San Bernardino	34.08665, -117.2005	Rural Minor Arterial	Dry, No-Freeze
6	6_8151	California	San Bernardino	34.73344, -115.55631	Rural Principal Arterial - Interstate	Dry, No-Freeze
6	6_8201	California	Kern	35.3971, -118.89844	Rural Minor Arterial	Dry, No-Freeze
6	6_8202	California	Kings	36.24775, -119.81438	Rural Principal Arterial - Other	Dry, No-Freeze

10	10_1450	Delaware	Kent	39.02399, -75.46056	Rural Principal Arterial - Other	Wet, No-Freeze
13	13_4092	Georgia	Thomas	31.02252, -84.0583	Rural Principal Arterial - Other	Wet, No-Freeze
13	13_4093	Georgia	Thomas	31.05289, -84.071	Rural Principal Arterial - Other	Wet, No-Freeze
13	13_4096	Georgia	Early	31.39442, -84.91713	Rural Minor Collector	Wet, No-Freeze
13	13_4420	Georgia	Bryan	31.90419, -81.36331	Rural Principal Arterial - Other	Wet, No-Freeze
22	22_3056	Louisiana	Rapides	30.97511, -92.29541	Rural Principal Arterial - Interstate	Wet, No-Freeze
24	24_1632	Maryland	Calvert	38.37197, -76.44649	Rural Principal Arterial - Other	Wet, No-Freeze
24	24_2401	Maryland	Harford	39.47668, -76.31859	Rural Principal Arterial - Other	Wet, No-Freeze
24	24_2805	Maryland	Frederick	39.40476, -77.35893	Rural Principal Arterial - Interstate	Wet, No-Freeze
28	28_2807	Mississippi	Lafayette	34.3551, -89.65572	Rural Principal Arterial - Other	Wet, No-Freeze
28	28_3018	Mississippi	Tishomingo	34.78364, -88.18126	Rural Principal Arterial - Other	Wet, No-Freeze
28	28_3083	Mississippi	Marshall	34.57342, -89.57943	Rural Principal Arterial - Other	Wet, No-Freeze
28	28_3085	Mississippi	Marshall	34.58128, -89.51599	Rural Principal Arterial - Other	Wet, No-Freeze
28	28_3087	Mississippi	Lafayette	34.44038, -89.49888	Rural Principal Arterial - Other	Wet, No-Freeze
28	28_3089	Mississippi	Lafayette	34.35236, -89.71305	Rural Principal Arterial - Other	Wet, No-Freeze
28	28_3090	Mississippi	Panola	34.4384, -90.17786	Rural Principal Arterial - Other	Wet, No-Freeze
28	28_3094	Mississippi	Jackson	30.43772, -88.62936	Rural Principal Arterial - Interstate	Wet, No-Freeze
29	29_5403	Missouri	Dunklin	36.11975, -90.17342	Rural Minor Arterial	Wet, No-Freeze
29	29_5413	Missouri	Dunklin	36.19655, -90.09112	Rural Principal Arterial - Other	Wet, No-Freeze
34	34_1638	New Jersey	Gloucester	39.80973, -75.10505	Urban Principal Arterial - Other	Wet, No-Freeze

					Freeways or Expressways	
37	37_1645	North Carolina	Columbus	34.34798, -78.64848	Rural Principal Arterial - Other	Wet, No-Freeze
37	37_2819	North Carolina	Guilford	35.93444, -79.82775	Rural Principal Arterial - Other	Wet, No-Freeze
37	37_2824	North Carolina	Chatham	35.70581, -79.42908	Rural Principal Arterial - Other	Wet, No-Freeze
37	37_2825	North Carolina	Mecklenburg	35.14218, -80.91683	Urban Minor Arterial	Wet, No-Freeze
38	38_2001	North Dakota	Grand Forks	47.93283, -97.42706	Rural Principal Arterial - Other	Wet, Freeze
41	41_2002	Oregon	Washington	45.59618, -123.01224	Rural Principal Arterial - Other	Wet, No-Freeze
47	47_2001	Tennessee	Dyer	36.18272, -89.22298	Rural Principal Arterial - Other	Wet, No-Freeze
47	47_2008	Tennessee	Gibson	35.85907, -88.74781	Rural Principal Arterial - Other	Wet, No-Freeze
48	48_1049	Texas	Nacogdoches	31.65924, -94.67828	Urban Other Principal Arterial	Wet, No-Freeze
48	48_2108	Texas	Galveston	29.34739, -94.92651	Rural Principal Arterial - Other	Wet, No-Freeze
48	48_2176	Texas	Hale	34.16527, -101.70905	Rural Major Collector	Wet, No-Freeze
48	48_3669	Texas	Angelina	31.32793, -94.78652	Rural Minor Arterial	Wet, No-Freeze
48	48_3679	Texas	Angelina	31.37204, -94.50556	Rural Minor Arterial	Wet, No-Freeze
48	48_3689	Texas	Polk	30.70597, -94.85921	Rural Principal Arterial - Other	Wet, No-Freeze
51	51_1417	Virginia	Fauquier	38.60894, -77.78757	Rural Principal Arterial - Other	Wet, No-Freeze
51	51_1419	Virginia	Russell	36.96552, -81.91914	Rural Principal Arterial - Other	Wet, Freeze
56	56_2015	Wyoming	Laramie	41.58895, -104.86954	Rural Principal Arterial - Interstate	Dry, Freeze
56	56_2017	Wyoming	Campbell	43.63396, -105.70391	Rural Minor Arterial	Dry, Freeze
56	56_2018	Wyoming	Natrona	43.00828, -106.7299	Rural Principal Arterial - Other	Dry, Freeze

56	56_2019	Wyoming	Campbell	44.1646, -105.44451	Rural Minor Arterial	Dry, Freeze
56	56_2020	Wyoming	Sheridan	44.9392, -107.2021	Rural Principal Arterial - Interstate	Dry, Freeze
56	56_2037	Wyoming	Sweetwater	41.66055, -107.74695	Rural Minor Arterial	Dry, Freeze
56	56_7772	Wyoming	Hot Springs	43.67094, -108.27953	Rural Minor Arterial	Dry, Freeze
56	56_7773	Wyoming	Natrona	42.66406, -106.48698	Rural Minor Arterial	Dry, Freeze
81	81_2812	Alberta	Highway District #6	51.72784, -113.24142	Rural Principal Arterial - Other	Dry, Freeze

APPENDIX II

Table 1: Inputs for MEPDG Analysis

A:Asphalt thickness (mm)	B:Cement thickness (mm)	C:Modulus of rupture (Psi)	D:Elastic modulus (MPa)	E:Speed (Kmph)	F:Crack spacing (ft)	G:Traffic (AADTT)	H:Subgrade	J:Temperature	K:Moisture	Equivalent climate for factor J and K
40	110	150	10342	60	25	1500	Fine	Freeze	Dry	Wyoming
40	320	150	13789.5	20	25	1500	Coarse	No Freeze	Wet	Tennessee
300	110	150	10342	20	25	1500	Coarse	No Freeze	Wet	Tennessee
40	110	150	10342	60	10	1500	Fine	No Freeze	Dry	New Mexico
300	110	150	13789.5	20	10	1500	Coarse	Freeze	Dry	Wyoming
40	320	150	10342	60	25	200	Fine	Freeze	Wet	Minnesota
40	320	150	10342	20	25	200	Fine	Freeze	Dry	Wyoming
40	110	150	13789.5	20	25	1500	Fine	No Freeze	Dry	New Mexico
300	110	150	13789.5	60	10	1500	Coarse	No Freeze	Wet	Tennessee
40	320	150	13789.5	20	10	1500	Coarse	Freeze	Wet	Minnesota
40	320	150	10342	60	10	200	Fine	No Freeze	Wet	Tennessee
300	110	150	10342	60	10	1500	Coarse	Freeze	Dry	Wyoming
300	320	150	13789.5	20	25	1500	Fine	Freeze	Wet	Minnesota
300	110	150	13789.5	20	10	1500	Coarse	No Freeze	Dry	New Mexico
300	110	150	13789.5	60	25	1500	Coarse	Freeze	Wet	Minnesota
300	320	150	13789.5	20	10	200	Coarse	No Freeze	Wet	Tennessee
300	320	150	10342	60	10	1500	Fine	Freeze	Wet	Minnesota
40	320	150	13789.5	60	25	1500	Coarse	No Freeze	Dry	New Mexico
40	110	150	13789.5	20	25	200	Coarse	No Freeze	Dry	New Mexico
40	110	150	13789.5	20	10	200	Coarse	Freeze	Dry	Wyoming
40	320	150	13789.5	60	25	200	Fine	No Freeze	Dry	New Mexico
300	110	150	10342	20	25	200	Fine	No Freeze	Wet	Tennessee
40	110	150	10342	20	25	200	Coarse	Freeze	Wet	Minnesota
300	110	150	10342	60	10	200	Fine	Freeze	Dry	Wyoming
300	320	150	10342	20	25	200	Coarse	No Freeze	Dry	New Mexico
40	320	150	10342	20	10	1500	Coarse	No Freeze	Dry	New Mexico
300	320	150	13789.5	60	25	1500	Fine	Freeze	Dry	Wyoming

40	110	150	13789.5	60	10	1500	Fine	Freeze	Wet	Minnesota
300	320	150	10342	20	10	1500	Fine	Freeze	Dry	Wyoming
40	110	150	13789.5	60	25	1500	Fine	No Freeze	Wet	Tennessee
40	320	150	10342	20	25	1500	Coarse	Freeze	Dry	Wyoming
300	110	150	13789.5	60	25	200	Fine	Freeze	Wet	Minnesota
300	110	150	13789.5	20	10	200	Fine	No Freeze	Dry	New Mexico
300	110	150	13789.5	60	10	200	Fine	No Freeze	Wet	Tennessee
40	110	150	13789.5	60	25	200	Coarse	No Freeze	Wet	Tennessee
40	320	150	10342	20	10	200	Fine	No Freeze	Dry	New Mexico
40	110	150	10342	60	25	200	Coarse	Freeze	Dry	Wyoming
300	110	150	10342	20	10	200	Fine	Freeze	Wet	Minnesota
300	110	150	10342	20	10	1500	Coarse	Freeze	Wet	Minnesota
300	320	150	13789.5	20	10	1500	Fine	No Freeze	Wet	Tennessee
300	320	150	10342	60	25	200	Coarse	No Freeze	Wet	Tennessee
40	110	150	10342	20	25	1500	Fine	Freeze	Wet	Minnesota
40	110	150	13789.5	20	10	1500	Fine	Freeze	Dry	Wyoming
40	110	150	10342	20	10	200	Coarse	No Freeze	Wet	Tennessee
300	320	150	13789.5	60	10	200	Coarse	No Freeze	Dry	New Mexico
300	320	150	10342	60	25	1500	Fine	No Freeze	Wet	Tennessee
40	110	150	10342	60	10	200	Coarse	No Freeze	Dry	New Mexico
40	320	150	10342	60	25	1500	Coarse	Freeze	Wet	Minnesota
40	320	150	10342	60	10	1500	Coarse	No Freeze	Wet	Tennessee
40	320	150	13789.5	20	10	200	Fine	Freeze	Wet	Minnesota
40	110	150	13789.5	60	10	200	Coarse	Freeze	Wet	Minnesota
300	320	150	13789.5	20	25	200	Coarse	Freeze	Wet	Minnesota
40	320	150	13789.5	60	10	200	Fine	Freeze	Dry	Wyoming
40	110	150	10342	20	10	1500	Fine	No Freeze	Wet	Tennessee
300	110	150	13789.5	20	25	200	Fine	Freeze	Dry	Wyoming
300	320	150	10342	20	10	200	Coarse	Freeze	Dry	Wyoming
40	320	150	13789.5	60	10	1500	Coarse	Freeze	Dry	Wyoming
300	320	150	10342	60	10	200	Coarse	Freeze	Wet	Minnesota
40	320	150	13789.5	20	25	200	Fine	No Freeze	Wet	Tennessee
300	320	150	13789.5	60	25	200	Coarse	Freeze	Dry	Wyoming
300	320	150	13789.5	60	10	1500	Fine	No Freeze	Dry	New Mexico
300	320	150	10342	20	25	1500	Fine	No Freeze	Dry	New Mexico

300	110	150	10342	60	25	1500	Coarse	No Freeze	Dry	New Mexico
300	110	150	10342	60	25	200	Fine	No Freeze	Dry	New Mexico
40	320	300	13789.5	20	10	200	Coarse	No Freeze	Dry	New Mexico
40	320	300	10342	60	10	1500	Fine	Freeze	Dry	Wyoming
40	110	300	10342	60	25	1500	Coarse	No Freeze	Wet	Tennessee
40	320	300	10342	20	10	200	Coarse	Freeze	Wet	Minnesota
300	320	300	10342	60	10	1500	Coarse	No Freeze	Dry	New Mexico
40	320	300	10342	60	25	200	Coarse	No Freeze	Dry	New Mexico
300	320	300	10342	60	25	200	Fine	Freeze	Dry	Wyoming
300	320	300	13789.5	20	25	1500	Coarse	No Freeze	Dry	New Mexico
40	110	300	13789.5	20	10	200	Fine	No Freeze	Wet	Tennessee
40	110	300	13789.5	60	25	200	Fine	Freeze	Dry	Wyoming
40	110	300	10342	20	10	1500	Coarse	Freeze	Dry	Wyoming
40	110	300	10342	20	25	1500	Coarse	No Freeze	Dry	New Mexico
300	110	300	13789.5	60	10	200	Coarse	Freeze	Dry	Wyoming
300	320	300	13789.5	20	10	200	Fine	Freeze	Dry	Wyoming
40	110	300	13789.5	20	10	1500	Coarse	No Freeze	Wet	Tennessee
40	320	300	10342	60	10	200	Coarse	Freeze	Dry	Wyoming
300	320	300	13789.5	20	25	200	Fine	No Freeze	Dry	New Mexico
300	110	300	13789.5	20	10	200	Coarse	Freeze	Wet	Minnesota
40	110	300	10342	20	10	200	Fine	Freeze	Dry	Wyoming
300	110	300	10342	60	10	1500	Fine	No Freeze	Wet	Tennessee
300	110	300	13789.5	20	25	1500	Fine	No Freeze	Wet	Tennessee
40	320	300	13789.5	60	10	200	Coarse	No Freeze	Wet	Tennessee
300	320	300	10342	20	25	200	Fine	Freeze	Wet	Minnesota
300	320	300	10342	60	25	1500	Coarse	Freeze	Dry	Wyoming
300	320	300	10342	60	10	200	Fine	No Freeze	Dry	New Mexico
40	320	300	13789.5	20	25	200	Coarse	Freeze	Dry	Wyoming
40	320	300	13789.5	20	10	1500	Fine	No Freeze	Dry	New Mexico
300	110	300	10342	60	25	200	Coarse	Freeze	Wet	Minnesota
300	110	300	10342	60	10	200	Coarse	No Freeze	Wet	Tennessee
300	110	300	10342	20	10	1500	Fine	No Freeze	Dry	New Mexico
40	110	300	10342	60	25	200	Fine	No Freeze	Wet	Tennessee
40	320	300	13789.5	60	25	200	Coarse	Freeze	Wet	Minnesota
40	320	300	10342	20	25	200	Coarse	No Freeze	Wet	Tennessee
40	110	300	13789.5	20	25	1500	Coarse	Freeze	Wet	Minnesota
300	110	300	13789.5	60	25	1500	Fine	No Freeze	Dry	New Mexico

40	110	300	13789.5	20	25	200	Fine	Freeze	Wet	Minnesota
300	110	300	13789.5	20	10	1500	Fine	Freeze	Wet	Minnesota
300	110	300	10342	60	25	1500	Fine	Freeze	Wet	Minnesota
300	320	300	13789.5	60	10	1500	Coarse	Freeze	Wet	Minnesota
40	110	300	13789.5	60	25	1500	Coarse	Freeze	Dry	Wyoming
300	320	300	13789.5	60	25	1500	Coarse	No Freeze	Wet	Tennessee
40	110	300	10342	60	10	200	Fine	Freeze	Wet	Minnesota
40	320	300	13789.5	20	25	1500	Fine	Freeze	Dry	Wyoming
40	110	300	13789.5	60	10	1500	Coarse	No Freeze	Dry	New Mexico
40	110	300	10342	60	10	1500	Coarse	Freeze	Wet	Minnesota
300	110	300	10342	20	25	200	Coarse	Freeze	Dry	Wyoming
40	110	300	10342	20	25	200	Fine	No Freeze	Dry	New Mexico
40	320	300	13789.5	60	10	1500	Fine	No Freeze	Wet	Tennessee
300	320	300	13789.5	60	25	200	Fine	No Freeze	Wet	Tennessee
300	320	300	13789.5	20	10	1500	Coarse	Freeze	Dry	Wyoming
300	320	300	10342	20	10	200	Fine	No Freeze	Wet	Tennessee
40	320	300	13789.5	60	25	1500	Fine	Freeze	Wet	Minnesota
40	320	300	10342	20	10	1500	Fine	Freeze	Wet	Minnesota
300	110	300	10342	20	25	1500	Fine	Freeze	Dry	Wyoming
300	320	300	13789.5	60	10	200	Fine	Freeze	Wet	Minnesota
300	320	300	10342	20	25	1500	Coarse	Freeze	Wet	Minnesota
300	110	300	13789.5	60	25	200	Coarse	No Freeze	Dry	New Mexico
40	320	300	10342	20	25	1500	Fine	No Freeze	Wet	Tennessee
300	110	300	13789.5	20	25	200	Coarse	No Freeze	Wet	Tennessee
40	110	300	13789.5	60	10	200	Fine	No Freeze	Dry	New Mexico
300	320	300	10342	20	10	1500	Coarse	No Freeze	Wet	Tennessee
300	110	300	10342	20	10	200	Coarse	No Freeze	Dry	New Mexico
40	320	300	10342	60	25	1500	Fine	No Freeze	Dry	New Mexico
300	110	300	13789.5	60	10	1500	Fine	Freeze	Dry	Wyoming

Note: All the values used in the software application were converted to U.S unit.

Table 2: Response to the input factors in New Mexico (Dry- No Freeze)

Distresses	Terminal IRI (in/mile)	Total Pavement Deformation (inch)	AC total fatigue cracking: bottom up + reflective (% lane area)	AC total transverse cracking: thermal + reflective (ft/mile)	AC thermal cracking (ft/mile)	AC top-down fatigue cracking (ft/mile)	AC permanent deformation- AC only (inch)	Chemically stabilized layer-fatigue fracture (%)
Limit	172	0.75	25	2500	1000	2000	0.25	25
Obtained (red colour suggests value outside limit)	211.2	0.19	75.55	5488	1	2457.04	0.01	75
	188.0	0.19	75.55	2167.	1.42	542.46	0.02	75
	182.1	0.1	39.84	5447.	1	3005.23	0.05	39.3
	158.2	0.08	42.64	2182	10.77	256.67	0.03	42.1
	176.3	0.12	75.54	2170.	4.18	260.44	0.02	75
	168.3	0.08	46.74	2176.	8.93	1308.48	0.01	46.2
	120.8	0.06	0.54	618.8	1	2535.57	0.03	0.12
	181.2	0.09	39.74	5479	10.77	257.2	0.04	39.2
	164.1	0.08	0.54	3567	1	13164.58	0.03	43
	192.0	0.09	45.94	5460	8.93	2932.88	0.02	45.4
	122.8	0.06	0.54	862	1	1797.47	0.02	0.19
	199.6	0.12	75.54	5449	4.18	260.44	0.02	75
	178.3	0.08	18.74	5452	1	1405.53	0.04	18.2
	150.3	0.1	9.59	2168	1	2099	0.06	9.05
	155	0.09	36.64	2166	1	1905.81	0.04	36.1
	152.8	0.08	0.55	2090	1	13803.88	0.02	58.9
	160.4	0.07	0.72	5463	10.77	256.65	0.02	0.18
	161.8	0.08	0.69	5453	1	3666.31	0.04	0.15
	145.7	0.06	20.34	2178	10.77	256.52	0.02	19.8
	140.0	0.09	0.72	2168	1	6674.14	0.06	0.19
	177	0.15	74.64	2172	4.18	282.77	0.03	74.1
	129	0.06	0.54	622	1	881.65	0.03	0.06
	131	0.06	0.54	889	1	461.05	0.02	0.04
	175	0.1	10.24	5468	8.93	256.48	0.04	9.7
	183	0.11	8.23	5444	1	13803.41	0.05	7.69
	152.	0.1	14.64	2165	1	257.2	0.04	14.1
	201	0.14	75.54	5451	4.18	282.65	0.02	75
	185	0.15	75.54	2166	1.42	303.14	0.01	75
	129	0.07	0.54	14731	1	775.19	0.02	0.16

Table 1: Response to the input factors in Tennessee (Wet- No Freeze)

Distresses	Terminal IRI (in/mile)	Total Pavement Deformation	AC total fatigue cracking: bottom up + reflective (% lane area)	AC total transverse cracking: thermal +	AC thermal cracking (ft/mile)	AC top-down fatigue cracking (ft/mile)	AC permanent deformation- AC only (inch)	Chemically stabilized layer- fatigue fracture (%)
Limit	172	0.75	25	2500	1000	2000	0.25	25
Obtained (red colour suggests value outside limit)	164.75	0.12	2.29	4858.4	1858.56	258.22	0.05	1.75
	176.88	0.14	47.16	3233.7	789.34	2916.53	0.07	46.6
	202.27	0.12	51.07	6886.64	798.34	1405.73	0.05	50.5
	220.79	0.09	46.74	9069.78	1911.36	266.61	0.02	46.2
	136.51	0.08	0.54	1608.88	798.34	256.5	0.05	0.64
	163.89	0.1	0.54	3829.94	796.22	329.01	0.04	45
	207.5	0.21	75.55	4043.31	1341.12	613.23	0.02	75
	174.33	0.09	0.55	5391.6	796.22	274.67	0.03	53.6
	198.58	0.13	75.54	4446.24	1605.12	250.82	0.02	75
	204.03	0.12	38.24	6891.31	797.28	480.91	0.08	37.7
	134.95	0.07	0.54	1483.47	798.34	2305.9	0.03	0.2
	224.78	0.14	75.54	8489.96	1605.12	261.06	0.02	75
	166.03	0.1	13.44	3233.88	797.28	322.03	0.06	12.9
	212.26	0.1	42.94	9083.99	1921.92	256.7	0.03	42.4
	232.96	0.21	75.55	7986.14	1351.68	681.83	0.02	75
	203.04	0.11	64.34	4939.35	1911.36	261.67	0.02	63.8
	200.48	0.17	75.54	4450.32	1605.12	285.35	0.03	75
	230.11	0.16	75.54	7944.86	1341.12	331.25	0.01	75
	226.72	0.17	75.54	8484.77	1605.12	286.86	0.03	75
	191.23	0.12	12.24	6880.92	796.22	371.1	0.05	11.7
	179.64	0.14	37.24	3229.86	796.22	266.22	0.07	36.7
	190.6	0.07	0.82	9083.99	1921.92	256.58	0.02	0.28
	151.83	0.08	0.54	3459.48	798.34	966.69	0.03	0.17
	204.9	0.16	75.54	4047.97	1351.68	314.09	0.01	75
	162.69	0.08	0.73	4958.18	1921.92	256.72	0.03	0.19
	151.18	0.1	0.75	3235.17	798.34	256.53	0.06	0.21
	205.89	0.1	13.54	9069.79	1911.36	256.49	0.04	13
	143.36	0.07	0.54	1490.83	797.28	269.06	0.04	0.07
	145.15	0.08	0.54	1618.95	797.28	286.05	0.05	0.06
	176.29	0.12	7.93	4943.6	1911.36	256.49	0.05	7.39
	139.18	0.09	0.54	1830.54	798.34	1968.48	0.04	0.81
	182.8	0.12	0.73	6894.14	798.334	9366.72	0.08	0.19

Table 4: Response to the Input Factors in Wyoming (Dry- Freeze)

Distresses	Terminal IRI (in/mile)	Total Pavement Deformation (inch)	AC total fatigue cracking: bottom up + reflective (% lane area)	AC total transverse cracking: thermal + reflective (ft/mile)	AC thermal cracking (ft/mile)	AC top-down fatigue cracking (ft/mile)	AC permanent deformation- AC only (inch)	Chemically stabilized layer-fatigue fracture (%)
Limit	172	0.75	25	2500	1000	2000	0.25	25
Obtained (red colour suggests value outside limit)	186.69	0.1	40.84	5446.88	1	2978.84	0.05	40.3
	149.56	0.09	0.54	2163.75	1	291.02	0.02	46
	184.14	0.09	37.54	5445.21	1	1854.36	0.04	37
	167.4	0.13	0.54	5420.74	1.73	264.32	0.01	75
	178.58	0.08	0.54	4947.32	1	13803.03	0.02	45.9
	164.6	0.09	28.94	2167.94	1	3405.6	0.05	28.4
	184.35	0.1	16.24	5452.32	1	5391.04	0.06	15.7
	162.36	0.09	41.24	2173.7	2.29	257.17	0.03	40.7
	162.36	0.09	41.24	2173.7	2.29	257.17	0.03	40.7
	142.89	0.13	0.54	2164.77	1.63	263.85	0.01	75
	216.11	0.21	75.55	5444.74	1	629.63	0.02	75
	173.45	0.09	0.57	5437.18	1	876.7	0.02	46.7
	152.59	0.09	0.54	1685.02	1	11779.57	0.03	43.6
	125.96	0.06	0.54	681.07	1	2507.2	0.03	0.12
	186.76	0.09	43.34	5449.12	2.29	256.68	0.02	42.8
	124.52	0.06	0.54	598.09	1	1503.89	0.02	0.2
	176.7	0.1	5.45	5444.64	1	256.49	0.03	4.91
	148.64	0.07	0.54	2163.87	1	356.49	0.02	0.9
	154.28	0.15	3.65	2164.37	1	375.12	0.01	75
	205.69	0.16	74.64	5450.7	1.63	307.59	0.02	74.1
	139.97	0.07	0.54	2175.31	1	756.73	0.02	0.17
	137.82	0.07	0.54	964.12	1	2475.54	0.04	0.06
	164.18	0.07	0.54	5411.45	2.29	256.52	0.02	0.12
	189.8	0.16	10.19	5438.99	1	13389.31	0.01	75
	141.37	0.08	0.69	2167.9	1	0.04	0.15	
	139.9	0.07	0.54	2160.31	2.29	256.66	0.02	0.19
	182.71	0.16	75.54	2172.92	1.63	305.03	0.02	75
	155.95	0.11	11.24	2166.05	1	256.55	0.04	10.7
	128.52	0.07	0.54	893.52	1	1420.2	0.03	0.11
	167.8	0.09	0.72	5452.58	1	5358.86	0.05	0.18
	164.07	0.11	9.86	2165.54	1	13699.95	0.05	9.32
	215.71	0.2	75.55	5457.47	1	903.54	0.01	75

Table 5: Response to the input factors in Minnesota (Wet-Freeze)

Distresses	Terminal IRI (in/mile)	Total Pavement Deformation (inch)	AC total fatigue cracking: bottom up + reflective (% lane area)	AC total transverse cracking: thermal + reflective (ft/mile)	AC thermal cracking (ft/mile)	AC top-down fatigue cracking (ft/mile)	AC permanent deformation- AC only (inch)	Chemically stabilized layer-fatigue fracture (%)
Limit	172	0.75	25	2500	1000	2000	0.25	25
Obtained (red colour suggest value outside limit)	175.78	0.09	0.54	5185.05	2090.88	268.58	0.01	46.4
	219.27	0.11	44.94	9343.43	2112	257.65	0.03	44.4
	177.41	0.1	36.94	2800.62	484	1332.74	0.05	36.4
	172.21	0.1	41.84	2820.97	501.6	1543.34	0.04	41.3
	188	0.08	10.34	6310	484.7	686.24	0.04	9.8
	171.17	0.15	0.54	5224.49	2112	303.25	0.01	75
	244.79	0.22	75.55	9169.66	1985.28	627.31	0.02	75
	156.41	0.08	0.54	2573.47	463.58	1187.22	0.02	43.6
	179.35	0.09	0.54	4431.89	463.58	13803.51	0.03	46.7
	196.89	0.12	40.84	6334.74	501.6	2703.07	0.05	40.3
	218.3	0.22	75.55	5061.34	1985.28	694.31	0.01	75
	190.19	0.1	43.24	5279.99	2112	257.14	0.02	42.7
	203.85	0.11	0.54	9314.24	2090.88	480.91	0.02	55.6
	198.97	0.15	0.54	9343.43	21112	267.18	0.01	75
	135.67	0.07	0.54	1229.54	517.44	426.7	0.03	0.51
	139.14	0.06	0.54	1634.5	517.44	1723.73	0.02	0.16
	167.62	0.08	0.54	5228.02	2112	256.59	0.02	38.8
	153.59	0.08	0.54	3264.27	501.6	1412.99	0.03	0.59
	143.83	0.07	0.54	1194.99	484.7	465.6	0.03	0.05
	144.56	0.08	0.54	2183.36	501.6	651.87	0.02	0.14
	167.19	0.07	0.54	5233.54	2112	256.54	0.02	0.25
	210.37	0.19	75.54	5276.37	2112	537	0.02	75
	178.78	0.17	0.54	5012.54	1985.28	331.15	0.01	75
	208.53	0.11	33.94	6257.9	463.58	13803.77	0.04	33.4
	163.55	0.1	9.27	2768.1	463.58	299.1	0.03	8.73
	175.66	0.08	0.72	6369.66	517.44	651.11	0.04	0.18
	205.96	0.17	0.54	9152.12	1985.28	318.56	0.01	75
	237.19	0.19	75.34	9343.43	2112	326.55	0.02	74.8
	182.75	0.09	13.14	5242.43	2090.88	256.49	0.03	12.6
	208.73	0.11	7.58	9314.24	2090.88	288.94	0.03	7.04
	147.32	0.06	0.54	1622.61	484.7	349.63	0.02	0.06
	154.18	0.1	0.7	2844.98	517.44	6528.27	0.05	0.16

The equations used in the MEPDG analysis is given below

AC Fatigue

$N_f = 0.00432 \times C \times \beta_{f1} k_1 \left(\frac{1}{\varepsilon_1}\right)^{k_2\beta_{f2}} \left(\frac{1}{E}\right)^{k_3\beta_{f3}}$ ....Equation 1

$C = 10^M$ ....Equation 2

$M = 4.84\left(\frac{V_a}{V_a+V_b} - 0.69\right)$ ....Equation 3

$k_1 = 3.75$

$k_2 = 2.87$

$k_3 = 1.46$

$\beta_{f1} = 0.02054$

$\beta_{f2} = 1.38$

$\beta_{f3} = 0.88$

Asphalt Rutting

$\frac{\varepsilon_p}{\varepsilon_r} = k_z \beta_{r1} 10^{k_1} T^{k_2\beta_{r2}} N^{k_2} N^{k_3\beta_{r3}}$ ....Equation 4

$K_z = (C_1 + C_2 \times \text{depth}) \times 0.328196^{\text{depth}}$ ....Equation 5

$C_1 = -0.1039 \times H_a^2 + 2.4868 \times H_a - 17.342$ ....Equation 6

$C_2 = 0.0172 \times H_a^2 - 17331 \times H_a + 27.428$ ....Equation 7

Where:

$\varepsilon_p =$ Plastic strain (in/in)

$\varepsilon_r =$ Elastic strain(in/n)

$T =$ Layer temperature(F)

$N =$ Number of load repetitions

$K_1 = 2.45$

$K_2 = 3.01$

$K_3 = 0.22$

$\beta_{r1} = 0.128$

$\beta_{r2} = 0.52$

$\beta_{r3} = 1.36$

CSM Fatigue

$N_f = 10^{\left(\frac{K_1 \beta_{c1} \left(\frac{\sigma_s}{M_r}\right)}{K_2 \beta_{c1}}\right)}$ …………………………………………………………………Equation 8

$N_f =$ Number of repetitions to fatigue cracking

$\sigma_s =$ Tensile stress(psi)

$M_r =$ Modulus of rupture(psi)

$K_1 = 0.972$

$K_2 = 0.0825$

$\beta_{c1} = 1$

$\beta_{c2} = 1$

AC Cracking

AC top-down cracking

$FC_{top} = \left(\frac{C_4}{1 + e^{\left(c_1 - c_2 \times \log_{10}(\text{Damage})\right)}}\right) \times 10.56$ ……………...…………………………………Equation 9

$C_1 = 7$

$C_2 = 3.5$

$C_3 = 0$

$C_4 = 1000$

AC Bottom-Up Cracking

$FC_{bottom} = \left(\frac{6000}{1 + e^{\left(c_1 \times c_1' - c_2 \times c_2' \times \log_{10}(100)\right)}}\right) \times \frac{1}{60}$……………………………………………...…Equation 10

$c_2' = -0.240874 - 39.748 \times (1 + h_a c)^{-2.856}$ ……..……………………………………..Equation 11

$c_1' = 2 \times c_2'$……………………………………………………………………….....…Equation 12

$c_1 = 1.31$

$c_2 = 2.1585$

$c_3 = 6000$

Cement Stabilized Material (CSM) Cracking

$FC_{ctb} = C_1 + \left(\frac{C_2}{1+ e^{(c_3 - c_4 \times \log_{10}(\text{Damage}))}}\right)$……………………………………………..……Equation 13

$c_1 = 0$

$c_2 = 75$

$c_3 = 2$

$c_4 = 2$

Reflective Cracking

$\Delta C = k_1 \Delta_{\text{bending}} + k_2 \Delta_{\text{shearing}} + k_3 \Delta_{\text{thermal}}$………………………………………….Equation 14

$\Delta D = \frac{C_1 k_1 \Delta_{\text{bending}} + C_2 k_2 \Delta_{\text{shearing}} + C_3 k_3 \Delta_{\text{thermal}}}{h_O L}$……………………………………………Equation 15

$\Delta_{\text{bending}} = A(\text{SIF})_B^n$

$\Delta_{\text{shearing}} = A(\text{SIF})_S^n$

$\Delta_{\text{Thermal}} = A(\text{SIF})_T^n$

$$D = \sum_{i=1}^{N} \Delta D$$

$$RCR = \left(\frac{100}{C_4 + e^{C_5 \log D}}\right) \times EX_C RK$$

$\Delta C =$ Crack length increment (in)

$\Delta D =$ Incremental damage ratio

$K_1, K_2, K_3, C_1, C_2, C_3 =$ Calibrationfactors (local and global)

$\Delta_{\text{bending}} + \Delta_{\text{shearing}} + \Delta_{\text{thermal}}$ = Crack length increments caused by bending, shearing, and thermal loading

$D =$ Damage ratio

$A, n =$ HMA material fracture properties

$N =$ Total number of days

$(\text{SIF})_B, (\text{SIF})_S, (\text{SIF})_T$

$=$ Stress intensity factors caused by bending, shearing and thermal loading

h_{OL} = Overlay thickness (in)

RCR = Crack in the underlying layers reflected (%)

EX_CRK =

Transverse cracking in underlying pavement layers, ft mile (transverse cracking);

Alligator cracking in underlying pavement layers, %(alligator cracking)

Transverse cracking constant in semi rigid pavement, $K_1 = 0.45$; $K_2 = 0.05$; $K_3 = 1$; $C_1 = 0.09809$; $C_2 = 0.19$; $C_3 = 0.19$; $C_4 = 165.3$; $C_5 = -5.1048$

Fatigue cracking constant in semi − rigid pavement, $K_1 = 0.45$; $K_2 = 0.05$; $K_3 = 1$; $C_1 = 1.64$; $C_2 = 1.1$; $C_3 = 0.19$; $C_4 = 62.1$; $C_5 = -404.6$

APPENDIX III

Table 1: Cement treated layer effect thickness in different climatic regions

Different input factors	Dry freeze		Dry no freeze		Wet freeze		Wet no freeze	
Subgrade	Fine	Coarse	Fine	Coarse	Fine	Coarse	Fine	Coarse
Traffic, AADTT	High	High	High	High	High	High	High	High
Crack spacing, mm	High	High	High	High	High	High	High	High
Speed, kmph	Low	Low	Low	Low	Low	Low	Low	Low
Asphalt thickness, mm	101.472	**132**	125	139.37	196.33	178	158	160
Cemented base layer thickness, mm	319.939	218	317.57	260.28	319.9	320	320	252
Elastic modulus, MPa	Low	Low	Low	Low	Low	Low	Low	Low
Modulus of rupture, MPa	High	High	High	High	High	High	High	High
IRI, in/mile	160.47	160	160.7	157.238	166.399	169	172	175.512
Total deformation, in	0.1096	0.1096	0.108	0.1	0.1069	0.104	0.114	0.119
AC total fatigue cracking (%)	12.15	8.66	9.12	4.672	6.89	2.29	7.17	4.5
AC total transverse cracking (%)	2220.3	2450	2372	2533.8	3324.9	4175.1	3735	4189
Asphalt thermal cracking (ft/mile)	1.74	1.74	2.23	2.47	825.29	1105.17	1329	1525
AC top-down cracking (ft/mile)	582.817	521.38	619.8	544.35	344.29	691.84	320	617
AC deformation (inch)	0.039569	0.0329	0.043	0.045	0.0446	0.0429	0.060	0.059

APPENDIX IV-TRB Paper

Factors Affecting the Design of Inverted Pavement System

Shahbaz Khan
(Corresponding author)
Memorial University of Newfoundland
St. John's, Newfoundland, A1B3X5, CANADA
Email: shahbazk@mun.ca

Kamal Hossain
Adjunct Professor, Department of Civil Engineering
Memorial University of Newfoundland
St. John's, Newfoundland, A1B3X5, CANADA
Email: kamalh@mun.ca
&
Assistant Professor, Department of Civil and Environmental Engineering
Carleton University
Ottawa, CANADA
Email: kamal.hossain@carleton.ca

Carlos Bazan
Assistant Professor, Department of Civil Engineering
Memorial University of Newfoundland
St. John's, Newfoundland, A1B3X5, CANADA
Email: cabazan@mun.ca

Paper submitted to 101th Annual Meeting of the Transportation Research Board, January 2022

Word count= 5 table (250) + 4627 (text) = 5887

Submitted on August 1, 2021

Submitted for: Presentation and Publication

ABSTRACT

The inverted pavement system is an alternative to the flexible pavement and rigid pavement system. Inverted pavement consists of a bituminous layer and an aggregate layer (crack relief layer) on top of a stabilized base. The design of an inverted pavement system can be understood as similar to the flexible pavement design. The critical stress and strain in the design of the pavement are a vertical compressive strain on the top of a subgrade, horizontal tensile strain situated below the bituminous layer and the cement treated base layer. The factors considered in pavement design are material properties, layer thickness and tyre pressure. The objective of this study is to determine the critical factors affecting the design of inverted pavement in terms of strains at the critical location. This study used Crosspave software to determine the strains in the pavement. Also, the design of the experiment evaluated the main factors out of ten factors affecting the design of inverted pavement at two levels. The result suggests that aggregate modulus is not a significant factor in the design of inverted pavement. The horizontal tensile strain below the bituminous layer is affected by the aggregate interlayer thickness and tyre pressure. Interesting enough, the same factors that affect horizontal tensile strain below the cement-treated base layer also affect vertical compressive strain above subgrade with the predicted R^2 value of more than 92%.

Keywords: Inverted pavement, design factors, Crosspave, optimization.

INTRODUCTION

The pavement industry is constantly looking for ways to improve the performance of pavement. Many researchers studied an inverted pavement system (e.g., [1]–[4]) to better understand its performance as an alternative to flexible and rigid pavements. As the name implies, inverted pavements use rigid supporting layers beneath the bituminous layer, unlike conventionally flexible pavements, where the layers stiffness decreases with depth. In inverted pavements, a weak layer (aggregate layer) is sandwiched between two strong layers (cement-treated base and bituminous layer). There is a schematic diagram of inverted pavement in **Figure 1**. In some cases, the cement-treated subbase can also be used along with cement-treated base layer.

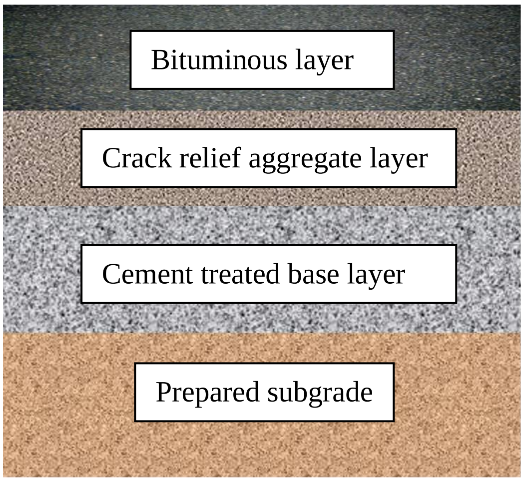

Figure 1 Inverted pavement system

Like other pavement systems, the design of inverted pavement is based on a combination of design load, optimal thickness, and the material properties of each layer. The material properties include the resilient modulus and poison's ratio of each layer. The inverted pavement design is based on the stress and strain at the critical locations The critical locations are vertical compressive strain at top of subgrade, horizontal tensile strain below bituminous layer and cement-treated base layer. Thickness of each layer plays an essential role in pavement performance. The bituminous layer is normally thin in an inverted pavement system [3]. The aggregate layer is typically used as the crack relief layer to prohibit reflective cracking from reaching the bituminous layer. This layer can be modelled as anisotropic (different properties in different directions) or isotropic and stress-dependent material [4],[5]. The minimum thickness of the aggregate layer is recommended to be 100 mm [6]. The cement-treated base layer should have minimum strength in unconfined strength (UCS). The UCS is mainly dependent on the cement type and the cement content. The cement content is generally kept low to avoid shrinkage and cracking. Many agencies who determine the specifications of pavement limit the cement content in the cement-treated base layer below 4% to avoid problems related to cracking [7]. This UCS value is related to the elastic modulus, indirect tensile strength, and flexural strength. Similarly, there is a lower cement content in the cement treated subbase layer. The inverted pavement has lower vertical compressive stress at the top subgrade and deflection at the surface[8].

Theoretical Framework for Design of Inverted Pavement System

This design system is not readily available in the North American pavement design software, MEDPG, so the design equations were adopted from Indian Specification and Austroads (it is collection of Australian and New Zealand transport agencies). In the present case, all the design equation used for various responses in inverted pavement layers consists of life in fatigue and rutting given were adopted from Indian Specification and it is given **Equations 1, 2 and 3** [9], [10].

$$N_f = 2.21 * 10^{-4}\left(\frac{1}{\varepsilon_{tb}}\right)^{3.89}\left(\frac{1}{E}\right)^{0.854} \text{..Equation 1}$$

$$N_R = 4.1656 * 10^{-8}\left(\frac{1}{\varepsilon_v}\right)^{4.5337} \text{..Equation 2}$$

$$N = RF\left[\frac{\frac{11300^{0.0804}}{E_c}+191}{\varepsilon_t}\right]^{12} \text{..Equation 3}$$

N_f = Number of cumulative standard axles to produce 20 % cracked surface
N_R = Number of cumulative standard axles to produce rutting of 20 mm
E = Elastic modulus of the bituminous surface at 35℃
E_C = Elastic modulus of the cementitious layer
ε_t = Horizontal tensile stress at the bottom of the cement-treated base layer
ε_{tb} = Horizontal tensile stress at the bottom of the bituminous layer
ε_v = Vertical compressive strain at the top of the subgrade
N = Number of cumulative standard axles for fatigue cracking
RF= Reliability factor

OBJECTIVE

The objective of the study is to determine the factors significantly affect the design of inverted pavement. Furthermore, it attempts to understand whether the use of the crack relief layer has any structural effects on the performance of the pavement in terms of strain or stress.

METHODOLOGY

The methodology for determining the critical parameters for the design of inverted pavement is given below.

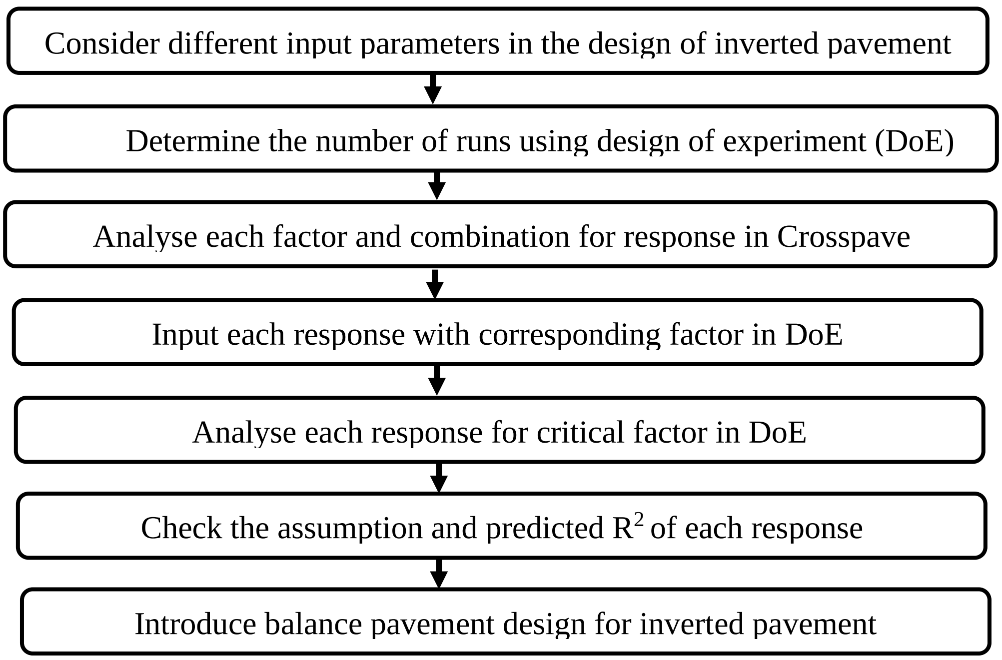

Figure 1 Steps for determining the critical parameter for design of inverted pavement

Factors Affecting Design of Inverted Pavement System

All the potential factors considered for the design of an inverted pavement system are similar to designing a flexible pavement system. The factors considered for the study are thickness, the modulus of various layers including the bituminous layer, the aggregate layer, the cement-treated base layer, the cement-treated subbase layer, and soil strength in terms of CBR and loading pressure. Each factor is considered at two levels to represent low and high values based on the specifications [9] and it is given below

11. Bituminous layer thickness

The minimum design thickness of a bituminous layer considered is 40 mm for a design traffic of 5 million standard axles and maximum value of 100 mm for a design traffic of 50 million standard axles with 5% CBR value. The design thickness is dependent on the traffic.

12. Bituminous layer modulus

The resilient modulus value is considered at two-level for viscosity grade (VG)-30 and VG – 40. The resilient modulus value for VG-30 and VG-40 binder are 2000 MPa and 3000 MPa, respectively at 35 °C. These two binders are considered in the majority of the state in India.

13. Aggregate layer thickness

The aggregate layer is used as the crack relief layer. Two scenarios are considered in the present study: one with an aggregate layer thickness of 100 mm and the other with no aggregate layer. A value of 100 mm is recommended [6][9][11].

14. Aggregate layer modulus

The highest modulus considered for good quality aggregate is 450 MPa. South African researchers recommended this value, and it is adopted in IRC: 37. However, many researchers ([4] [12] [5][13]) have pointed out the aggregate layer's stress-dependent and cross anisotropic properties in the inverted pavement due to its proximity to the bituminous layer. Therefore, anisotropy is considered at two levels such as 0.5 and 1 (representing 450 MPa modulus). The value of 0.5 represents the modulus in the horizontal direction is 0.5 times in the vertical direction.

15. Cement treated base layer thickness

The most vital layer in the inverted pavement design is the cement-treated base layer. The minimum thickness recommended in the IRC specifications is 100 mm and the maximum value is suggested up to 200 mm for a different design condition and subgrade condition [9].

16. Cement treated base layer modulus

The minimum recommended modulus after a 28-day curing period is 5000 MPa in IRC: 37. AASHTO 1993 has given a nomograph to determine elastic modulus from unconfined compressive strength (UCS) of the material. Many published specifications [9] [10] report that the elastic modulus after 28 days is 1000-1250 times the UCS value. However, the minimum curing period in many research studies is seven days. So, there is some discrepancy in the curing period and minimum strength required, i.e., the UCS value is considered at 7 days but the elastic modulus is considered at 28 days. Both should be kept for 7 days or 28 days to make it consistent for designers and practitioners. Therefore, the elastic modulus of 7 days and 28 days are considered in the present case from published literature [14]. The elastic modulus value at 7 and 28 days is 7475 MPa and 11525 MPa, respectively.

17. Cement treated subbase layer thickness

The present IRC specification suggests a minimum and maximum value of 100 mm and 200 mm, respectively, for different design compositions [9]. Therefore, these levels are considered in our case.

18. Cement treated subbase layer modulus

The subbase can be either stabilized with cement and can also be of the granular layer. The modulus value of 600 MPa is suggested in the present IRC specification for stabilized subbase [9]. The value of 200 MPa is indicated for the granular layer.

19. CBR

The subgrade CBR varied from 5% and 15 % in the present IRC specification. However, two levels of 5% and 10% are considered in the analysis to simulate the minimum and fair subgrade condition. The corresponding modulus value for 5% and 10% subgrade is 50 MPa and 76 MPa, respectively using the standard relation to covert CBR to modulus value.

20. Pressure

The standard pressure considered for the design of pavements is 0.56 MPa. Therefore, a condition with higher pressure is also considered with 0.7 MPa value.

Input Parameter in DoE

The concept of inverted pavement has been recently introduced in the Indian design code. Indian Road Congress (IRC) specification was used for input parameters. The number of factors for DoE has been decided based on the IRC: 37-2018. The various factors used in the design of the experiment is given in **Table 1**.

Table 1 Input parameter used in the DoE analysis

Factor	Name	Units	Type	Minimum	Maximum
A	Bituminous layer modulus	MPa	Numeric	-1	1
B	Bituminous layer thickness	mm	Numeric	-1	1
C	Aggregate interlayer modulus	MPa	Numeric	-1	1
D	Aggregate interlayer thickness	mm	Numeric	-1	1
E	Cement treated base layer, modulus	MPa	Numeric	-1	1
F	Cement treated base layer, thickness	mm	Numeric	-1	1
G	Cement treated subbase layer, modulus	MPa	Numeric	-1	1
H	Cement treated subbase layer, thickness	mm	Numeric	-1	1
J	Subgrade, modulus	MPa	Numeric	-1	1
K	Pressure	MPa	Numeric	-1	1

The upper and lower limit of the factors are based on the Indian Road Congress specification. Initially, a minimum run 2^K factorial design was used with center points. As a result, curvature was found to be significant. The central composite design was therefore employed with one face-centered point and 77 runs of the software using a minimum run resolution of five. Response Surface Methodology (RSM) design called Central Composite designs (CCD) are based on 2-level factorial designs, augmented with center and axial points are used to fit the model. RSM is used for the optimization of the input factors[15].

Response in DoE from Crosspave

The pavement responses in terms of vertical compressive strain on the subgrade and horizontal tensile strain below the bituminous layer and cemented base layer are the main interests for the designer. The pavement responses were calculated from pavement design software, named Crosspave. The software is validated with the standard result and more details about software application can be found in the research paper by Brundaban et al., 2020 [12]. All the possible combination of input from the data set was employed using face centered CCD model. The box plot of the response data is shown in **Figure 2**.

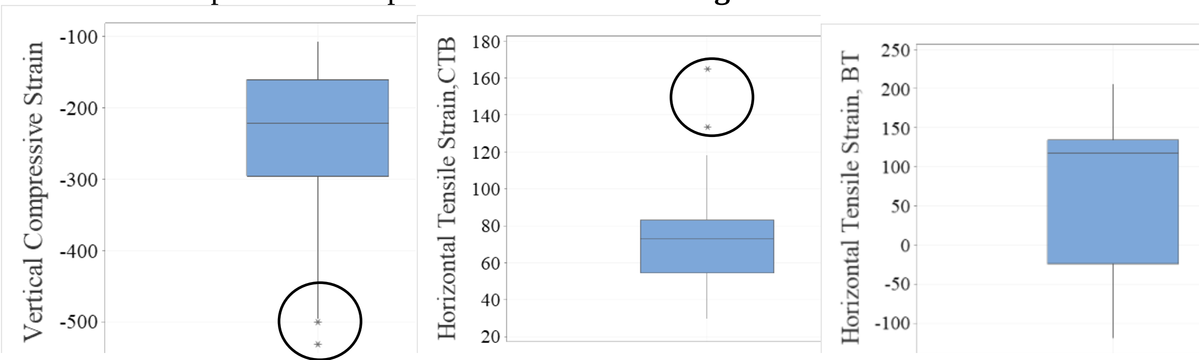

Figure 2 Box plot for the pavement response from Crosspave showing outliers

Model Considered in DoE

Response surface method (RSM), a collection of mathematical and statistical techniques useful for the modeling and analyzing problems in which a response of interest is influenced by several variables and the objective is to optimize the response. In RSM, the form of the relationship between the response and the independent variable is unknown [16]. Equation 4 and 5 depending upon the type of relationship.

- To find a suitable approximation of the true functional relationship between y and the set of independent variables. In the linear function between the independent variables, **Equation 4** is used to represent the first-order model.
- If the curvature is significant based on the system's response, the higher-order equation is used as given in **Equation 5**.

$$y = \beta_0 + \beta_1 x_1 + \beta_2 x_2 + \cdots \dots \dots . + \beta_k x_k + \varepsilon \dots \dots \dots \dots \dots \text{Equation 4}$$

$$y = \beta_0 + \sum_{1}^{k} \beta_i x_i + \sum_{1}^{k} \beta_{ii} x_i^2 + \sum \sum_{i<j} \beta_{ij} x_i x_j + \varepsilon \dots \dots \dots . \text{Equation 5}$$

where β_0 is the constant term, β_i, β_{ij} and β_{ii} are the coefficients of the linear, interaction and quadratic, respectively, and ε is the residual associated to the experiments.

There are different RSMs available in DoE, such as the Box Behnken Design (BBD) and the Central Composite Design (CCD). The CCD has an advantage over BBD when the number of factors is more than four [15]. Furthermore, three types of central composite designs, namely circumscribed, face-centered and inscribed, are available [17]. In the present case, we have used face centered design with three levels and one centre point as the response factor in the design is obtained from pavement software.

To obtain a pavement response at critical locations, the Crosspave software was used. Crosspave is software whose results are previously validated [12] and can model stress-dependent properties and accommodate anisotropic pavement layers' behavior. All the critical pavement responses in terms of vertical compressive strain, horizontal tensile strain in bituminous layer and cement treated base layer are considered. The total number of runs is based on the combination of different input factors.

Analysis with Design of Experiment

Three pavement responses were studied including vertical compressive strain, horizontal tensile strain below the cement-treated base and horizontal tensile strain below bituminous layer. The outlier in the figure was excluded from the study as given in **Figure 2**. Various models available for different response is given in **Table 2**. For example, for the response of vertical compressive strain, linear and quadratic models are available, but the linear model exhibited a higher R^2 value than the quadratic model.

Table 2 Various available models available for response

Response 1: Vertical Compressive Strain			
Source	Sequential p-value	Adjusted R^2	Predicted R^2
Linear	< 0.0001	0.98	0.9745
Quadratic	0.026	0.9969	0.7222
Response 2: Horizontal Tensile Strain, Cement Treated Layer			
Source	Sequential p-value	Adjusted R^2	Predicted R^2
Linear	< 0.0001	0.9311	0.9239
2FI	0.9942	0.8785	-15.867
Quadratic	0.1959	0.9177	-8.936
Response 3: Horizontal Tensile Strain, Bituminous Layer			
Source	Sequential p-value	Adjusted R^2	Predicted R^2
Linear	< 0.0001	0.82	0.8157

From **Table 2**, it is clear that all the response parameters have a linear model as the best fit for the input data. For example, in **Table 2**, response 2 of horizontal tensile strain shows the linear, 2 FI (factor interaction) and quadratic model as the possible models for input parameter but the linear model shows the best p-value and predicted R^2. Now, for each response, the most significant input term affecting the pavement response has been determined. Also, for each response, the assumption of the model such as normality plot of residuals, residuals versus predicted, residuals versus the run, and box cox transformation is checked. The box-cox transformation is used to check the most probable search to determine the transformed data. It is recommended power transform for vertical compressive strain, logarithmic transformation for horizontal tensile strain for a cement-treated base layer, and power transform for horizontal tensile strain below bituminous layer. The model's assumption is met for each response. The assumption for vertical compressive strain is given below in Figure 3. The prediction equation of vertical compressive strain, horizontal tensile strain below cement-treated layer and bituminous layer is given in **Equation 6, 7**, and **8**. The individual term in the **Equation 6,7** and **8** have been previously defined in **Table 1**.

$$(Vertical\ Compressive\ Strain + 585.00)^{2.59} = 10^5(44.06 + 1.959A + 9.60B + 4.47D + 3.94E + 21.93F + 1.43G + 3.15H + 05 + 5.47J) \quad \text{Equation 6}$$

$$Log_{10}(Horizontal\ Tensile\ Strain, CTB) = +1.82 - 0.00984\ A - 0.0718\ B - 0.0425\ D - 0.0428E - 0.127\ F - 0.0397\ G - 0.0244\ H - 0.0191\ J \quad \text{Equation 7}$$

$$(Horizontal\ Tensile\ Strain, BT + 132.00)^{1.37} = 1477.39 + 888.28\ D + 95.31\ K \quad \text{Equation 8}$$

.
.

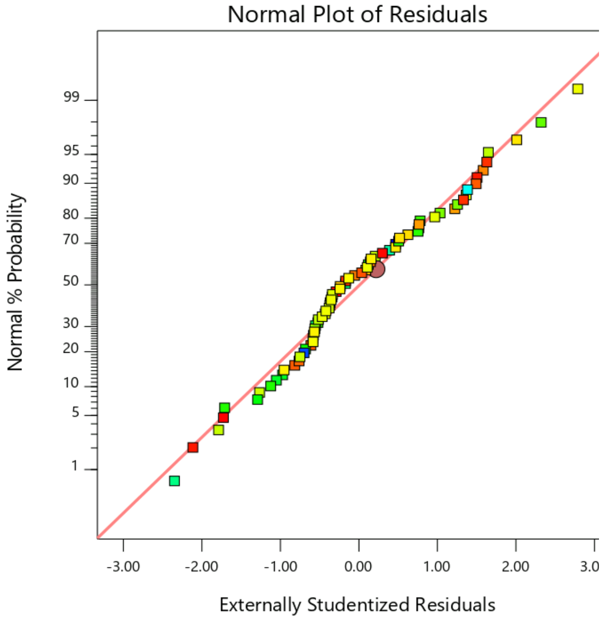

a) Normality plot of the residuals

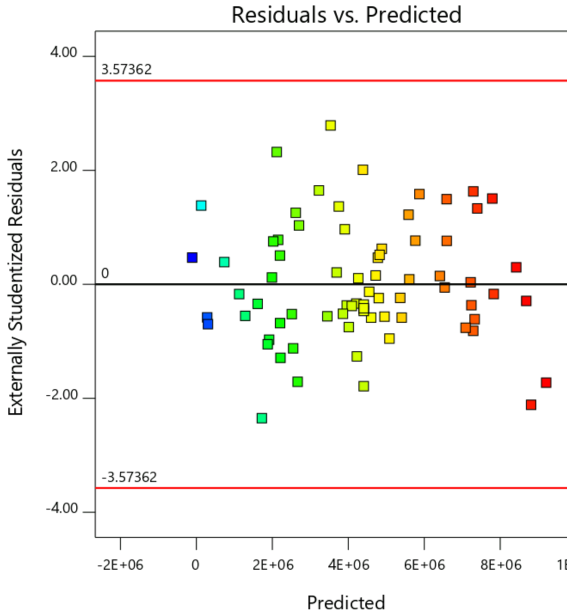

b) Scatter plot of dataset

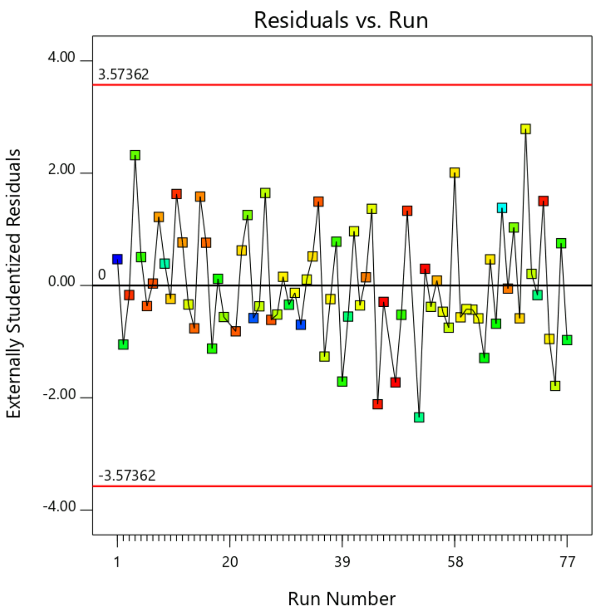

c) Randomness of the dataset

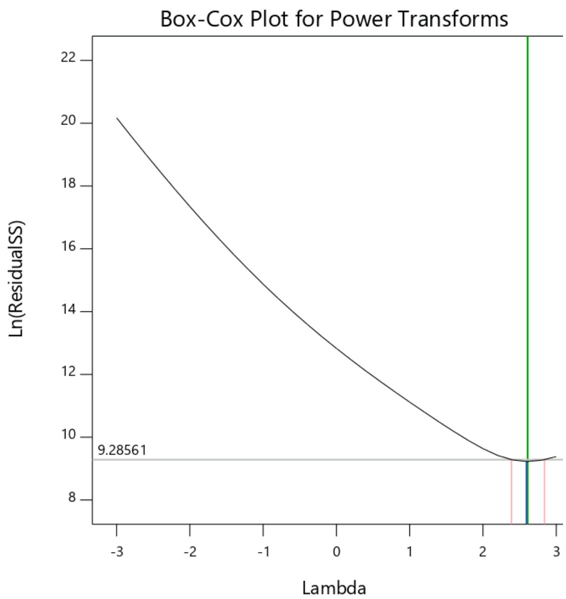

d) Box cox transformation of the dataset

Figure 3 Assumptions of the model for vertical compressive strain

Table 3 gives the coefficient of the pavement design's different responses, namely, vertical compressive strain, horizontal tensile strain below the cemented layer, horizontal tensile strain below the bituminous layer. The term CTB and BT in **Table 3** means cement-treated base and means bituminous layer respectively.

Table 3 The coefficient table for different responses considered in the model

The output of model and p-value	Intercept	A: Bituminous layer modulus	B: Bituminous layer thickness	C: Aggregate interlayer modulus	D: Aggregate interlayer	E: Cement treated base layer,	F: Cement treated base layer,	G: Cement treated subbase layer, modulus	H: Cement treated subbase layer, thickness	J: Subgrade, modulus	K: Pressure
(Vertical compressive strain + 585.00)^2.59	4.4E+06	195920	960050	Not Significant	447421	394145	2.19E+06	143049	315022	547470	
p-values		< 0.0001						0.0015	< 0.0001		
Adjusted R^2	0.98										
Log_{10}(Horizontal tensile strain, CTB)	1.8201	-0.00984	-0.07188	Not Significant	-0.04251	-0.04282	-0.12708	-0.0397	-0.02444	-0.01916	
p-values		0.0638	< 0.0001							0.0005	
Adjusted R^2	0.924										
(Horizontal tensile strain, BT + 132.00)^1.37	1477.3				888.286						95.3188
p-values					< 0.0001						0.051
Adjusted R^2	0.82										

Furthermore, the predicted versus the actual response of the parameter is given in **Figure 4**. The predicted versus the actual value are close to the line of equality for the response (vertical compressive strain). Similar results were obtained for other responses such as horizontal tensile strain below the bituminous layer and the cement-treated base layer.

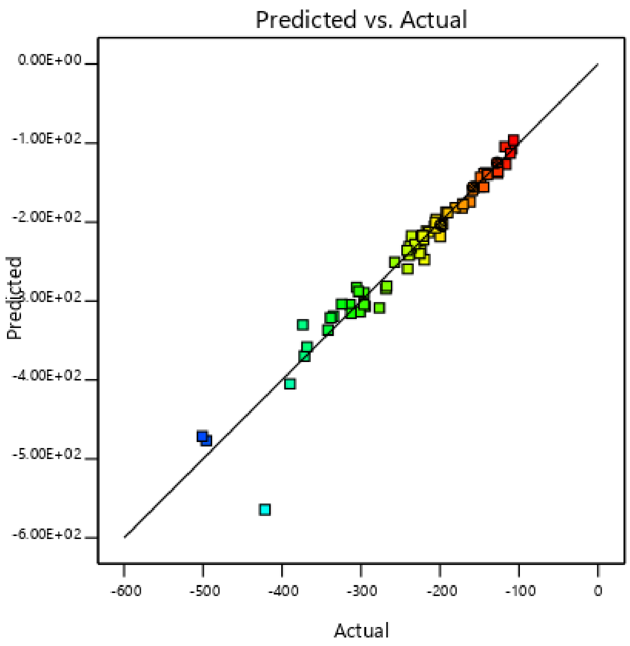

Figure 41 Predicted versus the actual response parameter for the design of the vertical compressive strain

Balance Strain Pavement Design for Inverted Pavement

The pavement is typically designed to handle traffic in the given design while requiring minimal maintenance. Pavement layers are designed to have strains within allowable limits. Among the failure issues associated with asphalt and cement-treated layers are the considerable stresses generated at their bottoms. By limiting these strains, we can extend the pavement's lifespan. For example, the designer of the perpetual pavement kept strains within the allowable limits to resolve this issue. However, the previous research focused primarily on asphalt [18] as a result of this problem. An inverted pavement system combines the various layers, the asphalt layer, the crack relief aggregate layer, the cement-treated base layer, the cement-treated subbase layer, and the subgrade. It is possible to achieve the minimum target strain by combining these layers.

A new equilibrium pavement design concept is proposed here, in which the target strains should be kept zero in the asphalt layer and below the endurance limit in the cement-treated base layer. There is bottom-up cracking in the asphalt layers caused by tensile strain, and in the cement-treated layers, where reflective cracking from CTB to the asphalt layer is already an issue, the combination of these two strains increases the problem. A tensile strain less than 50 µm should be maintained in the cement-treated layer based on literature [19] and the tensile strain beneath the asphalt layer should be kept close to zero. In a layer with a strain value of zero, there is no tension or compression.

The aggregate layer modulus has not been considered in the optimization, as it has no significance in the present case. Past studies focused on one layer, either an asphalt in the perpetual pavement or cement layer in the semi-rigid pavement, to achieve the tensile layer within the allowable limit. In reality, various combinations lead to the target strain, and there is more than one way to achieve the target strain. In this paper, the optimization of an inverted pavement within prescribed constraints was to achieve no tensile strain at the bottom of the asphalt layer and within the endurance limit of the cement treatment layer.

During the design of cement-treated pavements, it is essential to note that the failure of the base layer will eventually lead to failure of the entire pavement, and the need to do full-depth reclamation must be taken into consideration. However, when the asphalt pavement or concrete pavement fails, the surface layers can be repaired or recycled, which cannot be done when a base layer of semi-rigid pavement fails. Therefore, it is crucial to keep the tensile stress below the cement-treated layer within the limit of its endurance for the best pavement performance.

The optimization problem is addressed for low-volume to medium-volume roads. In India, low-volume roads are defined as roads with traffic less than 2 million standard axles (MSA) (IRC SP-72). Medium-volume roads have traffic of about 30 MSA's. The factors chosen for input are carefully selected to maximize the probability of an output response constraint.

According to **Table 3**, the aggregate layer modulus is not considered a significant factor in the design. In addition, the bituminous layer modulus and thickness are kept to a minimum to simulate low volume traffic. Subbase modulus treated with cement is considered to have a high value of 600 MPa, and similarly, the base layer modulus treated with cement is considered to have a high value achieved after 28 days. The concept of numerical optimization allows for the optimization of any combination of multiple goals. Goals can apply to both factors and responses. There are four achievable goals: maximization, minimization, setting targets, and staying within range. Numerical optimization uses hill-climbing techniques. A set of random points is checked along with the design points to see if there is a better solution. **Table 4** presents the different constraints used for the optimization of a balance pavement design.

Table 4 Constraint used for the optimization of pavement system

Input/Output	Value	Reason for considering this value
Bituminous layer modulus	Minimum	The modulus value in the bituminous layer is considered for low volume road
Bituminous layer thickness	Minimum	The thickness value in the bituminous layer is considered for low volume road
Aggregate interlayer modulus	NA	Not a significant factor
Aggregate interlayer thickness	In range	The range varies from 0 to 100 mm
Cement treated base layer, modulus	Maximum	The modulus value is considered after 28 days curing time
Cement treated base layer, thickness	In range	The range varies from 100 to 200 mm
Cement treated subbase layer, modulus	Maximum	The option consists of an untreated modulus of 200 MPa and a treated modulus of 600 MPa
Cement treated subbase layer, thickness	In range	The codal value recommendation is considered.
Subgrade, modulus	Minimum	The average CBR of 5% is considered
Pressure	In range	Two levels are considered in the design in overloading and normal loading. The minimum value corresponds to normal loading
Vertical Compressive Strain	Not controlled	If we can control strain in the above layers, the vertical compressive strain will always be safe
Horizontal Tensile Strain, CTB	50 µm	The endurance limit is chosen
Horizontal Tensile Strain, BT	Zero	The newly developed concept of balance strain is chosen.

Using the constraint in **Table 4**, the pavement has been optimized. The output of the pavement system with the target value of tensile strain below the bituminous layer and cement treated layer is given in **Table 5**.

Table 5 Values of input level for balance mix pavement design

Factors	**Value (in range between -1 and 1)**
Bituminous layer modulus	-0.985427 (minimum)
Bituminous layer thickness	-0.99968 (minimum)
Aggregate interlayer thickness	-0.76 (in range)
Cement treated base layer modulus	0.999 (maximum)
Cement treated base layer thickness	0.9758 (this value was set in range but maximum is obtained)
Cement treated subbase layer modulus	0.999 (maximum)
Cement treated subbase layer thickness	0.6115 (in range)
Subgrade modulus	0.704 (in range)
Pressure	0.0136 (in range)
Vertical compressive strain on top of subgrade, microstrain	-166.5
Horizontal tensile strain below cement-treated layer, microstrain	50
Horizontal tensile strain below bituminous layer, microstrain	-0.10

CONCLUSION

This study comprehensively considered all the design parameters used for the design of inverted pavement. In general, past studies focused on studying a limited number of factors. In our case, we have considered ten factors. Critical pavement response parameters were chosen to determine the most critical factors affecting the three responses: horizontal tensile strain under the bituminous layer, cement-treated base layer, and vertical compressive strain. Based on the DoE, the following conclusions have been obtained.

- The previously published articles ([4], [5], [12], and [20]) considered stress-dependent behaviour of the crack relief aggregate layer. In this research, the anisotropy behaviour of the aggregate interlayer was considered. However, the results suggest that aggregate modulus significantly does not affect output either vertically or horizontally in either the bituminous layer or the cement-treated layer. As a result, this result is a departure from the literature. The result can be understood as aggregate modulus having a low modulus of 450 MPa, whereas layers underlying cement-treated and overlaid with bituminous have a high modulus. Originally, the purpose of this layer was to prevent reflective cracking in the cement-treated base layer from extending into the underlying layer.
- Aside from the modulus and thickness of the bituminous layer, the cement-treated base layer, and the cement-treated subbase layer, vertical compression strain is influenced by the subgrade modulus and aggregate interlayer thickness. Interestingly, the same factors affect the horizontal tensile strain in the cement-treated base layer as they do the vertical compressive strain on top of the subgrade. In general, the adjusted R^2 value is more than 92%. Only the coefficient and p-value of the individual factors differ, as shown in **Table 3**.
- The optimized thickness using the concept of balance pavement design is given in **Table 5**. It is possible to have a minimum thickness of the bituminous layer (40 mm)

and still have zero strain and be within the endurance limit of the cement-treated layer. In comparison, it is almost impossible to have 40 mm thickness and zero strain in perpetual pavements. Long-lasting pavements can be achieved with this design.
- Finally, the existing criteria of 7 days UCS should be continued to accelerate the construction, but the cement layer modulus of 28 days curing is recommended to have strength and factor of safety in the pavement design. It is similar to building design, wherein the formworks are removed earlier in the field to accelerate construction, but the design strength is considered after 28 days.

LIMITATION OF THE STUDY

The present study detailed the comprehensively various factors used for pavement design using a linear elastic software, Crosspave. However, despite being a comprehensive study, the following are the limitation of the study.

- More sophisticated pavement design software such as MEPDG could not be used as the software does not design for the inverted pavement system.
- The layer interface was considered to be fully bonded. However, in actual field conditions, it may be partially bonded depending upon the construction practice.
- The present paper analysed the inverted pavement from linear elastic software. The use of finite element software could have been better.
- The optimized thickness is based on the theoretical concept. In the field, practical consideration may affect the actual values.
- The fatigue properties of cement stabilized affect the performance of the inverted pavement. Alternatively, cumulative fatigue damage should be carried out to understand whether the optimized pavement could take the design load.
- Finally, the critical factor found for a different response should be validated with some field results as they are statistically found out and validated through software only.

AUTHOR CONTIBUTION

The authors confirm contribution to the paper as follows: study conception and design: Shahbaz Khan, data collection: Shahbaz Khan; analysis and interpretation of results: Shahbaz Khan; draft manuscript preparation: Shahbaz Khan, Kamal Hossain and Carlos Bazan. All authors reviewed the results and approved the final version of the manuscript.

FUNDING

The funding of the corresponding author is supported by Natural Sciences and Engineering Research Council.

ACKNOWLEDGMENT

The authors are thankful to Assistant Professor Umesh Chandra and Brundaban Beriha, Ph.D scholar, IIT Bhubaneshwar for providing the software used in the analysis.

REFERENCES

[1] E. Papadopoulos and J. C. Santamarina, "Inverted base pavements: construction and performance," International Journal of Pavement Engineering, pp. 1–7, May 2017, doi: 10.1080/10298436.2017.1326237.

[2] E. Papadopoulos and J. C. Santamarina, "Analysis of inverted base pavements with thin-asphalt layers," International Journal of Pavement Engineering, vol. 17, no. 7, pp. 590–601, 2016, doi: 10.1080/10298436.2015.1007232.

[3] D. D. Cortes and J. C. Santamarina, "The LaGrange case history: Inverted pavement

system characterisation and preliminary numerical analyses," International Journal of Pavement Engineering, vol. 14, no. 5, pp. 463–471, 2013, doi: 10.1080/10298436.2012.742192.

[4] D. R. Biswal, U. Chandra Sahoo, and S. Ranjan Dash, "Structural response of an inverted pavement with stabilised base by numerical approach considering isotropic and anisotropic properties of unbound layers," Road Material and Pavement Design., 2020, doi: 10.1080/14680629.2019.1595701.

[5] E. Papadopoulos, D. D. Cortes, and J. Carlos Santamarina, "In-situ assessment of the stress-dependent stiffness of unbound aggregate bases: application in inverted base pavements," International Journal of Pavement Engineering., 2016, doi: 10.1080/10298436.2015.1022779.

[6] A. Sha, Z. Han, L. Jiao, L. Hu, and H. Li, "Optimal Structure Combination for Inverted Asphalt Pavement Incorporating Cracks in Cement-Treated Subbase," Transportation Research Record., 2020, doi: 10.1177/0361198119899056.

[7] A. Ismail et al., "Laboratory investigation on the strength characteristics of Cement-Treated Base," In Applied mechanics and materials, 2014 (Vol. 507, pp. 353-360) vol. 507, pp. 353–360, 2014, doi: 10.4028/www.scientific.net/AMM.507.353.

[8] E. Tutumluer and R. D. Barksdale, "Inverted flexible pavement response and performance," Transportation Research Record, no. 1482, pp. 102–110, 199..

[9] IRC:37, "Guidelines for design of flexible pavement," Indian Road Congress, New Delhi, 2018.

[10] Austroads.Pavement design:, "Pavement design: A guide to the structural design of road pavements." 2004,

[11] "AASHTO Guide for Design of Pavement Structures," in AASHTO, 2003.

[12] D. Beriha, B., Sahoo, U. C., & Mishra, "Crosspave: a multi-layer elastic analysis programme considering stress-dependent and cross-anisotropic behaviour of unbound aggregate pavement layers.," International Journal of Pavement Engineering, pp. 1-15., 2020.

[13] E. Papadopoulos, D. D. Cortes, and J. Carlos Santamarina, "In-situ assessment of the stress-dependent stiffness of unbound aggregate bases: application in inverted base pavements," International Journal of Pavement Engineering, vol. 17, no. 10, pp. 870–877, 2016, doi: 10.1080/10298436.2015.1022779.

[14] A. Sounthararajah, H. H. Bui, N. Nguyen, P. Jitsangiam, and J. Kodikara, "Early-Age Fatigue Damage Assessment of Cement-Treated Bases under Repetitive Heavy Traffic Loading," Journal of Material in Civil Enginering, 2018, doi: 10.1061/(asce)mt.1943-5533.0002250.

[15] L. Lye, "Applications of DOE in Engineering and Science: A Collection of 2^6 Case Studies.," 2019.

[16] D. C. Montgomery, Design and analysis of experiments. John wiley & sons. 2017.

[17] P. . El Hami, A., & Pougnet, Embedded Mechatronic Systems 2: Analysis of Failures, Modeling, Simulation and Optimization (Vol. 2). Elsevier Ltd, 2020.

REFERENCES

1. Ahmed, A., Labi, S., Li, Z., & Shields, T. (2013). Aggregate and disaggregate statistical evaluation of the performance-based effectiveness of long-term pavement performance specific pavement study-5 (LTPP SPS-5) flexible pavement rehabilitation treatments. Structure and Infrastructure Engineering, 9(2), 172-187.
2. Babashamsi, P., Yusoff, N. I. M., Ceylan, H., Nor, N. G. M., & Jenatabadi, H. S. (2016). Evaluation of pavement life cycle cost analysis: Review and analysis. International Journal of Pavement Research and Technology, 9(4), 241-254.
3. Banerjee, A., Aguiar-Moya, J., & Prozzi, J. A. (2009). Texas experience using LTPP for calibration of the MEPDG permanent deformation models. Transportation Research Record, 2094, 12-20.
4. Barksdale, R. D., and H. A. Todres. A Study of Factors Affecting Crushed Stone Base Course Performance. Atlanta, Georgia, 1983.
5. Bayomy, F., Salem, H., & Vosti, L. (2006). Analysis of the long-term pavement performance data for the Idaho GPS and SPS sections. Moscow: Idaho Transportation Department.
6. Beriha, B., & Sahoo, U. C. (2020). Analysis of flexible pavement with cross-anisotropic material properties. International Journal of Pavement Research and Technology, 13(4), 411-416.
7. Bhattacharya, B. B., Von Quintus, H. L., & Darter, M. I. (2015). Implementation and local calibration of the MEPDG transfer functions in wyoming (No. FHWA 16/02F). Wyoming. Dept. of Transportation.
8. Biswal, D. R., Chandra Sahoo, U., & Ranjan Dash, S. (2020). Structural response of an inverted pavement with stabilised base by numerical approach considering isotropic

and anisotropic properties of unbound layers. Road Materials and Pavement Design, 21(8), 2160-2179.

9. Brundaban Beriha, Umesh C. Sahoo & Debakanta Mishra (2020) Crosspave: a multi-layer elastic analysis programme considering stress-dependent and cross-anisotropic behaviour of unbound aggregate pavement layers, International Journal of Pavement Engineering, DOI: 10.1080/10298436.2020.1821025
10. Burnos, P., & Rys, D. (2017). The effect of flexible pavement mechanics on the accuracy of axle load sensors in vehicle weigh-in-motion systems. Sensors, 17(9), 2053.
11. Cai, L., Wang, H., & Fu, Y. (2013). Freeze–thaw resistance of alkali–slag concrete based on response surface methodology. Construction and Building Materials, 49, 70-76.
12. Carvalho, R., Ayres, M., Shirazi, H., Selezneva, O., & Darter, M. (2011). Impact of design features on pavement response and performance in rehabilitated flexible and rigid pavements (No. FHWA-HRT-10-066). Turner-Fairbank Highway Research Center.
13. Chen, S., You, Z., Sharifi, N. P., Yao, H., & Gong, F. (2019). Material selections in asphalt pavement for wet-freeze climate zones: A review. Construction and Building Materials, 201, 510-525.
14. Daleiden, J. F., Rauhut, J. B., Killingsworth, B., Antwi, E. O., Darter, M. I., & Ahmad, R. (1994). Evaluation of the AASHTO design equations and recommended improvements (No. SHRP-P-394). Strategic Highway Research Program.
15. Daleiden, J. F., Simpson, A., & Rauhut, J. B. (1998). Rehabilitation performance trends: early observations from long-term pavement performance specific pavement

studies. Publication FHWA-RD-97-099. Office of Infrastructure Research and Development, FHWA.

16. Dong, Q., & Huang, B. (2015). Failure probability of resurfaced preventive maintenance treatments: investigation into long-term pavement performance program. Transportation Research Record, 2481(1), 65-74.
17. Donnelly, P. (1984). Design and analysis of experiments, -Montgomery, DC.
18. El Hami, A., & Pougnet, P. (Eds.). (2020). Embedded mechatronic systems 2: analysis of failures, modeling, simulation and optimization (Vol. 2). Elsevier.
19. Gu, F., & Tran, N. (2019). Best practices for determining life cycle costs of asphalt pavements (No. NCAT Report 19-03).
20. Guo, X. (2013). Local calibration of the MEPDG using test track data (Doctoral dissertation).
21. Haas, R., & Kazmierowski, T. (1996). Tac's new pavement design and management guide. In cost effectiveness through innovation: proceedings of the 1996 tac annual conference, charlottetown, prince edward island, october 6-9, 1997.
22. Haider, S. W., & Chatti, K. (2009). Effect of design and site factors on fatigue cracking of new flexible pavements in the LTPP SPS-1 experiment. International Journal of Pavement Engineering, 10(2), 133-147.
23. Hall, K. T., Simpson, A. L., & Correa, C. E. (2002). LTPP data analysis: effectiveness of maintenance and rehabilitation options. Washington, DC: National Cooperative Highway Research Program.
24. Hanson, Jonathan Russell, "Cracking and roughness of asphalt pavements constructed using cement-treated base materials" (2006). Theses and Dissertations. 396. https://scholarsarchive.byu.edu/etd/396
25. Highway Research Board (1962). The AASHO Road Test.

26. Huang, Y. H. (2004). Pavement design and analysis. Pearson/Prentice Hall.

27. IRC 37-2012. Guidelines for design of flexible pavement. Indian Road Congress, New Delhi, 2012.

28. IRC 37-2018. Guidelines for design of flexible pavement. Indian Road Congress, New Delhi, 2018.

29. Jackson, D. J. (2001). Pavement preventive maintenance guidelines. In Second International Symposium on Maintenance and Rehabilitation of Pavements and Technological Control. Auburn University, University of Mississippi (No. 01-128).

30. Jackson, N., Puccinelli, J., & Engineers, N. C. (2006). Long-term pavement performance program (LTPP) data analysis support: National Pooled Fund Study TPF-5 (013). Effects of multiple freeze cycles and deep frost penetration on pavement performance and cost (No. FHWA-HRT-06-121; 123210-8). Turner-Fairbank Highway Research Center.

31. Kennedy, M., & Krouse, D. (1999). Strategies for improving fermentation medium performance: a review. Journal of Industrial Microbiology and Biotechnology, 23(6), 456-475.

32. Ker, H. W., Lee, Y. H., & Wu, P. H. (2008). Development of fatigue cracking prediction models using long-term pavement performance database. Journal of Transportation Engineering, 134(11), 477-482.

33. Lewis, D. E., K. Ledford, T. Georges, and D. M. Jared. Construction and performance of inverted pavements in Georgia. Transportation Research Record: Journal of the Transportation Research Board, 2012

34. Long Term Pavement Performance (LTPP), 2018, LTPP InfoPave - Data Selection and Download (dot.gov), accessed on 1st March, 2020

35. Lye, L. 2020. ENGI 9516: Simulitude, modelling and data analysis-course notes, Memorial University of Newfoundland and Labrador, Canada.

36. Mallela, J., Glover, L. T., Darter, M. I., Von Quintus, H., Gotlif, A., Stanley, M., & Sadasivam, S. (2009). Guidelines for implementing NCHRP 1-37A ME Design Procedures in Ohio: Volume 1--Summary of Findings, Implementation Plan, and Next Steps (No. FHWA/OH-2009/9A). Ohio. Dept. of Transportation.

37. Mamlouk, M. S., & Dosa, M. (2014). Verification of effectiveness of chip seal as a pavement preventive maintenance treatment using LTPP data. International Journal of Pavement Engineering, 15(10), 879-888.

38. Miller, J. S., & Bellinger, W. Y. (2003). Distress identification manual for the long-term pavement performance program (No. FHWA-RD-03-031). United States. Federal Highway Administration. Office of Infrastructure Research and Development.

39. Miller, H. J., Guthrie, W. S., Crane, R. A., & Smith, B. (2006). Evaluation of cement-stabilized full-depth-recycled base materials for frost and early traffic conditions.

40. Moghaddam, T. B., Soltani, M., Karim, M. R., & Baaj, H. (2015). Optimization of asphalt and modifier contents for polyethylene terephthalate modified asphalt mixtures using response surface methodology. Measurement, 74, 159-169.

41. Muthadi, N. R., & Kim, Y. R. (2008). Local calibration of mechanistic-empirical pavement design guide for flexible pavement design. Transportation Research Record, 2087(1), 131-141.

42. Nassar, A. I., Thom, N., & Parry, T. (2016). Optimizing the mix design of cold bitumen emulsion mixtures using response surface methodology. Construction and Building Materials, 104, 216-229.

43. Papadopoulos, E., and J. C. Santamarina. Inverted base pavements: construction and performance. International Journal of Pavement Engineering, Vol. 8436, No. May, 2017, pp. 1–7. https://doi.org/10.1080/10298436.2017.1326237.

44. Papadopoulos, E., D. D. Cortes, and J. Carlos Santamarina. In-Situ assessment of the stress-dependent stiffness of unbound aggregate bases: application in inverted base pavements. International Journal of Pavement Engineering, Vol. 17, No. 10, 2016, pp. 870–877. https://doi.org/10.1080/10298436.2015.1022779.

45. Perera, R. W., & Kohn, S. D. (1999). International roughness index of asphalt concrete overlays: Analysis of data from long-term pavement performance program SPS-5 projects. Transportation research record, 1655(1), 100-109.

46. Perera, R. W., & Kohn, S. D. (2001). LTPP data analysis: Factors affecting pavement smoothness. Washington, DC, USA: Transportation Research Board, National Research Council.

47. Peshkin, D. G., Hoerner, T. E., & Zimmerman, K. A. (2004). Optimal timing of pavement preventive maintenance treatment applications (Vol. 523). Transportation Research Board.

48. Rooholamini, H., Hassani, A., & Aliha, M. R. M. (2018). Evaluating the effect of macro-synthetic fibre on the mechanical properties of roller-compacted concrete pavement using response surface methodology. Construction and Building Materials, 159, 517-529.

49. Santamarina, J., and E. Papadopoulos. Inverted Base Pavements: New Field Test & Design Catalogue. 2014.

50. Sha, A., Han, Z., Jiao, L., Hu, L., & Li, H. (2020). Optimal structure combination for inverted asphalt pavement incorporating cracks in cement-treated subbase. Transportation Research Record, 2674(1), 68-78.

51. Simpson, A. L., Schmalzer, P. N., & Rada, G. R. (2007). Long-term pavement performance project laboratory materials testing and handling guide (No. FHWA-HRT-07-052). United States. Federal Highway Administration.

52. Smith, B., & Nair, H. (2015). Development of local calibration factors and design criteria values for mechanistic-empirical pavement design (No. FHWA/VCTIR 16-R1). Virginia Center for Transportation Innovation and Research.

53. Souliman, M. I., Mamlouk, M. S., El-Basyouny, M. M., & Zapata, C. E. (2010). Calibration of the AASHTO MEPDG for flexible pavement for Arizona conditions. In Proceedings of the Transportation Research Board 89th Annual Meeting (p. 22). Washington, DC, USA: Transportation Research Board.

54. Sounthararajah, A., Bui, H. H., Nguyen, N., Jitsangiam, P., & Kodikara, J. (2018). Early-age fatigue damage assessment of cement-treated bases under repetitive heavy traffic loading. Journal of Materials in Civil Engineering, 30(6), 04018079.

55. Su, N., Xiao, F., Wang, J., & Amirkhanian, S. (2017). Characterizations of base and subbase layers for Mechanistic-Empirical Pavement Design. Construction and Building Materials, 152, 731-745.

56. Tarefder, R., & Rodriguez-Ruiz, J. I. (2013). Local calibration of MEPDG for flexible pavements in New Mexico. Journal of Transportation Engineering, 139(10), 981-991.

57. Theyse, H., M. De Beer, and F. Rust. Overview of south african mechanistic pavement design method. Transportation Research Record: Journal of the Transportation Research Board, Vol. 1539, 1996, pp. 6–17. https://doi.org/10.3141/1539-02.

58. Tutumluer, E. Practices for unbound aggregate pavement layers. Washington, DC, 2013.

59. Tutumluer, E., and R. D. Barksdale. Inverted flexible pavement response and performance. Transportation research record, No. 1482, 1995, pp. 102–110.

60. Visintine, B. A., Simpson, A. L., & Rada, G. R. (2017). Validation of pavement performance measures using LTPP data: Final Report. Report No. FHWA-HRT-17-089. Federal Highway Administration, Washington, DC.

61. Walker, D., & Cebon, D. (2011). The Metamorphosis of long-term pavement performance traffic data. TR News-Transportation Research Board, (277), 9.

62. Wang, H., & Wang, Z. (2013). Evaluation of pavement surface friction subject to various pavement preservation treatments. Construction and Building Materials, 48, 194-202.

63. Wang, H., Zhao, J., & Wang, Z. (2015). Impact of overweight traffic on pavement life using weigh-in-motion data and mechanistic-empirical pavement analysis. In 9th International Conference on Managing Pavement Assets.

64. Williams, R. C., & Shaidur, R. (2013). Mechanistic-empirical pavement design guide calibration for pavement rehabilitation (No. SPR 718). Oregon. Dept. of Transportation. Research Section.

65. Wu, Z., Yang, X., & Zhang, Z. (2013). Evaluation of MEPDG flexible pavement design using pavement management system data: Louisiana experience. International Journal of Pavement Engineering, 14(7), 674-685.

66. Yuan, X. X., & Nemtsov, I. (2018). Local calibration of the MEPDG distress and performance models for Ontario’s flexible roads: Overview, impacts, and reflection. Transportation Research Record, 2672(40), 207-216.

67. Zuniga-Garcia, N., Martinez-Alonso, W., de Fortier Smit, A., Hong, F., & Prozzi, J. A. (2018). Economic analysis of pavement preservation techniques. Transportation Research Record, 2672(12), 10-19.